

Relic Densities of Dark Matter in the $U(1)$ -Extended NMSSM and the Gauged Axion Supermultiplet

^aClaudio Corianò, ^bMarco Guzzi and ^aAntonio Mariano

^a *Department of Physics, Università del Salento
and INFN Sezione di Lecce, Via Arnesano 73100 Lecce, Italy*¹

^b *Department of Physics, Southern Methodist University,
Dallas TX 75275, USA*²

Abstract

We compute the dark matter relic densities of neutralinos and axions in a supersymmetric model with a gauged anomalous $U(1)$ symmetry, kinetically mixed with $U(1)_Y$ of hypercharge. The model is a variant of the USSM (the $U(1)$ extended NMSSM), containing an extra $U(1)$ symmetry and an extra singlet in the superpotential respect to the MSSM, where gauge invariance is restored by Peccei-Quinn interactions using a Stückelberg multiplet. This approach introduces an axion ($\text{Im } b$) and a saxion ($\text{Re } b$) in the spectrum and generates an axino component for the neutralino. The Stückelberg axion ($\text{Im } b$) develops a physical component (the gauged axion) after electroweak symmetry breaking. We classify all the interactions of the Lagrangian and perform a complete simulation study of the spectrum, determining the neutralino relic densities using micrOMEGAs. We discuss the phenomenological implications of the model analyzing mass values for the axion from the milli-eV to the MeV region. The possible scenarios that we analyze are significantly constrained by a combination of WMAP data, the exclusion limits from direct axion searches and the veto on late entropy release at the time of nucleosynthesis.

¹claudio.coriano@unisalento.it, antonio.mariano@unisalento.it

²mguzzi@physics.smu.edu

1 Introduction

Axions have been studied along the years both as a realistic attempt to solve the strong CP problem [1, 2],[3, 4, 5, 6, 7][8], to which they are closely related, but also as a possible candidate to answer more recent puzzles in cosmology, such as the origin of dark energy, whose presence has found confirmation in the study of Type I supernovae [9, 10]. In this second case it has been pointed out that they can contribute to the vacuum energy, a possibility that remains realistic if their mass m_a - which in this case should be $\sim 10^{-33}$ eV and smaller - is of electroweak [11] and not of QCD origin. In this case they differ significantly from the standard (Peccei-Quinn, PQ) invisible axion.

According to this scenario, the vacuum misalignment (see [12, 13] for a discussion in the PQ case) induced at the electroweak scale would guarantee that the degree of freedom associated with the axion field remains frozen, rolling down very slowly towards the minimum of the non-perturbative instanton potential, with m_a much smaller than the current Hubble rate. Given the rather tight experimental constraints which have significantly affected the parameter space (axion mass and gauge couplings) for PQ axions [14, 15, 16], the study of these types of fields has also taken into account the possibility to evade the current bounds [17, 18]. These are summarized both into an upper and a lower bound on the size of f_a , the axion decay constant, which sets the scale of the misalignment angle θ , defined as the ratio of the axion field (a) over the PQ scale v_{PQ} ($v_{PQ} \sim f_a$).

Axion-like particles can be reasonably described by pseudoscalar fields characterized by an enlarged parameter space for mass and couplings, with a direct coupling to the gauge fields (of the form $aF\tilde{F}$) whose strength remains unrelated to their mass. They have been at the center of several recent and less recent studies (see for instance [19, 20] [21, 22, 23, 18, 24, 25]). They are supposed to inherit most of the properties of a typical invisible axion - a PQ axion - while acquiring some others which are not allowed to it.

We recall that the axion mass (which in the PQ case is $O(\Lambda_{QCD}^2/f_a)$ and the axion coupling to the gauge fields are indeed related by the same constant f_a . In the PQ case f_a ($\sim 10^{10} - 10^{12}$ GeV) makes the axion rather light ($\sim 10^{-3} - 10^{-5}$ eV) and also very weakly coupled. The same (large) scale plays a significant role in establishing the axion as a possible dark matter candidate, contributing significantly to the relic densities of cold dark matter. A much smaller value of f_a , for instance, would diminish significantly the axion contribution to cold dark matter due to the suppression of its abundance (Y_χ) which depends quadratically on f_a .

It is quite immediate to realize that the gauging of the axionic symmetries by introducing a local anomalous $U(1)$ - inherited from an underlying anomalous structure, i.e. a gauge anomaly - allows to leave the mass and the coupling of the axion to the gauge fields unrelated [26, 27], offering a natural theoretical justification for the origin of axion-like particles. We just recall that effective low energy models incorporating gauged PQ interactions emerge in several string and supergravity constructions, for instance in orientifold vacua of string theory and in gauged supergravities (see for instance [28, 29]).

The analysis that we perform in this work has the goal to capture the relevant phenomenological features of the axions present in this class of models, extending a previous study presented in a non-supersymmetric context [30]. We will be following, as in previous studies, a bottom-up approach. This

allows to identify the low energy effective action on the basis of a rather simple operatorial structure typical of anomalous abelian models. The theory is then fixed by the condition of gauge invariance of the anomalous effective action, amended by operators of dimension-5 (Wess-Zumino or PQ-like terms) which appear in the action suppressed by a suitable scale, the Stückelberg mass (M_{St}).

The introduction of the Stückelberg multiplet (or axion multiplet), while necessary for the restoration of gauge invariance, is in general expected to raise some concerns at cosmological level because of the presence, among its components, of a scalar modulus, the saxion. In supersymmetric (ordinary) PQ formulations this has a mass of the order of the weak scale or smaller and poses severe problems to the standard cosmological scenario. A late time decay of this particle, for instance, could cause an entropy release with a low reheating temperature ($T_{RH} < 5 \text{ MeV}$) which is unacceptable for nucleosynthesis. Just for comparison, we mention that in the case of string moduli, for instance, the interaction of these states with the rest of the fields of the low energy spectrum is suppressed by the Planck scale. In turn, this forces the mass of these states to be quite large (100 TeV or so) [31, 32] in order to enhance the phase space for their decay, for a similar reason.

In our construction the scalar modulus of the axion multiplet acquires a mass of the order of the Stückelberg scale and has sizeable interactions with the other fields of the model, thereby decaying pretty fast ($\sim 10^{-23} \text{ s}$). Therefore, smaller values of its mass - in the TeV range - turn out to be compatible with the standard scenario for nucleosynthesis.

Few more comments are in order concerning the structure of these Lagrangians and the possible models which can be constructed using our bottom-up approach. One is about the kinetic term of the Stückelberg multiplet, that due to gauge invariance, necessarily has to take the Stückelberg form, generating a mass term at tree level for the anomalous gauge boson. In fact, the introduction of this term is the only way to render the axion a dynamical field, while preserving gauge invariance. Obviously, this points towards the generality of the supersymmetric construction. A second comment concerns the form of the superpotential, which here, for simplicity, is assumed to be that of the NMSSM. As explained in [33], this corresponds to the simplest structure which supports a physical axion in the spectrum. The presence of just one extra singlet superfield respect to the superpotential of the MSSM makes the analysis, in this case, more manageable. However, we expect that the analysis of more general superpotentials incorporating anomalous symmetries should follow quite closely our approach.

1.1 Cosmological bounds on the Stückelberg mass and supersymmetry

One of the main conclusions of our study is that cosmological constraints on dark matter relics impose bounds on the value of the fundamental scales of the theory. For instance, we show - at least for the superpotential that we analyze - that cosmological constraints on the allowed values of the relic densities of dark matter set an upper bound on the Stückelberg mass of about 1.5 TeV. This constraint emerges only after a detailed analysis, showing that important information on the consistency of many constructions of this type can be gathered only as a result of extensive numerical studies and can't be predicted beforehand. Therefore, the possibility to extend important numerical tools - for the analysis of particle spectra, interactions and relic densities - from the MSSM to new models is an important and open avenue

for future studies.

Concerning the approach that we have followed in our analysis, we just remark that all the studies of the (quite sizeable) mass matrices have been performed numerically after the identification of the relevant region in parameter space. At the same time, the spectrum has been scanned thoroughly in order to identify the most significant regions where all the consistency constraints are satisfied.

The scenario that we have mostly investigated is that of low scale supersymmetry, with the corresponding scale M_{susy} around 1 TeV, although other scenario could be investigated as well. As we have mentioned, the strongest constraint on the model comes from the bounds on the relic densities of neutralinos from WMAP [34], which favour a dark matter (DM) contribution to $\Omega h^2 = \rho/\rho_c h^2$ around $10 - 14\%$ ($\Omega_{DM} h^2 \sim 0.1$). This forces the Stückelberg scale M_{St} to lay around the SUSY breaking scale M_{susy} . This result poses stringent limits on the mass of the extra Z prime in these models, especially if combined with the lower bound on the mass of new neutral gauge interactions from direct searches [35].

We discuss the way a physical axion emerges in these models, and the mechanisms of vacuum misalignments which are typical of these types of constructions, extending a previous analysis [30]. These mechanisms are referred to, in the literature on axions, as being “non thermal” [12, 13]. A non-thermal population of axions, given the bounds obtained on the Stückelberg mass, as we are going to see, is then found to be negligible. Our study, however, does not exclude the possibility of having a thermal population of the same particles. The answer to this question requires a separate and quite involved study, given the presence of several (and all relevant) low energy scales below the TeV region to be considered.

1.2 The USSM-A

Non-supersymmetric versions of the class of models that we are going to analyze have been discussed in details in [36, 26, 27]. Recently [33, 37], an extension of a specific supersymmetric model, the USSM (the $U(1)$ -extended Next-to-Minimal Supersymmetric Standard Model of [38]) has been presented, in which the $U(1)$ symmetry is anomalous. This model supports an axion-like particle in its spectrum. It has been named the “USSM-A”, to recall both its supersymmetric origin and its anomalous abelian gauge structure. It is also close to a similar $U(1)'$ extension of the MSSM (the $U(1)'$ Minimal Supersymmetric Standard Model) [39], which supports an axino component among the interaction eigenstates of the neutralino sector, but not a gauged axion, due to the structure of the MSSM superpotential. The study of relic densities in this model have been performed in [40, 41]. In the non-supersymmetric case the identification of a physical axion in the spectra of these models has been discussed in detail in [36], a realization called “the Minimal Low Scale Orientifold Model” or MLSOM for short.

Both in the USSM-A and in the model of [39], the extra $U(1)$ symmetry takes an anomalous form and the violation of gauge invariance requires supersymmetric PQ interactions, with a Stückelberg supermultiplet for the restoration of the gauge symmetry. The extra gauge boson of the anomalous $U(1)$ symmetry is massive and in the Stückelberg phase, as in previous non-supersymmetric constructions [36, 26, 27]. As shown in the case of the MLSOM, axion-like particles appear in the CP-odd spectrum of these theories whenever Higgs-axion mixing [36] occurs. For this reason in this work we will be using the term “gauged supersymmetric axion” (or axi-Higgs, denoted equivalently as χ or H_0^5) to refer to this state.

As we have mentioned in the introduction, we will follow a minimal approach. This approach allows to define an effective theory on the basis of 1) an assigned gauge structure (the number of anomalous abelian interactions); 2) some conditions of anomaly cancellation and gauge invariance of the effective Lagrangian; 3) the choice of a suitable value of the Stückelberg mass scale characterizing the range in which the description of these effective models is compatible with unitarity [42]. As in a previous analysis for the LHC in the MLSOM [43], we will stress on the general features of these models, trying to fit them into a coherent scenario of particle cosmology, rather than on specific realizations or charge assignments which are less significant for our goals.

1.3 Organization of this work

In the first part of this work we perform several generalizations of the model discussed in [33, 37], with the introduction of a kinetic mixing between the hypercharge $U(1)_Y$ and the anomalous $U(1)_B$ symmetry. We analyze the entire formal structure of the model in this general setting, and include in the analysis of the CP-even sector also the real part of the Stückelberg field, the saxion, which had been removed in our previous study, having assumed its effective decoupling from the low energy spectrum. The saxion is indeed heavy, of the order of the Stückelberg mass (M_{St}), which in the scenario that we investigate is assumed to be in the TeV region. Its decay occurs far above the supersymmetry breaking scale M_{susy} , and as such does not pose any problem to the standard cosmological model, in particular to nucleosynthesis. We will study its decay under the worst possible scenario, assuming that it takes place close to the SUSY breaking scale, chosen around 1 TeV. Even within this scenario the cosmological problems are avoided. The interaction of the saxion with the other field of the Lagrangian is non-polynomial, and can be expanded in inverse powers of M_{St} .

At a second stage we turn to a quantification of the relic densities of the model, which involves, beside the saxion, an axion and a neutralino with an axino component. The axion, which is part of the Stückelberg multiplet $\hat{\mathbf{b}}$ (the imaginary part of the scalar component, $\text{Im } b$), acquires a mass via an extra potential (V') which, in our approach, is assumed to originate below the scale of supersymmetry breaking M_{susy} .

In the MLSOM [36], V' appears whenever the Stückelberg field b (which in that case is real) undergoes a mixing with the scalar sector of the model, effectively parameterizing the vacuum misalignment. Similar considerations entail in the supersymmetric case.

These corrections to the standard scalar potential (V) of the NMSSM (Next to Minimal MSSM) will tilt a flat (but physical) direction in field space in the scalar CP-odd sector. This direction in the vacuum manifold defines the gauged axion (χ) whose mass will be directly linked to the size of V' (the strength of the potential, parameterized by the dimensionless constant λ_{eff}). Obviously, under the assumption that these corrections are small, the axion χ will be a light pseudoscalar. They turn out to be proportional to the vevs of the two Higgses (v) and of the extra singlet S of the model beside the strength of the potential, which is $O(\lambda_{eff} v^4)$. As in a previous analysis performed in the context of the MLSOM [30], also in the supersymmetric case the mechanism of vacuum misalignment comes into the game not only at the electroweak scale but also at the QCD phase transition. In fact, the possibility of a sequential

misalignment of the physical axion is clearly justified by the gauge charge of the Stückelberg field $\text{Im } b$. From this field the physical axion χ inherits interactions of the form $\chi F \tilde{F}$ both with the strong and the electroweak sector (due to mixed $U(1) - SU(2)$ and $U(1) - SU(3)$ anomalies). In our case χ feels both the presence of an extra potential V' at the electroweak scale and the analogous one due to the QCD instantons at a later stage.

As we have mentioned, in the scenario that we analyze the breaking of supersymmetry takes place in the TeV region, with a neutralino ($\tilde{\chi}$) that becomes massive around this scale. Its decoupling occurs at a temperature $T_{dc} \sim O(m_{\tilde{\chi}}/20)$, in close analogy with typical studies of relic densities in the MSSM and in its extensions.

The neutralino mass matrix is enlarged due to the presence of an extra component (the axino) in the neutral sector and the spectrum is computed numerically for several values of the fundamental charges. The evaluation of the relic densities of the neutralinos is performed by a complete simulation of the 2-to-2 scattering cross sections of the model, which is characterized by approximately 400 interactions and is computationally rather challenging in the presence of Higgs-axion mixing.

In the absence of this mixing the Stückelberg ($\text{Im } b$) is just a Goldstone mode of a local gauge symmetry and can be gauged away (at all scales) as in [39]. In our model as in the MLSOM, a simple counting of the degrees of freedom shows that this is not the case. This field is an unphysical Goldstone mode only in the Stückelberg phase, i.e. above the electroweak scale. The reappearance of $\text{Im } b$ at the electroweak scale is the result of a simple rearrangements of the degrees of freedom in the CP-odd sector, occurring at this scale, as we will discuss in Sec. 7.

This situation is new compared to the PQ case, where the global nature of the $U(1)$ symmetry leaves the axion as a massless degree of freedom (a Goldstone mode of a global symmetry) that cannot be gauged away and that acquires a small mass only at the quark-hadron transition. This detail is particularly important in regard to the constraints imposed by the isocurvature perturbations on axion models [44], and their interplay with inflation. In our case, these problems are avoided since at the time of inflation $\text{Im } b$ is not a physical field [43].

Coming to the numerical analysis, which is the central part of our work and that motivates our conclusions, this is quite challenging, given the large number of interactions. Several numerical codes have been developed in order to automate the calculation of the relic densities, codes which are of wide use. In particular, micrOMEGAs [45], the code in which we have implemented the Lagrangian, allows to perform these computations in supersymmetric models that include R-parity conservation. This allows to have a stable supersymmetric particle. Besides, the program allows the inclusion of co-annihilations whenever the mass of the next-to-lowest mass neutralino is close to the mass of the lowest eigenstate. We show that the co-annihilation mechanism is crucial in order to satisfy the WMAP constraints on dark matter and forces the Stückelberg mass (the tree-level mass of the anomalous extra Z prime of the model) to lay around the SUSY breaking scale.

Regarding the cross section calculation implemented in the Boltzmann equation, micrOMEGAs relies on CalcHEP [46], a package that allows the calculation of tree-level cross sections and decay rates in any given model. The particle content and vertices of the model have to be specified completely in some input files. In our case the CalcHEP input files have been generated using LanHEP[47] and we have developed

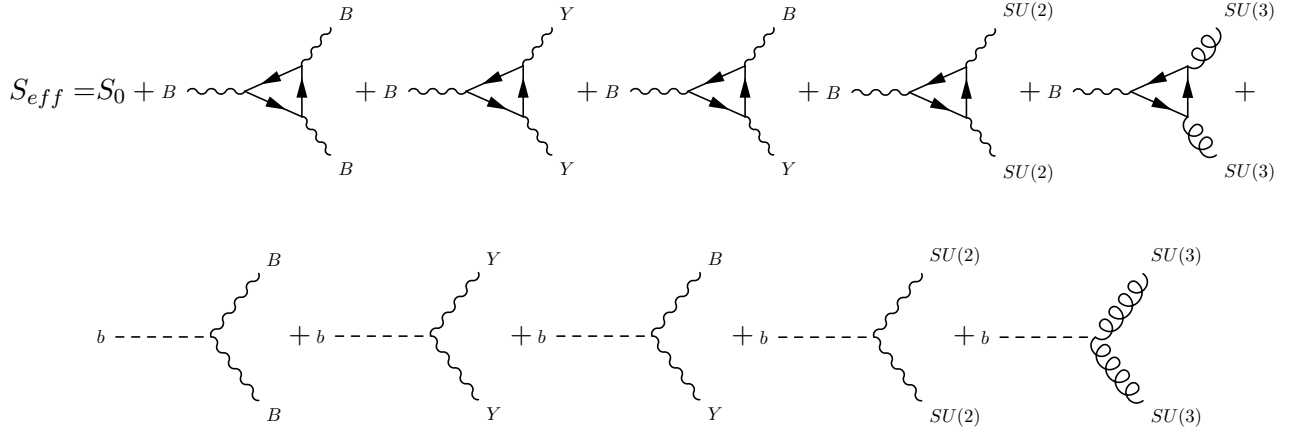


Figure 1: Anomalous contributions to the Lagrangian and WZ counterterms

a translator to interface the results of our symbolic computation of all the (about 400) vertices of the model with LanHEP. This has allowed us to speed up the analysis considerably.

The expressions of most of the vertices are quite lengthy and have not been included in the appendix, except for some basic ones. We have run micrOMEGAs under general conditions, and tried to determine the dependence of the model on the fundamental parameters, such as the Stückelberg mass, M_{St} and the supersymmetric soft breaking terms M_{susy} , which are the most significant ones. The results of these simulations are discussed in detail.

One final comment concerns the treatment of the gauge kinetic mixing in this paper. It is identified by a parameter α ($\sin \alpha$) that we will keep nonzero in some parts of the discussion, especially in the analysis of the spectrum of the model. This has been computed numerically (and completely) for small values of the parameter. We think that the discussion of kinetic mixing in the model is interesting on its own, especially in view of further expansion of our analysis, but we have found that it plays a marginal role in the determination of the relic densities of the axions and neutralinos, and in the dynamics of the saxion, which are all controlled by far more relevant parameters, first among them the Stückelberg mass. Therefore, we have decided to illustrate the modifications induced on the analytical forms of the mass matrices for nonzero α , giving the explicit dependence of the gauge boson masses, Goldstones etc. on this parameter, since these results might be of wider interest, but we have set α to zero in the numerical analysis.

2 General Features of the Model

The gauge structure of the model is of the form $SU(3)_c \times SU(2) \times U(1)_Y \times U(1)_B$, where B is the anomalous gauge boson, and with a matter content given by the usual generations of the Standard Model (SM). In all the Lagrangians below we implicitly sum over the three fermion generations. A list of the fundamental superfields and charge assignments is summarized in Tab. 1. Beside the standard kinetic terms of the USSM-A [33], the Lagrangian is characterized by the presence of a kinetic mixing between

the two $U(1)$'s which will be accounted for separately in \mathcal{L}_{KM} , and by the presence of Fayet-Iliopoulos terms in \mathcal{L}_{FI} allowed by the two abelian gauge symmetries. Explicitly we have

$$\mathcal{L}_{USSM-A} = \mathcal{L}_{USSM} + \mathcal{L}_{KM} + \mathcal{L}_{FI} + \mathcal{L}_{axion} \quad (1)$$

where the Lagrangian of the USSM (\mathcal{L}_{USSM}) has been modified by the addition of \mathcal{L}_{axion} to compensate for the anomalous variation of the corresponding effective action due to the anomalous charge assignments. The former is given by

$$\mathcal{L}_{USSM} = \mathcal{L}_{lep} + \mathcal{L}_{quark} + \mathcal{L}_{Higgs} + \mathcal{L}_{gauge} + \mathcal{L}_{SMT} + \mathcal{L}_{GMT} \quad (2)$$

with contributions from the leptons, quarks and Higgs plus gauge kinetic terms. The matter contributions from leptons and quarks

$$\mathcal{L}_{lep} = \int d^4\theta \left[\hat{L}^\dagger e^{2g_2\hat{W}+g_Y\hat{Y}+g_B\hat{B}} \hat{L} + \hat{R}^\dagger e^{2g_2\hat{W}+g_Y\hat{Y}+g_B\hat{B}} \hat{R} \right] \quad (3)$$

$$\mathcal{L}_{quark} = \int d^4\theta \left[\hat{Q}^\dagger e^{2g_s\hat{G}+2g_2\hat{W}+g_Y\hat{Y}+g_B\hat{B}} \hat{Q} + \hat{U}_R^\dagger e^{2g_s\hat{G}+g_Y\hat{Y}+g_B\hat{B}} \hat{U}_R + \hat{D}_R^\dagger e^{2g_s\hat{G}+g_Y\hat{Y}+g_B\hat{B}} \hat{D}_R \right] \quad (4)$$

are accompanied by a sector which involves two Higgs $SU(2)$ doublet superfields, \hat{H}_1 and \hat{H}_2 , and one singlet \hat{S}

$$\mathcal{L}_{Higgs} = \int d^4\theta \left[\hat{H}_1^\dagger e^{2g_2\hat{W}+g_Y\hat{Y}+g_B\hat{B}} \hat{H}_1 + \hat{H}_2^\dagger e^{2g_2\hat{W}+g_Y\hat{Y}+g_B\hat{B}} \hat{H}_2 + \hat{S}^\dagger e^{g_B\hat{B}} \hat{S} + \mathcal{W}\delta^2(\bar{\theta}) + \bar{\mathcal{W}}\delta^2(\theta) \right] \quad (5)$$

with the superpotential chosen of the form

$$\mathcal{W} = \lambda \hat{S} \hat{H}_1 \cdot \hat{H}_2 + y_e \hat{H}_1 \cdot \hat{L} \hat{R} + y_d \hat{H}_1 \cdot \hat{Q} \hat{D}_R + y_u \hat{H}_2 \cdot \hat{Q} \hat{U}_R. \quad (6)$$

This superpotential, as shown in [33, 37], allows a physical axion in the spectrum. The gauge content plus the soft breaking terms in the form of scalar mass terms (SMT) are identical to those of the USSM

$$\begin{aligned} \mathcal{L}_{gauge} &= \frac{1}{4} \int d^4\theta \left[\mathcal{G}^\alpha \mathcal{G}_\alpha + W^\alpha W_\alpha + W^{Y\alpha} W_\alpha^Y + W^{B\alpha} W_\alpha^B \right] \delta^2(\bar{\theta}) + h.c. \\ \mathcal{L}_{SMT} &= - \int d^4\theta \delta^4(\theta, \bar{\theta}) \left[M_L^2 \hat{L}^\dagger \hat{L} + m_R^2 \hat{R}^\dagger \hat{R} + M_Q^2 \hat{Q}^\dagger \hat{Q} + m_U^2 \hat{U}_R^\dagger \hat{U}_R + m_D^2 \hat{D}_R^\dagger \hat{D}_R \right. \\ &\quad + m_1^2 \hat{H}_1^\dagger \hat{H}_1 + m_2^2 \hat{H}_2^\dagger \hat{H}_2 + m_S^2 \hat{S}^\dagger \hat{S} + (a_\lambda \hat{S} \hat{H}_1 \cdot \hat{H}_2 + h.c.) + (a_e \hat{H}_1 \cdot \hat{L} \hat{R} + h.c.) \\ &\quad \left. + (a_d \hat{H}_1 \cdot \hat{Q} \hat{D}_R + h.c.) + (a_u \hat{H}_2 \cdot \hat{Q} \hat{U}_R + h.c.) \right]. \end{aligned} \quad (7)$$

As usual, $M_L, M_Q, m_R, m_{U_R}, m_{D_R}, m_1, m_2, m_S$ are the mass parameters of the explicit supersymmetry breaking, while a_e, a_λ, a_u, a_d are dimensionful coefficients. The soft breaking due to gaugino mass terms (GMT) now include a mixing mass parameter M_{YB}

$$\begin{aligned} \mathcal{L}_{GMT} &= \int d^4\theta \left[\frac{1}{2} (M_G \mathcal{G}^\alpha \mathcal{G}_\alpha + M_w W^\alpha W_\alpha + M_Y W^{Y\alpha} W_\alpha^Y + M_B W^{B\alpha} W_\alpha^B \right. \\ &\quad \left. + M_{YB} W^{Y\alpha} W_\alpha^B) + h.c. \right] \delta^4(\theta, \bar{\theta}). \end{aligned} \quad (8)$$

Superfields	SU(3)	SU(2)	$U(1)_Y$	$U(1)_B$
$\hat{\mathbf{b}}(x, \theta, \bar{\theta})$	1	1	0	s
$\hat{S}(x, \theta, \bar{\theta})$	1	1	0	B_S
$\hat{L}(x, \theta, \bar{\theta})$	1	2	-1/2	B_L
$\hat{R}(x, \theta, \bar{\theta})$	1	1	1	B_R
$\hat{Q}(x, \theta, \bar{\theta})$	3	2	1/6	B_Q
$\hat{U}_R(x, \theta, \bar{\theta})$	$\bar{3}$	1	-2/3	B_{U_R}
$\hat{D}_R(x, \theta, \bar{\theta})$	$\bar{3}$	1	+1/3	B_{D_R}
$\hat{H}_1(x, \theta, \bar{\theta})$	1	2	-1/2	B_{H_1}
$\hat{H}_2(x, \theta, \bar{\theta})$	1	2	1/2	B_{H_2}

Table 1: Charge assignment of the model

Given the presence of two abelian gauge factors, we include a kinetic mixing term

$$\mathcal{L}_{km} = \frac{\sin \alpha}{2} \int d^2\theta \hat{W}_Y \hat{W}_B + h.c. \quad (9)$$

and the Fayet-Iliopoulos (FI) terms

$$\mathcal{L}_{FI} = \xi_B D_B + \xi_Y D_Y \quad (10)$$

where D_B and D_Y are the auxiliary fields of the two abelian scalar supermultiplets of the model.

The superfield $\hat{\mathbf{b}}$ describes the Stückelberg multiplet,

$$\hat{\mathbf{b}} = b + i\sqrt{2}\theta\psi_{\mathbf{b}} - i\theta\sigma^\mu\bar{\theta}\partial_\mu b + \frac{\sqrt{2}}{2}\theta\theta\bar{\theta}\bar{\sigma}^\mu\partial_\mu\psi_{\mathbf{b}} - \frac{1}{4}\theta\theta\bar{\theta}\bar{\theta}\square b + \theta\theta F_{\mathbf{b}}, \quad (11)$$

and contains the Stückelberg axion (a complex b field) and its supersymmetric partner, referred to as the axino ($\psi_{\mathbf{b}}$), which combines with the neutral gauginos and higgsinos to generate the neutralinos of the model. Details on the notation for the superfields components can be found in Tab. 2. We just recall that we denote with λ_B and λ_Y the two gauginos of the two vector superfields (\hat{B}, \hat{Y}) corresponding to the anomalous $U(1)_B$ and to the hypercharge vector multiplet. The singlet superfield \hat{S} has as components the scalar "singlet" S and its supersymmetric partner, the singlino, denoted as \tilde{S} .

The interactions and dynamics of axion superfield are defined in \mathcal{L}_{axion} , the Lagrangian that contains both the kinetic (Stückelberg) term, responsible for the mass of the anomalous gauge boson (which reaches the electroweak symmetry breaking scale already in a massive state), the kinetic term of the saxion and of the axino, and the Wess-Zumino terms, which are needed for anomaly cancellation. We recall that Stückelberg fields appear both in anomalous and in non-anomalous contexts. In this second have been analyzed recently in [48].

In our case, this Lagrangian is given by

$$\mathcal{L}_{axion/saxion} = \mathcal{L}_{St} + \mathcal{L}_{WZ} \quad (12)$$

Superfield	Bosonic	Fermionic	Auxiliary
$\hat{\mathbf{b}}(x, \theta, \bar{\theta})$	$b(x)$	$\psi_{\mathbf{b}}(x)$	$F_{\mathbf{b}}(x)$
$\hat{S}(x, \theta, \bar{\theta})$	$S(x)$	$\tilde{S}(x)$	$F_S(x)$
$\hat{L}(x, \theta, \bar{\theta})$	$\tilde{L}(x)$	$L(x)$	$F_L(x)$
$\hat{R}(x, \theta, \bar{\theta})$	$\tilde{R}(x)$	$\bar{R}(x)$	$F_R(x)$
$\hat{Q}(x, \theta, \bar{\theta})$	$\tilde{Q}(x)$	$Q(x)$	$F_Q(x)$
$\hat{U}_R(x, \theta, \bar{\theta})$	$\tilde{U}_R(x)$	$\bar{U}_R(x)$	$F_{U_R}(x)$
$\hat{D}_R(x, \theta, \bar{\theta})$	$\tilde{D}_R(x)$	$\bar{D}_R(x)$	$F_{D_R}(x)$
$\hat{H}_1(x, \theta, \bar{\theta})$	$H_1(x)$	$\tilde{H}_1(x)$	$F_{H_1}(x)$
$\hat{H}_2(x, \theta, \bar{\theta})$	$H_2(x)$	$\tilde{H}_2(x)$	$F_{H_2}(x)$
$\hat{B}(x, \theta, \bar{\theta})$	$B_\mu(x)$	$\lambda_B(x)$	$D_B(x)$
$\hat{Y}(x, \theta, \bar{\theta})$	$A_\mu^Y(x)$	$\lambda_Y(x)$	$D_Y(x)$
$\hat{W}^i(x, \theta, \bar{\theta})$	$W_\mu^i(x)$	$\lambda_{W^i}(x)$	$D_{W^i}(x)$
$\hat{G}^a(x, \theta, \bar{\theta})$	$G_\mu^a(x)$	$\lambda_{g^a}(x), \bar{\lambda}_{g^a}(x)$	$D_{G^a}(x)$

Table 2: Superfields and their components.

where \mathcal{L}_{St} is the supersymmetric version of the Stückelberg mass term [49], while \mathcal{L}_{WZ} denotes the WZ counterterms responsible for the axion-like nature of the pseudoscalar b . Specifically

$$\begin{aligned}
\mathcal{L}_{St} &= \frac{1}{4} \int d^4\theta (\hat{\mathbf{b}} + \hat{\mathbf{b}}^\dagger + 2M_{St}\hat{B})^2 \\
\mathcal{L}_{WZ} &= -\frac{1}{2} \int d^4\theta \left\{ \left[\frac{1}{2} \frac{c_G}{M_{St}} \text{Tr}(\mathcal{G}\mathcal{G})\hat{\mathbf{b}} + \frac{1}{2} \frac{c_W}{M_{St}} \text{Tr}(WW)\hat{\mathbf{b}} \right. \right. \\
&\quad \left. \left. + \frac{c_Y}{M_{St}} \hat{\mathbf{b}} W_\alpha^Y W^{Y,\alpha} + \frac{c_B}{M_{St}} \hat{\mathbf{b}} W_\alpha^B W^{B,\alpha} + \frac{c_{YB}}{M_{St}} \hat{\mathbf{b}} W_\alpha^Y W^{B,\alpha} \right] \delta(\bar{\theta}^2) + h.c. \right\},
\end{aligned} \tag{13}$$

where we have denoted with \mathcal{G} the supersymmetric field-strength of $SU(3)_c$, with W the supersymmetric field-strength of $SU(2)$, with W^Y and with W^B the supersymmetric field-strength of $U(1)_Y$ and $U(1)_B$ respectively. The Lagrangian \mathcal{L}_{St} is invariant under the $U(1)_B$ gauge transformations

$$\begin{aligned}
\delta_B \hat{B} &= \hat{\Lambda} + \hat{\Lambda}^\dagger \\
\delta_B \hat{\mathbf{b}} &= -2M_{St}\hat{\Lambda}
\end{aligned} \tag{14}$$

where $\hat{\Lambda}$ is an arbitrary chiral superfield. So the scalar component of $\hat{\mathbf{b}}$, that consists of the saxion and the axion field, shifts under a $U(1)_B$ gauge transformation.

The coefficients $c_I \equiv (c_G, c_W, c_Y, c_B, c_{YB})$ are dimensionless, fixed by the conditions of gauge invariance, and are functions of the free charges B_i of the model (as shown below in Eq. (16))

$$\begin{aligned}
c_B &= -\frac{\mathcal{A}_{BBB}}{384\pi^2} & c_Y &= -\frac{\mathcal{A}_{BY Y}}{128\pi^2} & c_{YB} &= -\frac{\mathcal{A}_{BY B}}{128\pi^2} \\
c_W &= -\frac{\mathcal{A}_{BWW}}{64\pi^2} & c_G &= -\frac{\mathcal{A}_{BGG}}{64\pi^2}.
\end{aligned} \tag{15}$$

The coefficients \mathcal{A} , in turn, are defined by the conditions of gauge invariance of the effective action, related to the anomalies $\{U(1)_B^3\}$, $\{U(1)_B, U(1)_Y^2\}$, $\{U(1)_B^2, U(1)_Y\}$, $\{U(1)_B, SU(2)^2\}$, $\{U(1)_B, SU(3)^2\}$. Below we use the notation \mathcal{A}_{BBB} , \mathcal{A}_{BY^2} and \mathcal{A}_{BBY} , \mathcal{A}_{BWW} and \mathcal{A}_{BGG} to denote them. Using the conditions of gauge invariance these coefficients assume the form

$$\begin{aligned}
\mathcal{A}_{BBB} &= -3B_{H_1}^3 - 3B_{H_1}^2(3B_L + 18B_Q - 7B_S) - 3B_{H_1}(3B_L^2 + (18B_Q - 7B_S)B_S) \\
&\quad + 3B_L^3 + B_S(27B_Q^2 - 27B_S B_Q + 8B_S^2) \\
\mathcal{A}_{BY^2} &= \frac{1}{2}(-3B_L - 9B_Q + 7B_S) \\
\mathcal{A}_{BBY} &= 2B_{H_1}(3B_L + 9B_Q - 5B_S) + (12B_Q - 5B_S)B_S \\
\mathcal{A}_{BWW} &= \frac{1}{2}(3B_L + 9B_Q - B_S) \\
\mathcal{A}_{BGG} &= \frac{3}{2}B_S.
\end{aligned} \tag{16}$$

We have expressed all the anomaly equations in terms of 4 charges, $B_i \equiv (B_{H_1}, B_S, B_Q, B_L)$ ordered from 1 to 4 (left to right). Notice that these charges can be taken as fundamental parameters of the model. Their independent variation allows to scan the entire spectra of these models with no reference to any specific construction. These relations appear in the anomalous variation (δ_B) of the supersymmetric 1-loop effective action of the model, which forces the introduction of supersymmetric PQ-like interactions (WZ terms) for its overall vanishing. Formally we have the relation

$$\delta_B(B_i)\mathcal{S}_{1loop} + \delta_B(c_I(B_i))\mathcal{S}_{WZ} = 0, \tag{17}$$

where the anomalous variation can be parameterized by the 4 charges B_i together with the coefficients $c_J(B_i)$ in front of the WZ counter-terms. In these notations, the uppercase index J runs over all the 5 mixed-anomaly conditions $B^3, BY^2, B^2Y, BW^2, BG^2$, ordered from 1 to 5 (left to right).

It is convenient, at this point, to define our benchmark charge assignments. The function (f) which allows to identify all the charges in terms of the free ones is formally given by

$$f(B_Q, B_L, B_{H_1}, B_S) = (B_Q, B_{U_R}, B_{D_R}, B_L, B_R, B_{H_1}, B_{H_2}, B_S). \tag{18}$$

These depend only upon the four free parameters B_Q , B_L , B_{H_1} and B_S . In our analysis, the charges of Eq. (18) have been assigned as

$$f(2, 1, -1, 1) = (2, -2, -1, 1, 0, -1, 0, 1). \tag{19}$$

The dependence of our results on this choice of this parametric charges is quite small. Instead, as we will see, the relevant parameters of our analysis turn out to be: 1) the anomalous coupling of the gauge boson g_B , which controls the decay rate of the saxion and of the axion and 2) the Stückelberg mass.

3 Axions and Saxions and all orders interactions ($\alpha = 0$)

The contributions of the axions and saxions to the total Lagrangian are derived from the combination of the Stückelberg and Wess-Zumino terms. The complete axion/saxion Lagrangian expressed in terms of

component fields is given by

$$\mathcal{L}_{axion/saxion} \equiv \mathcal{L}_{St} + \mathcal{L}_{WZ} \quad (20)$$

and contains a mixing among the D terms which is rather peculiar, as we are going to show. The off-shell expression of this Lagrangian is given by

$$\begin{aligned} \mathcal{L}_{axion/saxion} = & \frac{1}{2} (\partial_\mu \text{Im } b + M_{St} B_\mu)^2 + \frac{1}{2} \partial_\mu \text{Re } b \partial^\mu \text{Re } b + \frac{i}{2} \psi_{\mathbf{b}} \sigma^\mu \partial_\mu \bar{\psi}_{\mathbf{b}} + \frac{i}{2} \bar{\psi}_{\mathbf{b}} \bar{\sigma}^\mu \partial_\mu \psi_{\mathbf{b}} + \frac{1}{2} F_{\mathbf{b}} F_{\mathbf{b}}^\dagger + \\ & M_{St} \text{Re } b D_B - \frac{M_{St}}{\sqrt{2}} (\psi_{\mathbf{b}} \lambda_B + h.c.) + \frac{1}{8} \frac{c_G}{M_{St}} G_{\mu\nu}^a G^{a\mu\nu} \text{Re } b + \\ & \frac{1}{8} \frac{c_W}{M_{St}} W_{\mu\nu}^i W^{i\mu\nu} \text{Re } b + \frac{1}{2} \frac{c_Y}{M_{St}} F_{\mu\nu}^Y F^{Y\mu\nu} \text{Re } b + \frac{1}{2} \frac{c_B}{M_{St}} F_{\mu\nu}^B F^{B\mu\nu} \text{Re } b + \\ & \frac{1}{2} \frac{c_{YB}}{M_{St}} F_{\mu\nu}^Y F^{B\mu\nu} \text{Re } b - \frac{1}{16} \frac{c_G}{M_{St}} \epsilon^{\mu\nu\rho\sigma} G_{\mu\nu}^a G_{\rho\sigma}^a \text{Im } b - \frac{1}{16} \frac{c_W}{M_{St}} \epsilon^{\mu\nu\rho\sigma} W_{\mu\nu}^i W_{\rho\sigma}^i \text{Im } b - \\ & \frac{1}{4} \frac{c_Y}{M_{St}} \epsilon^{\mu\nu\rho\sigma} F_{\mu\nu}^Y F_{\rho\sigma}^Y \text{Im } b - \frac{1}{4} \frac{c_B}{M_{St}} \epsilon^{\mu\nu\rho\sigma} F_{\mu\nu}^B F_{\rho\sigma}^B \text{Im } b - \frac{1}{4} \frac{c_{YB}}{M_{St}} \epsilon^{\mu\nu\rho\sigma} F_{\mu\nu}^Y F_{\rho\sigma}^B \text{Im } b + \\ & \frac{1}{4} \frac{c_W}{M_{St}} \left[\frac{1}{4} \text{Im } b \lambda_{W^i} \sigma^\mu D_\mu \bar{\lambda}_{W^i} - \frac{i}{4\sqrt{2}} \psi_{\mathbf{b}} \lambda_{W^i} \sigma^\mu \bar{\sigma}^\nu W_{\mu\nu}^i + \right. \\ & \left. \frac{1}{4} F_{\mathbf{b}} \lambda_{W^i} \lambda_{W^i} + \frac{1}{2\sqrt{2}} \psi_{\mathbf{b}} \lambda_{W^i} D^i + h.c. \right] + \frac{1}{4} \frac{c_G}{M_{St}} \left[\frac{1}{4} \text{Im } b \lambda_{g^a} \sigma^\mu D_\mu \bar{\lambda}_{g^a} - \right. \\ & \left. \frac{i}{4\sqrt{2}} \psi_{\mathbf{b}} \lambda_{g^a} \sigma^\mu \bar{\sigma}^\nu G_{\mu\nu}^a + \frac{1}{4} F_{\mathbf{b}} \lambda_{g^a} \lambda_{g^a} + \frac{1}{2\sqrt{2}} \psi_{\mathbf{b}} \lambda_{g^a} D^a + h.c. \right] + \\ & \frac{c_Y}{M_{St}} [\text{Im } b \lambda_Y \sigma^\mu D_\mu \bar{\lambda}_Y - \frac{i}{2\sqrt{2}} \psi_{\mathbf{b}} \lambda_Y \sigma^\mu \bar{\sigma}^\nu F_{\mu\nu}^Y + \frac{1}{2} F_{\mathbf{b}} \lambda_Y \lambda_Y + \frac{1}{\sqrt{2}} \psi_{\mathbf{b}} \lambda_Y D_Y + h.c.] + \\ & \frac{c_B}{M_{St}} [\text{Im } b \lambda_B \sigma^\mu D_\mu \bar{\lambda}_B - \frac{i}{2\sqrt{2}} \psi_{\mathbf{b}} \lambda_B \sigma^\mu \bar{\sigma}^\nu F_{\mu\nu}^B + \frac{1}{2} F_{\mathbf{b}} \lambda_B \lambda_B + \frac{1}{\sqrt{2}} \psi_{\mathbf{b}} \lambda_B D_B + h.c.] + \\ & \frac{c_{YB}}{M_{St}} [(\text{Im } b \lambda_Y \sigma^\mu \partial_\mu \bar{\lambda}_B - i \text{Re } b \lambda_Y \sigma^\mu \partial_\mu \bar{\lambda}_B - \frac{i}{2\sqrt{2}} \lambda_Y \sigma^\mu \bar{\sigma}^\nu F_{\mu\nu}^B \psi_{\mathbf{b}} + \frac{1}{2} F_{\mathbf{b}} \lambda_Y \lambda_B + \frac{1}{\sqrt{2}} \psi_{\mathbf{b}} \lambda_Y D_B - \\ & \text{Re } b D_Y D_B) + (Y \leftrightarrow B) + h.c.]. \end{aligned} \quad (21)$$

where for simplicity we have set the mixing parameter α to zero. In this case, the general expression of the auxiliary field $F_{\mathbf{b}}$, which in general is given by

$$\begin{aligned} F_{\mathbf{b}} = & -\frac{1}{16} \left(\frac{c_G}{M_{St}} \bar{\lambda}_{g^a} \bar{\lambda}_{g^a} + \frac{c_W}{M_{St}} \bar{\lambda}_{W^i} \bar{\lambda}_{W^i} \right) - \frac{1}{2} \left[\frac{c_B}{M_{St}} \bar{\lambda}_{B'} \bar{\lambda}_{B'} \sec^2 \alpha + \right. \\ & \left. 2 \frac{c_{YB}}{M_{St}} \bar{\lambda}_{B'} \sec \alpha (-\bar{\lambda}_{B'} \tan \alpha + \bar{\lambda}_{Y'}) + \frac{c_Y}{M_{St}} (\bar{\lambda}_{B'} \tan \alpha - \bar{\lambda}_{Y'})^2 \right], \end{aligned} \quad (22)$$

simplifies, after the obvious replacements $\sec \alpha \rightarrow 1, \tan \alpha \rightarrow 0$.

One important feature of the supersymmetric model is that b is a complex field with its real and imaginary parts. While $\text{Im } b$ may appear in the CP-odd part of the scalar sector and undergoes mixing with the Higgs sector, its real part, $\text{Re } b$, the saxion (or scalar axion) has a mass exactly equal to the Stückelberg mass, as expected from supersymmetry. We just recall that in the absence of SUSY breaking parameters, the components of the Stückelberg multiplet form, together with the vector multiplet of the anomalous gauge boson, a massive vector multiplet of mass M_{St} . This is composed of the massive anomalous gauge boson, whose mass is given by the Stückelberg term, the massive saxion and a massive Dirac fermion of mass M_{St} . The fermion is obtained by diagonalizing the 2-dimensional mass matrix

constructed in the basis of λ_B - the gaugino from the vector multiplet \hat{B} - and ψ_b , which is the axino of the Stückelberg multiplet. The diagonalization of this matrix trivially gives two Weyl eigenstates of the same mass M_{St} , which can be assembled into a single massive Dirac fermion of the same mass. Notice that in this re-identification of the degrees of freedom contained in $\hat{\mathbf{b}}$ and in the vector multiplet \hat{B} , $\text{Im } b$ takes the role of a Nambu-Goldstone mode and can be gauged away.

The saxion has typical interactions of the form $\text{Re } b F_i F_j$, with the gauge fields which have mixed-anomalies with $U(1)_B$, beside a non-polynomial interaction with the remaining fields of the theory. As we are going to elaborate, this features shows up because of the presence of a term proportional to the product of the two abelian D terms of the model (of $U(1)_Y \times U(1)_B$), which induce a factor $\sim 1/(1 - \sigma \text{Re } b^2/M_{St}^2)$ in the on-shell effective action, with $\sigma = 16c_{YB}^2$ being proportional to the counterterm of the mixed YYB anomaly.

To clarify this point, we recall that the general Lagrangian contains a supersymmetric Wess-Zumino term of the form

$$\mathcal{L}_{WZ,YB} = -\frac{1}{2} \int d^4\theta \left[\frac{c_{YB}}{M_{St}} \hat{\mathbf{b}} W_\alpha^Y W^{B,\alpha} \right] \delta(\bar{\theta}^2) + h.c. \quad (23)$$

which gives, after the expansion in components, a term that mixes the D-terms of $U(1)_Y$ and $U(1)_B$

$$\frac{c_{YB}}{M_{St}} \text{Re } b D_Y D_B. \quad (24)$$

In this case the equations of motion for the auxiliary fields D_Y and D_B are coupled. In the absence of kinetic mixing ($\alpha = 0$) these are given by

$$\begin{aligned} D_{B,OS} &= \frac{1}{12(-1 + 16 \text{Re } b^2 c_{YB}^2/M_{St}^2)} \left[12\xi_B + 6g_B (B_{H_1} H_1^\dagger H_1 + B_{H_2} H_2^\dagger H_2 + B_S S^\dagger S - B_{D_R} \tilde{D}_R^\dagger \tilde{D}_R - \right. \\ &\quad B_{U_R} \tilde{U}_R^\dagger \tilde{U}_R + B_Q \tilde{Q}^\dagger \tilde{Q} - B_R \tilde{R}^\dagger \tilde{R} + B_L \tilde{L}^\dagger \tilde{L}) + 8 \frac{c_{YB}}{M_{St}} g_Y \text{Re } b \left(-3H_1^\dagger H_1 + 3H_2^\dagger H_2 + 2\tilde{D}_R^\dagger \tilde{D}_R - \right. \\ &\quad 4\tilde{U}_R^\dagger \tilde{U}_R + \tilde{Q}^\dagger \tilde{Q} + 6\tilde{R}^\dagger \tilde{R} - 3\tilde{L}^\dagger \tilde{L} \left. \right) + 48 \frac{c_{YB}}{M_{St}} \xi_Y \text{Re } b + 12M_{St} \text{Re } b + 6\sqrt{2} \frac{c_B}{M_{St}} (\lambda_B \psi_{\mathbf{b}} + h.c.) + \\ &\quad 6\sqrt{2} \frac{c_{YB}}{M_{St}} (\lambda_Y \psi_{\mathbf{b}} + h.c.) + 24\sqrt{2} \frac{c_B c_{YB}}{M_{St}^2} \text{Re } b (\lambda_Y \psi_{\mathbf{b}} + h.c.) + 24\sqrt{2} \frac{c_{YB}^2}{M_{St}^2} \text{Re } b (\lambda_B \psi_{\mathbf{b}} + h.c.) \left. \right], \\ D_{Y,OS} &= \frac{1}{12(-1 + 16 \text{Re } b^2 c_{YB}^2/M_{St}^2)} \left[12\xi_Y + 2g_Y \left(-3H_1^\dagger H_1 + 3H_2^\dagger H_2 + 2\tilde{D}_R^\dagger \tilde{D}_R - 4\tilde{U}_R^\dagger \tilde{U}_R + \tilde{Q}^\dagger \tilde{Q} + \right. \right. \\ &\quad 6\tilde{R}^\dagger \tilde{R} - 3\tilde{L}^\dagger \tilde{L} \left. \right) + 24 \frac{c_{YB}}{M_{St}} g_B \text{Re } b \left(B_{H_1} H_1^\dagger H_1 + B_{H_2} H_2^\dagger H_2 + B_S S^\dagger S - B_{D_R} \tilde{D}_R^\dagger \tilde{D}_R - B_{U_R} \tilde{U}_R^\dagger \tilde{U}_R + \right. \\ &\quad B_Q \tilde{Q}^\dagger \tilde{Q} - B_R \tilde{R}^\dagger \tilde{R} + B_L \tilde{L}^\dagger \tilde{L} \left. \right) + 48 \frac{c_{YB}}{M_{St}} \xi_B \text{Re } b + 48c_{YB} \text{Re } b^2 + 6\sqrt{2} \frac{c_Y}{M_{St}} (\lambda_Y \psi_{\mathbf{b}} + h.c.) + \\ &\quad 6\sqrt{2} \frac{c_{YB}}{M_{St}} (\lambda_B \psi_{\mathbf{b}} + h.c.) + 24\sqrt{2} \frac{c_B c_{YB}}{M_{St}^2} \text{Re } b (\lambda_B \psi_{\mathbf{b}} + h.c.) + 24\sqrt{2} \frac{c_{YB}^2}{M_{St}^2} \text{Re } b (\lambda_Y \psi_{\mathbf{b}} + h.c.) \left. \right], \end{aligned} \quad (25)$$

showing that their on-shell expressions are characterized by the appearance of the saxion field in a non-polynomial form. The presence of the Stückelberg mass allows to perform an expansion of these terms to all orders (in $\text{Re } b/M_{St}$) obtaining

$$\frac{1}{(1 - 16c_{YB}^2 \text{Re } b^2/M_{St}^2)^2} = \sum_{n=0}^{\infty} (n+1) (4c_{YB} \text{Re } b/M_{St})^{2n}. \quad (26)$$

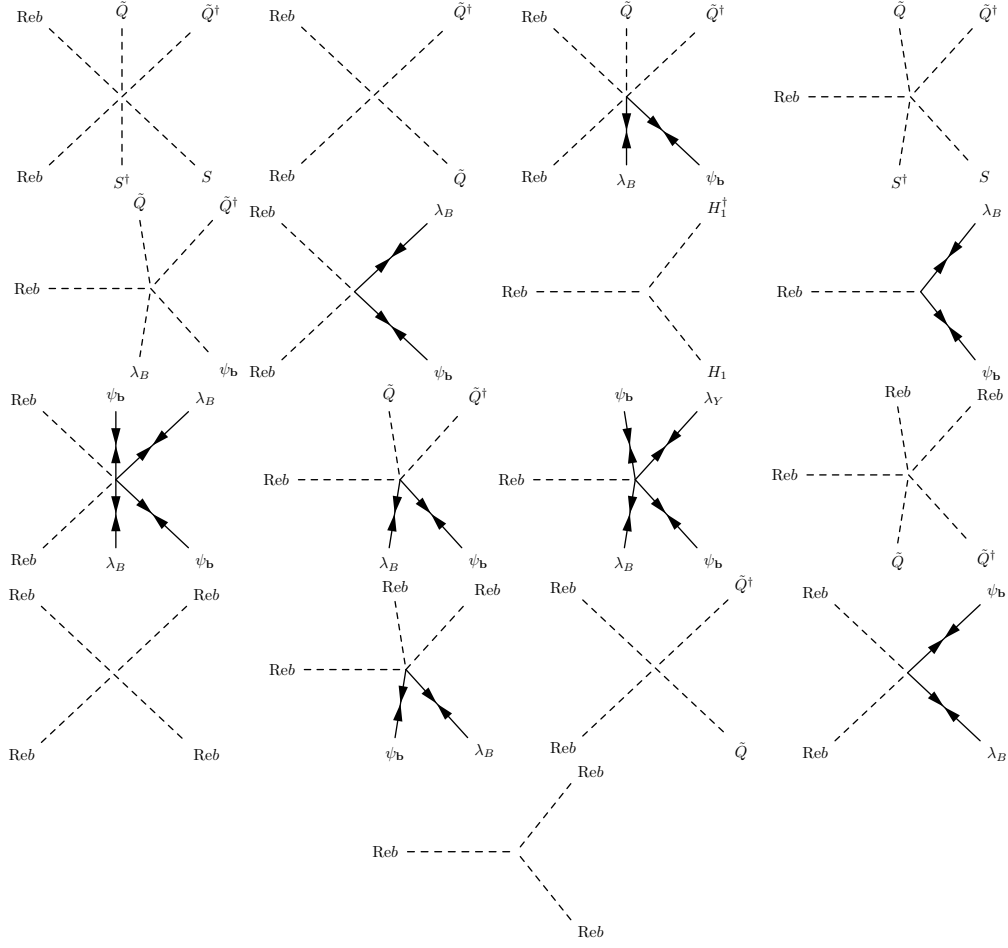


Figure 2: Saxion interactions to lowest order in $1/M_{St}$. An infinite number of additional higher order interactions (in powers of $1/M_{St}$) are generated by the insertion on these vertices of n powers of saxion lines. We use the double line notation for Majorana particles.

Defining \mathcal{L}_{D_Y, D_B} as the Lagrangian parts that collect all the terms containing D_Y and D_B fields, we get

$$\mathcal{L}_{D_B, D_Y} = -\frac{1}{2} \left[D_{B, OS}^2 - 8 \text{Re } b \frac{c_{YB}}{M_{St}} D_{Y, OS} D_{B, OS} + D_{Y, OS}^2 \right] \quad (27)$$

in terms of their on-shell expressions.

The Lagrangian of the saxion is then extracted from the complete expression of \mathcal{L}_{axion} and can be arranged as

$$\mathcal{L}_{saxion} = \frac{1}{2} \partial_\mu \text{Re } b \partial^\mu \text{Re } b - i b_{YB} \text{Re } b \left[\lambda_Y \sigma^\mu \partial_\mu \bar{\lambda}_B + (Y \leftrightarrow B) + h.c. \right] + \tilde{\mathcal{L}}_{D_Y} + \tilde{\mathcal{L}}_{D_B}; \quad (28)$$

where the terms $\tilde{\mathcal{L}}_{D_Y}$ and $\tilde{\mathcal{L}}_{D_B}$ are given by

$$\begin{aligned} \tilde{\mathcal{L}}_{D_Y} &= \mathcal{L}_{D_Y} - \mathcal{L}_{D_Y}(\text{Re } b \rightarrow 0), \\ \tilde{\mathcal{L}}_{D_B} &= \mathcal{L}_{D_B} - \mathcal{L}_{D_B}(\text{Re } b \rightarrow 0). \end{aligned} \quad (29)$$

In this expression we have simply subtracted the terms that do not depend on $\text{Re } b$. The mass term for $\text{Re } b$ is given by

$$\mathcal{L}_{\text{Re } b, \text{mass}} = -\frac{1}{2} \left[M_{St}^2 + 8c_{YB}\xi_Y + 16\frac{c_{YB}^2}{M_{St}^2} (\xi_B^2 + \xi_Y^2) \right] \text{Re } b^2 \quad (30)$$

which coincides with the Stückelberg mass in the absence of Fayet-Iliopoulos terms. We present a list of the vertices to leading order in $1/M_{St}$ in Fig. 2. Additional vertices (not shown) come with n insertions of $\text{Re } b$ and a suppression by higher powers ($2n$) of M_{St} .

A very large Stückelberg mass, in principle, would be sufficient to guarantee that the effect of reheating - caused by the decay of the saxion - takes place well above the temperature of nucleosynthesis (see for instance the discussion in [32]) thereby avoiding the problem of a possible late entropy release at that time. In this case one can essentially neglect the saxion from the low energy spectrum. For moduli of string origin the required mass value (~ 100 TeV), much larger than in our case, is justified by the suppressed gravitational interaction of the modulus with the rest of the matter fields and works as an enhancing factor for its decay. In our case, instead, such a suppression is absent and a fast decay of the saxion is guaranteed already by a Stückelberg mass around the TeV scale. We will see in the next sections that M_{St} can't be pushed too far above the TeV scale, since the neutralino is overproduced when this scale gets too large, and its relic densities are such to overclose the universe. A detailed analysis of the saxion decay is given in Sec. 6.

4 The scalar potential and the saxion

As we have mentioned, in this model there are three scalar fields which take a vev, H_1, H_2 and S , the scalar components of the \hat{S} scalar superfield. The scalar potential is composed by contributions coming from the D-terms, F-terms and scalar mass term

$$\begin{aligned} V &= V_D + V_F + V_{SMT} \\ V_D &= -\frac{1}{2} \left[\bar{D}_{B,OS}^2 - 8 \text{Re } b \frac{c_{YB}}{M_{St}} \bar{D}_{Y,OS} \bar{D}_{B,OS} + \bar{D}_{Y,OS}^2 \right] + \frac{g_2^2}{8} (|H_1|^2 + |H_2|^2)^2 + \frac{g_2^2}{2} |H_1^\dagger H_2|^2 \\ V_F &= |\lambda H_1 \cdot H_2|^2 + |\lambda S|^2 (|H_1|^2 + |H_2|^2) \\ V_{SMT} &= m_1^2 |H_1|^2 + m_2^2 |H_2|^2 + m_S^2 |S|^2 + (a_\lambda S H_1 \cdot H_2 + h.c.) \end{aligned} \quad (31)$$

where we have defined

$$\begin{aligned} \bar{D}_{B,OS} &= \frac{1}{12(-1 + 16 \text{Re } b^2 c_{YB}^2 / M_{St}^2)} \left[12\xi_B + 6g_B (B_{H_1} |H_1|^2 + B_{H_2} |H_2|^2 + B_S |S|^2) \right. \\ &\quad \left. - 24 \frac{c_{YB}}{M_{St}} g_Y \text{Re } b (|H_1|^2 - |H_2|^2) + 48 \frac{c_{YB}}{M_{St}} \xi_Y \text{Re } b + 12 M_{St} \text{Re } b \right], \\ \bar{D}_{Y,OS} &= \frac{1}{12(-1 + 16 \text{Re } b^2 c_{YB}^2 / M_{St}^2)} \left[12\xi_Y - 6g_Y (|H_1|^2 - |H_2|^2) + \right. \\ &\quad \left. 24 \frac{c_{YB}}{M_{St}} g_B \text{Re } b (B_{H_1} |H_1|^2 + B_{H_2} |H_2|^2 + B_S |S|^2) + 48 \frac{c_{YB}}{M_{St}} \xi_B \text{Re } b + 48 c_{YB} \text{Re } b^2 \right]. \end{aligned} \quad (32)$$

These are obtained from the Higgs and scalar singlet part of the on-shell expressions of the auxiliary fields D_Y and D_B , given in Eq. (25).

We introduce the following basis

$$H_1 = \frac{1}{\sqrt{2}} \begin{pmatrix} \text{Re}H_1^0 + i \text{Im}H_1^0 \\ \text{Re}H_1^- + i \text{Im}H_1^- \end{pmatrix} \quad H_2 = \frac{1}{\sqrt{2}} \begin{pmatrix} \text{Re}H_2^+ + i \text{Im}H_2^+ \\ \text{Re}H_2^0 + i \text{Im}H_2^0 \end{pmatrix} \quad S = \frac{1}{\sqrt{2}}(\text{Re}S + i \text{Im}S).$$

In correspondence of the minimum value of the potential we use the following parametrization for the Higgs fields and for the singlet

$$\langle H_1 \rangle = \frac{1}{\sqrt{2}} \begin{pmatrix} v_1 \\ 0 \end{pmatrix} \quad \langle H_2 \rangle = \frac{1}{\sqrt{2}} \begin{pmatrix} 0 \\ v_2 \end{pmatrix} \quad \langle S \rangle = \frac{v_S}{\sqrt{2}}. \quad (33)$$

It is straightforward to figure out that the superfield $\hat{\mathbf{b}}$ has no soft-breaking scalar mass term that can be added, and that the only tree-level mass acquired by $\text{Re}b$ comes from the kinetic Stückelberg Lagrangian. Notice also that the potential is flat in the direction of the saxion, in the absence of electroweak symmetry breaking ($v_1 = v_2 = 0$) and for a vanishing v_S . This can be easily inferred from the derivative of the potential with respect to $\text{Re}b$ which gives

$$\frac{\partial V}{\partial \text{Re}b} = \frac{1}{4} [g_B (B_{H_1} v_1^2 + B_{H_2} v_2^2 + B_S v_S^2) + 4\xi_B] \left[M_{St} + \frac{c_{YB}}{M_{St}} (g_Y (v_2^2 - v_1^2) + 4\xi_Y) \right], \quad (34)$$

that vanishes in the absence of FI terms and in the “exact phase”, i.e. before electroweak symmetry breaking and with $v_S = 0$. This implies that the mass matrix of the CP-even sector contains an eigenvalue, M_{St} , the saxion mass, which takes corrections proportional to the vevs of the model in the broken phase. Therefore, in general, the diagonalization of this sector involves a 4-by-4 matrix which in the exact phase is characterized by M_{St} and by three additional zero eigenvalues, while after the breaking has four positive eigenvalues, corresponding to the 4 physical states available in this sector (see Sec. B). However, as we are going to show, the saxion can be decoupled from the rest of the model since it decays pretty fast and has essentially turned into radiation at the onset of the electroweak era. We will come to discuss these points in more detail in the following. This result convalidates an assumption on the decoupling of the saxion, which has been at the basis of a previous analysis [37].

It is also obvious that the model, in general, contains runaway solutions for the saxion, since the stability condition, obtained by setting Eq. (34) to zero, can be violated, except for a suitable choice of the FI terms ($\xi_Y = 0, \xi_B \sim -M_{St}^2$). A second solution, corresponding to ($\xi_Y = 0, \xi_B = 0$) is, in principle, also possible. This however, would require a Stückelberg mass which has to be of electroweak origin ($M_{St} \sim v^2$) in order set to zero the second factor of (34). Such small values of the Stückelberg mass are in general considered excluded, since they would imply the existence of an extra Z' which would acquire a tree-level mass of the same order, which is clearly ruled out by current exclusion limits [50]. Therefore, this unlikely scenario will not be investigated any further in our analysis and we will select a range for M_{St} above 1 TeV in the following discussions. While the issue of moduli stabilization is a crucial feature of string theory that can be cured by the introduction of external fluxes in the compactification scheme, in our simplified case is less important, since the saxion, as we are going to show, decays extremely fast and contributes to radiation far before the TeV region. In this respect, we can still allow vanishing values of the FI terms, for simplicity, and focus on the most interesting features of these types of models and

the implications for the axion, which are all connected to the properties of the vacuum below the scale of SUSY breaking and at the electroweak and QCD phase transitions.

We finally recall that the three scalar sectors of the model are characterized in terms of

- **A Charged Higgs sector**

This sector involves the states $(\text{Re}H_2^1, \text{Re}H_1^2)$. It is not affected by the kinetic mixing and the analysis of the mass matrix in this sector proceeds exactly as in our previous work. We have one zero eigenvalue corresponding to a charged Goldstone boson and a mass eigenvalue corresponding to the charged Higgs

$$m_{H^\pm}^2 = \left(\frac{v_1}{v_2} + \frac{v_2}{v_1} \right) \left(\frac{1}{4}g^2 v_1 v_2 - \frac{1}{2}\lambda^2 v_1 v_2 + a_\lambda \frac{v_S}{\sqrt{2}} \right); \quad (35)$$

where $g^2 = g_2^2 + g_Y^2$.

- **A CP-even sector**

This sector is diagonalized starting from the basis $(\text{Re}H_1^1, \text{Re}H_2^2, \text{Re}S)$ with the saxion $\text{Re}b$ being already diagonal. The three physical states obtained in this sector are denoted, as H_0^1, H_0^2 and H_0^3 . Together with the charged physical state extracted before, H^\pm , they describe the 5 degrees of freedom of the CP-even sector.

- **A CP-odd sector**

This sector is diagonalized starting from the basis $(\text{Im}H_1^1, \text{Im}H_2^2, \text{Im}S, \text{Im}b)$. We obtain two physical states, H_0^4 and H_0^5 , and two Goldstone modes that provide the longitudinal degrees of freedom for the neutral gauge bosons, Z and Z' .

5 Diagonalizing the $U(1)_Y \times U(1)_B$ Kinetic Mixing

One of the features of models containing several extra $U(1)$'s is the possibility of having a kinetic mixing between the two abelian symmetries, feature which has never been addressed before in models of this type. For this reason in this section we are going to pause and proceed with a study of this mixing, giving a characterization of the spectrum of the model in this extended case.

In order to discuss the structure of the spectrum of the theory when we allow a kinetic mixing between two $U(1)$'s, we need to perform a first rotation in order to remove the mixing and then proceed with the diagonalization of the mass matrix of the neutral sector. This allows the identification of the mass eigenstates. For the identification of the Goldstone modes of the Z and Z' gauge bosons, instead, as discussed in [36], in models combining both the Higgs and the Stückelberg mechanisms, the best way is to collect the bilinear terms involving the massive neutral gauge bosons and one derivative coupling (i.e. those terms of the form $M_Z Z \partial G_Z, M_Z Z \partial G_{Z'}$). The expressions of G_Z and $G_{Z'}$ are obtained only after collecting all these contributions.

This unusual feature of the Stückelberg mechanism, respect to the Standard Model, owes its origin to the fact that the scalar potential is not sufficient to provide complete information on the massless excitation of the theory in the broken electroweak phase. In fact, an extra contribution to the Goldstones,

not present in the linear expansion around the electroweak vacuum, comes from the term $B^\mu \partial_\mu \text{Im} b$, which has to be taken into account. The procedure of diagonalization of the mixing is illustrated best using a simple model. This shares many similarities with the general theory that we are going to discuss next.

As an example we consider an anomalous theory with a gauge structure $U(1)_A \times U(1)_B$ and defined by the following Lagrangian

$$\begin{aligned} \mathcal{L}_0 = & |(\partial_\mu + ig_B q_B B_\mu) \phi|^2 - \frac{1}{4} F_A^2 - \frac{1}{4} F_B^2 + \frac{\sin \alpha}{2} F_A F_B + \frac{1}{2} (\partial_\mu a + M_1 B_\mu)^2 - \lambda \left(|\phi|^2 - \frac{v^2}{2} \right)^2 \\ & + \bar{\psi} i \gamma^\mu (\partial_\mu + ie A_\mu + ig_B \gamma^5 B_\mu) \psi - \lambda_1 \bar{\psi}_L \phi \psi_R - \lambda_1 \bar{\psi}_R \phi^* \psi_L. \end{aligned} \quad (36)$$

In this theory the B gauge boson is anomalous, due to the appearance of a single chiral fermion. We have also introduced a Higgs field (ϕ) plus the Stückelberg mass term for the B field, and an axion a , which is the (real) Stückelberg field. α is the mixing parameter in the term $\sin \alpha F_A F_B$, proportional to the product of the two abelian field strengths F_A and F_B .

The B gauge field acquires its mass by a combination of the Higgs (1st term) and Stückelberg (5th term) mechanisms. The A gauge boson remains massless after the spontaneous breaking of the $U(1)_B$ symmetry. We choose a specific redefinition of the two gauge fields that maintains one of the two new gauge fields massless (A'_μ) while removing the mixing term. This is given by

$$\begin{pmatrix} F_{A'} \\ F_{B'} \end{pmatrix} = \begin{pmatrix} 1 & -\tan \alpha \\ 0 & 1/\cos \alpha \end{pmatrix} \begin{pmatrix} F_A \\ F_B \end{pmatrix} \quad (37)$$

which implies the gauge fields redefinition

$$A'_\mu = A_\mu - \tan \alpha B_\mu, \quad B'_\mu = B_\mu / \cos \alpha. \quad (38)$$

With this choice the covariant derivative can be written as

$$\begin{aligned} D_\mu = & \partial_\mu + ie A_\mu + ig_B q_B B_\mu \\ = & \partial_\mu + ie A'_\mu + (-ie \tan \alpha + i \frac{g_B q_B}{\cos \alpha}) B'_\mu \\ = & \partial_\mu + ie A'_\mu + ig'_B q'_B B'_\mu \end{aligned} \quad (39)$$

where $g'_B = g_B / \cos \alpha$ and $q'_B = q_B - e/g'_B \tan \alpha$.

Writing the Lagrangian in terms of the redefined fields, we observe that if we consider small values of α , the gauge sectors are diagonal (see for instance [51])

$$\begin{aligned} \mathcal{L}_0 = & |(\partial_\mu + ig'_B q'_B B'_\mu) \phi|^2 - \frac{1}{4} F_{A'}^2 - \frac{1}{4} F_{B'}^2 + \frac{1}{2} (\partial_\mu a + M_1 B'_\mu)^2 - \lambda \left(|\phi|^2 - \frac{v^2}{2} \right)^2 \\ & + \bar{\psi} i \gamma^\mu [\partial_\mu + ie A'_\mu + i(e\alpha + g'_B \gamma^5) B'_\mu] \psi - \lambda_1 \bar{\psi}_L \phi \psi_R - \lambda_1 \bar{\psi}_R \phi^* \psi_L. \end{aligned} \quad (40)$$

There are some conclusions that we can draw from this simple example. We can clearly remove the abelian mixing and identify A'_μ with a physical photon. The interaction of the rotated field with the fermion is left invariant, since the old vector current $J_\mu = -e \bar{\psi} \gamma_\mu \psi$ is not modified, while B'_μ acquires a small vector coupling through the interaction with αJ_μ . At the same time the charges of the vector and axial vector currents ($J_{\mu 5} = -g'_B \bar{\psi} \gamma_\mu \gamma^5 \psi$) of the B gauge boson carry a dependence on the mixing parameter α . Finally, the form of the Stückelberg mass term (4th term in Eq. 40) remains invariant.

5.1 Massive gauge bosons and kinetic mixing

Moving to discuss the mixing in the complete supersymmetric model, the masses of the neutral gauge bosons are affected by the kinetic mixing. Also in this case we follow closely the approach presented in the simple model above. They are identified from the quadratic terms in the expansion of the Higgs derivatives and by the Stückelberg mass term contained in the bosonic part of \mathcal{L}_{St} . We have a rotation matrix O^A

$$\begin{pmatrix} A^\gamma \\ Z \\ Z' \end{pmatrix} = O^A \begin{pmatrix} W^3 \\ A'^Y \\ B' \end{pmatrix}, \quad (41)$$

which rotates from the basis (W^3, A', B') , in which the kinetic mixing has been eliminated, to the physical mass eigenstates (Z, Z', A^γ) , where A^γ denotes the photon.

The Lagrangian of the gauge sector is given by

$$\mathcal{L}_{gauge} = \frac{1}{4} \int d^2\theta \{W_Y W_Y + W_B W_B + 2 \sin \alpha W_Y W_B\} + h.c. \quad (42)$$

The kinetic mixing terms written in component fields is given by

$$\mathcal{L}_{km} = -i \sin \alpha (\bar{\lambda}^Y \bar{\sigma}^\mu \partial_\mu \lambda^B + \bar{\lambda}^B \bar{\sigma}^\mu \partial_\mu \lambda^Y) - \frac{\sin \alpha}{2} F^{Y\mu\nu} F_{\mu\nu}^B + \sin \alpha D^Y D^B. \quad (43)$$

This mixing is resolved using the same transformation as in Eq. (37), that is

$$\begin{pmatrix} W_{Y'} \\ W_{B'} \end{pmatrix} = \begin{pmatrix} 1 & -\tan \alpha \\ 0 & 1/\cos \alpha \end{pmatrix} \begin{pmatrix} W_Y \\ W_B \end{pmatrix}. \quad (44)$$

Notice that the mixing will involve also the D-terms of the abelian vector multiplet. The expression of the mass matrix of the gauge bosons after the rotation is given in an appendix, here we quote the result. The matrix has a null eigenvalue, corresponding to the photon, with the remaining two eigenvalues given by

$$\begin{aligned} M_{Z,Z'}^2 &= \frac{1}{8} (A \mp \sqrt{A^2 - B}) \\ A &= \sec^2 \alpha (4M_{st}^2 + N_{BB}) + g^2 v^2 + g_Y \tan \alpha (g_Y v^2 \tan \alpha + 2x_B \sec \alpha) \\ B &= 4g^2 \sec^2 \alpha [(4M_{st}^2 + N_{BB}) v^2 - x_B^2], \end{aligned} \quad (45)$$

where we have defined

$$\begin{aligned} N_{BB} &= g_B^2 (B_{H_1}^2 v_1^2 + B_{H_2}^2 v_2^2 + B_S^2 v_S^2), \\ x_B &= g_B (B_{H_1} v_1^2 - B_{H_2} v_2^2), \\ v^2 &= v_1^2 + v_2^2. \end{aligned} \quad (46)$$

Expanding up to second order in $1/M_{St}$ and first order in α we get

$$\begin{aligned} m_Z^2 &= \frac{1}{4} g^2 v^2 - \frac{g^2 x_B^2}{8M_{St}^2} - \alpha \frac{g^2 g_Y v^2 x_B}{4M_{St}^2}, \\ m_{Z'}^2 &= \frac{M_{St}^2}{2} + \frac{1}{4} N_{BB} + \frac{g^2 x_B^2}{8M_{St}} + \alpha \left(\frac{g_Y x_B}{2} + \frac{g^2 g_Y v^2 x_B}{4M_{St}^2} \right), \end{aligned} \quad (47)$$

showing the decoupling of Z' as M_{St} gets large.

The identification of the Goldstones in the case of gauge kinetic mixing, as we have mentioned, is obtained from the bilinear Lagrangian with derivative couplings (DC)

$$\mathcal{L}_{DC} = M_Z Z_\mu \partial^\mu G_Z + M_{Z'} Z'_\mu \partial^\mu G_{Z'}. \quad (48)$$

These expressions turn out to be identical to those given in [37]

$$\begin{aligned} M_Z G_Z = & -A \left[\frac{v_1}{2x_B} \left(f_1 + \sqrt{f_1^2 + 4g^2 x_B^2} \right) - v_1 g_B B_{H_1} \right] \text{Im } H_1^0 \\ & + A \left[\frac{v_2}{2x_B} \left(f_1 + \sqrt{f_1^2 + 4g^2 x_B^2} \right) + v_2 g_B B_{H_2} \right] \text{Im } H_2^0 \\ & + B_S g_B v_S A \text{Im } S + 2M_{st} A \text{Im } b \end{aligned} \quad (49)$$

$$\begin{aligned} M_{Z'} G_{Z'} = & A' \left[\frac{v_1}{2x_B} \left(\sqrt{f_1^2 + 4g^2 x_B^2} - f_1 \right) + v_1 g_B B_{H_1} \right] \text{Im } H_1^0 \\ & - A' \left[\frac{v_2}{2x_B} \left(\sqrt{f_1^2 + 4g^2 x_B^2} - f_1 \right) - v_2 g_B B_{H_2} \right] \text{Im } H_2^0 \\ & + B_S g_B v_S A' \text{Im } S + 2M_{st} A' \text{Im } b \end{aligned} \quad (50)$$

where

$$A = \sqrt{\frac{1}{8} - \frac{f_1}{8\sqrt{f_1^2 + 4g^2 x_B^2}}}, \quad A' = \sqrt{\frac{1}{8} + \frac{f_1}{8\sqrt{f_1^2 + 4g^2 x_B^2}}}, \quad f_1 = 4M_{St}^2 - g^2 v^2 + N_{BB}, \quad (51)$$

but now with the replacements

$$g_B \rightarrow g_B \sec \alpha \quad g_Y \rightarrow g_Y \tan \alpha. \quad (52)$$

G_Z and $G_{Z'}$ are orthonormal. It is then clear that the CP-odd sector is spanned by the triple $(\text{Im} S, \text{Im} H_1^0, \text{Im} H_2^0)$ together with $\text{Im } b$, even though the scalar potential does not provide any information on $\text{Im } b$, since this does not show up as a variable in its expression. As we have already mentioned, the small effect due to a nonzero α can be essentially absorbed by a suitable variation of the Stückelberg mass, as one can easily figure out from 47. A numerical analysis indeed shows that the spectrum is quite insensitive to small variations of this parameter. For this reason, in the following sections, we have set α to zero. We have left to an appendix, for completeness, the full expressions of the several terms of the Lagrangians (mass matrices, potential, ecc.) where it appears.

6 Saxion decay modes

Having summarized the basic structure of the model, we now turn to describe the leading contributions to the 2-body decays of the saxion (into squarks, sleptons and gauginos) which are provided by the D-terms. Since the mass of the saxion coincides with the Stückelberg mass M_{St} , which will be constrained to lay

below the 2 TeV region, we will consider a range of variation of M_{St} in our analysis that will respect this bound. It is then crucial to show that the total decay rate of the saxion is sufficiently large so not to interfere with the nucleosynthesis at later times.

We will compute its decay rate by considering the worst possible scenario, i.e. by assuming that this decay occurs around the SUSY breaking scale, or temperature T around 1 TeV. At this temperature, the decays of the saxion are parameterized by the typical SUSY breaking scales such as M_b and M_Y , both of $O(M_{susy})$. The model is in a symmetric electroweak phase ($M_{susy} > v$), which justifies the use of the interaction eigenstates (rather than the mass eigenstates) for the description of the final decay products.

The relevant interactions are described by the Lagrangian

$$\begin{aligned} \mathcal{L}_{int. \text{ saxion}} = & \text{Re } b \left[-\frac{1}{2} g_B M_{St} B_{H_1} H_1^\dagger H_1 - \frac{1}{2} g_B M_{St} B_{H_2} H_2^\dagger H_2 - \frac{1}{2} g_B M_{St} B_S S^\dagger S \right. \\ & - \frac{1}{2} g_B M_{St} B_Q \sum_{j=1}^3 \tilde{Q}_j^\dagger \tilde{Q}_j + \frac{1}{2} g_B M_{St} B_{D_R} \sum_{j=1}^3 \tilde{D}_{R,j}^\dagger \tilde{D}_{R,j} + \frac{1}{2} g_B M_{St} B_{U_R} \sum_{j=1}^3 \tilde{U}_{R,j}^\dagger \tilde{U}_{R,j} \\ & - \frac{1}{2} g_B M_{St} B_L \sum_{l=e,\mu,\tau} \tilde{L}_l^\dagger \tilde{L}_l + \frac{1}{2} g_B M_{St} B_R \sum_{l=e,\mu,\tau} \tilde{R}_l^\dagger \tilde{R}_l \\ & \left. - \frac{c_B}{\sqrt{2}} (\lambda_B \psi_{\mathbf{b}} + \bar{\lambda}_B \bar{\psi}_{\mathbf{b}}) - \frac{c_{YB}}{\sqrt{2}} (\psi_{\mathbf{b}} \lambda_Y + \bar{\psi}_{\mathbf{b}} \bar{\lambda}_Y) \right]. \end{aligned} \quad (53)$$

Here, the left-handed doublets of the squarks and the sleptons are defined as \tilde{Q}_j and \tilde{L}_l respectively, while the right-handed singlets are $\tilde{U}_{R,j}$, $\tilde{D}_{R,j}$ and \tilde{R}_l , with j, l labeling the fermion families. The leading tree level decay modes are the ones included in $\mathcal{L}_{int. \text{ saxion}}$. They involve CP-even and CP-odd massless scalars, the extra singlet scalar S , the squarks, the sleptons and the gauginos $\psi_{\mathbf{b}}$, λ_Y . We compute the total decay rate into fermions, squarks and sleptons, and Higgs scalars. Specifically we have

• Decays into fermions

Assuming that $M_{\mathbf{b}} \approx M_Y$ are slightly less than 1 TeV, the decay rates of the saxion into one gaugino and one axino are

$$\begin{aligned} \Gamma(\text{Re } b \rightarrow \bar{\lambda}_B \psi_{\mathbf{b}}) &= c_B^2 \frac{M_{\text{Re } b}}{32\pi} \left(1 - 4 \frac{M_{\mathbf{b}}^2}{M_{\text{Re } b}^2} \right)^{3/2}, \\ \Gamma(\text{Re } b \rightarrow \bar{\lambda}_Y \psi_{\mathbf{b}}) &= c_{YB}^2 \frac{M_{\text{Re } b}}{32\pi} \left(1 - 4 \frac{M_Y^2}{M_{\text{Re } b}^2} \right)^{3/2}, \end{aligned} \quad (54)$$

with the expressions of the coefficients c_B and c_{YB} determining the couplings given explicitly in Eq. (15).

• Decays into Squarks and Sleptons

In this channel we consider, for simplicity, the decay only into squarks and sleptons of the same type. Even in this case we are assuming that the masses of the squarks and of the sleptons are all equal and slightly below 1 TeV. The decay rate into the i -type sfermion is given by

$$\Gamma(\text{Re } b \rightarrow \tilde{f}_i^\dagger \tilde{f}_i) = \frac{g_i^2 \lambda^{1/2}}{16\pi M_{\text{Re } b}^3} \quad (55)$$

where the kinematic function λ is, in general, defined as $\lambda = \left(M_i^2 + M_j^2 - M_{\text{Re}b}^2\right)^2 - 4M_i^2 M_j^2$ (here with $M_i = M_j$), and the couplings g_i , in the various cases, are defined as

$$g_i = \begin{cases} N_c c_{U_R} & \text{R-handed singlet u-type squark,} \\ N_c c_{D_R} & \text{R-handed singlet quark d-type squark,} \\ N_c c_{Q_L} & \text{L-handed doublet squark,} \\ c_R & \text{R-handed singlet slepton } \tilde{e}, \tilde{\mu}, \tilde{\tau}, \\ c_L & \text{L-handed doublet slepton.} \end{cases} \quad (56)$$

Here $N_c = 3$ is the color factor and the various couplings are given as

$$\begin{aligned} c_{D_R} &= \frac{1}{2} g_B M_{St} B_{D_R}, & c_{U_R} &= \frac{1}{2} g_B M_{St} B_{U_R}, & c_{Q_L} &= -\frac{1}{2} g_B M_{St} B_Q, \\ c_L &= -\frac{1}{2} g_B M_{St} B_L, & c_R &= \frac{1}{2} g_B M_{St} B_R. \end{aligned} \quad (57)$$

• Decays into massless scalars

The decay rate into particles of the Higgs sector that we denote generically with $h_i = \text{Re}H_1, \text{Im}H_1, \dots$ is given by

$$\Gamma(\text{Re}b \rightarrow h_i h_i) = \frac{s_i^2}{32\pi M_{\text{Re}b}} \left(1 - 4 \frac{M_{s_i}^2}{M_{\text{Re}b}^2}\right)^{1/2}, \quad (58)$$

where the couplings s_i are defined as

$$s_i = \begin{cases} c_{H_1} & H_1 \text{ Higgs doublet} \\ c_{H_2} & H_2 \text{ Higgs doublet} \\ c_S & S \text{ Higgs singlet} \end{cases} \quad (59)$$

and the coefficients c_{H_1}, c_{H_2}, c_S are

$$c_{H_1} = -\frac{1}{4} g_B M_{St} B_{H_1}, \quad c_{H_2} = -\frac{1}{4} g_B M_{St} B_{H_2}, \quad c_S = -\frac{1}{4} g_B M_{St} B_S. \quad (60)$$

The total decay rate is obtained by summing over all the decay modes

$$\Gamma_{\text{tot}} = \Gamma(\text{Re}b \rightarrow \bar{\lambda}'_b \psi_{\mathbf{b}}) + \Gamma(\text{Re}b \rightarrow \bar{\lambda}_Y \psi_{\mathbf{b}}) + \sum_i \Gamma(\text{Re}b \rightarrow \tilde{f}_i \tilde{f}_i) + \sum_i \Gamma(\text{Re}b \rightarrow h_i h_i). \quad (61)$$

All the decay rates depend upon the value of the extra $U_B(1)$ coupling g_B , the Stückelberg mass M_{St} and the SUSY breaking scale M_{susy} .

The total decay rate and the lifetime of the saxion are shown in Fig. (3), with the saxion mass $M_{\text{Re}b}$ given by the Stückelberg scale ($M_{\text{Re}b} = M_{St}$) around 1.4 TeV, and with all the squarks and the sleptons in the final state taken of a mass of 700 GeV. All the particles of the Higgs sector are considered to be massless. For $g_B = 0.01$ we obtain a saxion whose decay rate is around 60 MeV if its mass is 1.7 TeV, and which decays rather quickly, since its lifetime is about 10^{-23} seconds. The lifetime decreases

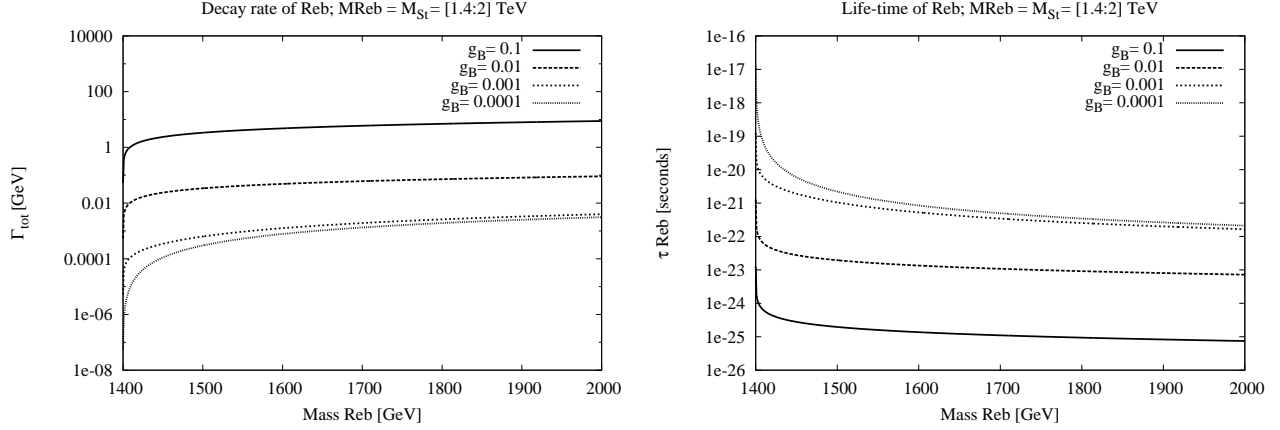


Figure 3: Total decay rate and lifetime of the saxion for different values of g_B as a function of the Stückelberg mass.

quite significantly as we increase the gauge coupling of the anomalous gauge symmetry. For instance, for $g_B = 0.1$ it decreases to $\sim 10^{-24}$ sec, since the phase space for the decay is considerably enhanced.

We conclude that the saxion decays sufficiently fast and does not generate any late entropy release at the time of nucleosynthesis. Therefore, in the analysis of the evolution of the contributions to the total energy density (ρ) of the universe, either due to matter (ρ_m) or to radiation (ρ_R), at temperatures $T \leq 2$ TeV, the contribution coming from the saxion is entirely accounted for by ρ_R .

At this point, having cleared the way of any possible obstruction due to the presence of moduli at the low energy stage ($T \leq 2$ TeV) of the evolution of our model, we are ready to discuss the relevant features of the Stückelberg field. In particular, we will discuss the appearance of a physical axion, the physical component of the Stückelberg, at the electroweak scale. This is extracted from the CP-odd sector and generated by the mechanism of vacuum misalignment taking place at the same scale. In particular, the discussion serves to illustrate how a flat - but physical - direction might be singled out from the vacuum manifold, acquiring a small curvature at the electroweak phase transition.

7 The flat direction of the physical axion from Higgs-axion mixing

In [33],[37] we have presented in some detail an approximate procedure in order to identify in the CP-odd sector one state that inherits axion-like interactions. The approach did not require the explicit expressions of the curvature terms in the CP-odd part of the supersymmetric potential, which are instead needed in the discussion of the angle of misalignment. Here we are going to extend this analysis by giving the explicit parameterization of these additional terms. The determination of the angle of misalignment and its parameterization in terms of the physical axion is based on an extension of the method presented in [30]. We are going to illustrate this point starting, for simplicity, from the non-supersymmetric case and then moving to the supersymmetric one.

7.1 The non-supersymmetric case

In the non-supersymmetric case the scalar sector contains two Higgs doublets $V_{PQ}(H_u, H_d)$ plus one extra contribution (a PQ breaking potential), denoted as $V_{\cancel{P}Q}(H_u, H_d, b)$ or V' , which mixes the Higgs sector with the Stückelberg axion b ,

$$V = V_{PQ}(H_u, H_d) + V_{\cancel{P}Q}(H_u, H_d, b). \quad (62)$$

The mixing induced in the CP-odd sector determines the presence of a linear combination of the Stückelberg field b and of the Goldstones of the CP-odd sector, called χ , which is characterized by an almost flat direction, whose curvature is controlled by the strength of the extra potential $V_{\cancel{P}Q}$. $V_{PQ}(H_u, H_d)$ is the ordinary potential of 2 Higgs doublets,

$$V_{PQ} = \mu_u^2 H_u^\dagger H_u + \mu_d^2 H_d^\dagger H_d + \lambda_{uu}(H_u^\dagger H_u)^2 + \lambda_{dd}(H_d^\dagger H_d)^2 - 2\lambda_{ud}(H_u^\dagger H_u)(H_d^\dagger H_d) + 2\lambda'_{ud}|H_u^T \tau_2 H_d|^2 \quad (63)$$

Concerning the V' contribution to the total potential, its structure is inferred just on the basis of gauge invariance and given by

$$V' = \lambda_0 (H_2^\dagger H_1 e^{-ig_B(B_{H_2}-B_{H_1})\frac{b}{2M_{St}}}) + \lambda_1 (H_2^\dagger H_1 e^{-ig_B(B_{H_2}-B_{H_1})\frac{b}{2M_{St}}})^2 + \lambda_2 (H_2^\dagger H_2)(H_2^\dagger H_1 e^{-ig_B(B_{H_2}-B_{H_1})\frac{b}{2M_{St}}}) + \lambda_3 (H_1^\dagger H_1)(H_2^\dagger H_1 e^{-ig_B(B_{H_2}-B_{H_1})\frac{b}{2M_{St}}}) + \text{h.c.} \quad (64)$$

These terms are the only ones allowed by the symmetry of the model and are parameterized by one dimensionful ($\lambda_0 \equiv \bar{\lambda}_0 v$) and three dimensionless constants ($\lambda_1, \lambda_2, \lambda_3$).

The CP-odd sector is then spanned by the three fields $(\text{Im}H_1, \text{Im}H_2, b)$, with the potential V_{PQ} a function only of H_1 and H_2 . Before electroweak symmetry breaking the potential allows the identification of one Goldstone mode, G_1^0 , while b is the second Goldstone.

After electroweak symmetry breaking, due to Higgs-axion mixing, only one component of b is an unphysical mode. This component is a linear combination of the two Goldstone modes of the total potential ($V_{PQ} + V'$), denoted as G_0^1, G_0^2 . The physical axion, χ , i.e. the component of b which is not proportional to the two Goldstones, can be identified using the rotation matrix O^χ which relates interaction and mass eigenstates in the CP-odd sector

$$\begin{pmatrix} G_0^1 \\ G_0^2 \\ \chi \end{pmatrix} = O^\chi \begin{pmatrix} \text{Im}H_1^0 \\ \text{Im}H_2^0 \\ b \end{pmatrix}. \quad (65)$$

χ inherits WZ interactions from b , since the Stückelberg field b , as we have just mentioned, can be expressed as a linear combination of the physical axion χ and the Goldstone modes via this matrix

$$b = O_{13}^\chi G_0^1 + O_{23}^\chi G_0^2 + O_{33}^\chi \chi. \quad (66)$$

From an explicit computation one finds that $O_{13}^\chi = 0$, $O_{23}^\chi \sim O(1)$ and $O_{33}^\chi \sim v/M_{St}$. The Goldstones of the two neutral gauge bosons, $G_Z, G_{Z'}$ are linear combinations of G_0^1 and G_0^2 and can be extracted from

the bilinear mixings after an expansion around the broken electroweak vacuum. Then, the entire CP-odd sector can be spanned by the basis $(G_Z, G_{Z'}, \chi)$. The presence of an extra degree of freedom in this sector has been established in [36] using a simple counting of the degrees of freedom. We review this point for clarity.

There are 9 degrees of freedom in the set $(A_Y, W_3, B, \text{Im}H_1, \text{Im}H_2)$ before electroweak symmetry breaking, as well as 9 in the set (A_γ, Z, Z', χ) , which is generated after the breaking. The direction determining the gauged axion χ is then physical but flat, in the absence of an extra potential which may depend explicitly on b . The potential V' is responsible for giving a small mass for χ and can be used to parameterize the mechanism of vacuum misalignment originated at the electroweak scale.

One can explore the structure of this potential and, in particular, investigate its periodicity. The phase of the potential is indeed parameterized by the ratio χ/σ_χ [30]

$$V' = 4v_1v_2 (\lambda_2v_1^2 + \lambda_3v_2^2 + \lambda_0) \cos\left(\frac{\chi}{\sigma_\chi}\right) + 2\lambda_1v_1^2v_2^2 \cos\left(2\frac{\chi}{\sigma_\chi}\right) \quad (67)$$

with a mass for the physical axion χ given by

$$m_\chi^2 = \frac{2v_1v_2}{\sigma_\chi^2} (\bar{\lambda}_0v^2 + \lambda_2v_1^2 + \lambda_3v_2^2 + 4\lambda_1v_1v_2) \approx \lambda_{eff}v^2, \quad (68)$$

with $\sigma_\chi \sim O(v)$. The size of this expression is the result of two factors which appear in Eq. (68): the size of the potential, parameterized by $(\bar{\lambda}_0, \lambda_1, \lambda_2, \lambda_3)$, and the electroweak vevs of the two Higgses. The appearance of χ in Eq. (67) - in the phase of the extra potential - shows explicitly that the angle of misalignment is entirely described by this field. The angle is defined as

$$\theta(x) \equiv \frac{\chi(x)}{\sigma_\chi}, \quad (69)$$

where

$$\sigma_\chi \equiv \frac{2v_1v_2M_{St}}{\sqrt{g_B^2(B_{H_2} - B_{H_1})^2v_1^2v_2^2 + 2M_{St}^2(v_1^2 + v_2^2)}} \quad (70)$$

is the new dimensionful constant which takes the same role of the scale f_a of the PQ case ($\theta(x) = a/f_a$). The potential is characterized by a small strength $\sim \lambda_{eff}v^4$, and for this reason one can think of χ as a pseudo Nambu-Goldstone mode of the theory.

At this stage, it is important to realize that the size of the extra potential is significant in order to establish whether the degree of freedom associated to the axion field remains frozen or not at the electroweak scale. For instance, if λ_{eff} is associated to electroweak instantons ($\lambda_{eff} \sim \lambda_{inst}$), then m_χ is very suppressed (see the discussion in Sec. 7.3) and far smaller than the corresponding Hubble rate at the electroweak scale

$$H(T) = \frac{1}{3} \sqrt{\frac{4}{5} \pi^3 g_{*,T}} \frac{T^2}{M_P} \quad (71)$$

which is about 10^{-5} eV. In the expression above g_{*,T_i} is the number of effective massless degrees of freedom of the model at a given temperature (T), while M_P denotes the Planck mass. We recall that the condition

$$m_\chi(T) \sim 3H(T) \quad (72)$$

which ensures the presence of oscillations and determines implicitly the oscillation temperature T_i , is indeed impossible to satisfy if the misalignment that generates the value of m_χ at the electroweak scale is assumed of being of instanton origin (see the discussion in Appendix E). This implies that the degree of freedom associated to this physical axion would be essentially frozen at the electroweak scale, and the oscillations could take place at a later stage in the early universe, only around the QCD hadron transition. Instead, a more sizeable potential, providing an axion mass larger than 10^{-5} eV, would allow such oscillations. For an axion mass around 1 MeV oscillations indeed occur, but are damped by the particle decay, given that its lifetime ($\tau_l \sim 10^{-4}$ sec) is much larger than period of their oscillation ($\tau_{osc} \sim 10^{-13}$ sec). This discussion is going to be expanded to the supersymmetric case.

7.2 Supersymmetry and the angle of misalignment

In the supersymmetric case the situation is analogous, in the sense that the physical direction χ can be identified by the same criteria. The superpotential that we are considering allows the presence of one extra degree of freedom, given by $\text{Im } S$, to appear in the CP-odd sector besides the states $(\text{Im } H_1, \text{Im } H_2, \text{Im } b)$, already present in the non-supersymmetric case.

From the supersymmetric potential V in (31), we identify two massless states, that we call G_1^0 and G_2^0 , and a massive eigenstate, called H_4^0 . G_1^0 and G_2^0 do not coincide with the true Goldstones of the model, as in the previous case, since the V potential does not include any contribution involving $\text{Im } b$. The correct neutral Goldstone modes are extracted from the derivative couplings between the CP-odd scalar fields and the neutral gauge bosons present in the Lagrangian. The physical axion is then identified as the massless direction which is orthogonal to the subspace spanned by $(G_Z, G_{Z'}, H_4^0)$. This state is called $H_0^5 \equiv \chi$ and is given by the linear combination

$$\chi = \frac{1}{N_\chi} [2M_{st}v_1v_2^2 \text{Im } H_1^0 + 2M_{st}v_1^2v_2 \text{Im } H_2^0 - 2M_{st}v^2v_S \text{Im } S + B_S g_B \sec \alpha (v^2v_S^2 + v_1^2v_2^2) \text{Im } b]$$

$$N_\chi = \sqrt{4M_{St}^2v^2(v^2v_S^2 + v_1^2v_2^2) + B_S^2g_B^2 \sec^2 \alpha (v^2v_S^2 + v_1^2v_2^2)^2}. \quad (73)$$

It is important to remark that this state is not constructed, at least at this stage, from the matrix O^χ , since the projection of $\text{Im } b$ on χ would be zero, if the matrix O_χ were derived just from the potential V_{PQ} . This should be obvious, since O_χ measures the curvature of the potential in the direction of $\text{Im } b$, and V_{PQ} does not depend on $\text{Im } b$.

Also in this case, the identification of the Goldstones of the two neutral massive gauge bosons (Z and Z') is obtained by looking at the bilinear mixing terms; these appear in the Lagrangian once this is rewritten in the physical basis (in the form $M_Z Z \partial G_Z$, and $M_{Z'} Z' \partial G_{Z'}$).

Then one can immediately figure out that the linear basis spanning the entire CP-odd sector can be completed by the addition of an extra, orthogonal state χ ($G_Z, G_{Z'}, H_4^0, \chi$). The new entry parameterizes a massless but physical direction in this sector. Once $\text{Im } b$ is re-expressed in terms of the physical axion χ and of the Goldstone modes $G_Z, G_{Z'}$ of the massive gauge bosons, χ will inherit from $\text{Im } b$ axion-like interactions and will be promoted to a generalized PQ axion.

At this point, having identified this flat but physical direction of the potential in the CP-odd sector, one can ask the obvious question whether the same potential can acquire a curvature. These effects are

indeed parameterized by the strength (λ_{eff}) of the potential V' (the “extra potential”) that we are going to identify below, and which remains a free parameter in the theory.

One special comments should be deserved for v_S , the vev of the scalar singlet, which is new compared to the standard MSSM scenario and which is part of the scalar potential. We recall that this new scale is essentially bound by the condition $\lambda v_S \sim \mu \sim 200 \text{ GeV}$ (see Eq. 6). This defines the typical range for the μ term, which sets the scale of the interaction for the two Higgs doublets in supersymmetric theories.

In our case we are allowed to parameterize this new non-perturbative contribution (V') to the potential, as discussed in the previous section, in a rather straightforward way, by classifying all the phase-dependent operators which can be constructed using the fundamental fields of the model. In analogy to the non-supersymmetric case (the MLSOM) [36] we rely only on gauge invariance as a guiding principle to identify them. These include, in particular, a dependence of V' , again in the form of a phase factor, from the Stückelberg field $\text{Im } b$.

The contributions appearing in V' don't need to be given necessarily in a supersymmetric form, since we are assuming that supersymmetry is already broken at the scale at which they appear ($v < M_{susy}$). They are parameterized in the form

$$V' = \sum_{i=1}^6 V_i \quad (74)$$

where

$$\begin{aligned} V_1 &= a_1 S^4 e^{-i4g_B B_S \frac{\text{Im } b}{2M_{St}}} + h.c. \\ V_2 &= e^{-ig_B B_S \frac{\text{Im } b}{2M_{St}}} \left(a_2 H_1 \cdot H_2 S^2 + b_2 H_1^\dagger H_1 S + b_3 H_2^\dagger H_2 S + b_4 S^\dagger S^2 + d_1 S \right) + h.c. \\ V_3 &= e^{-ig_B 2B_S \frac{\text{Im } b}{2M_{St}}} \left(a_3 H_1^\dagger H_1 S^2 + a_4 H_2^\dagger H_2 S^2 + a_5 S^\dagger S^3 + c_1 S^2 \right) + h.c. \\ V_4 &= a_6 (H_1 \cdot H_2)^2 e^{ig_B 2B_S \frac{\text{Im } b}{2M_{St}}} + h.c. \\ V_5 &= b_1 S^3 e^{-ig_B 3B_S \frac{\text{Im } b}{2M_{St}}} + h.c. \\ V_6 &= c_2 H_1 \cdot H_2 e^{ig_B B_S \frac{\text{Im } b}{2M_{St}}} + h.c.. \end{aligned} \quad (75)$$

In the expressions above we have grouped together terms that share the same phase factor. Notice that the parameters a_i, b_j, c_k and d_1 carry different mass dimensions. For these reasons they can be parameterized by suitable powers of the SUSY breaking mass M_{susy} times λ_{eff} . We explicitly obtain the estimates

$$a_i \sim \lambda_{eff} \quad b_j \sim \lambda_{eff} m_S \quad c_k \sim \lambda_{eff} m_S^2 \quad d_1 \sim \lambda_{eff} M_{susy}^3. \quad (76)$$

If we introduce any of the terms in Eq. (75), and recompute the CP-odd mass matrix using the new potential ($V + V'$), this gets modified, but we still find two massless eigenstates corresponding to the neutral Goldstone modes, which also in this case we call G_0^1 and G_0^2 . They can be expressed as linear combinations of the neutral Goldstone states coming from the derivative couplings between the gauge bosons and the CP-odd Higgs fields. An important point to remark is that these states (Goldstone modes) do not depend on the parameters of the Peccei-Quinn breaking potential, as we expect, since the presence of this extra potential doesn't affect the bilinear derivative couplings through which they are identified.

In the basis $(\text{Im}H_1^1, \text{Im}H_2^2, \text{Im}S, \text{Im}b)$ they are given by

$$G_0^1 = \left\{ \frac{v_1}{v}, \frac{-v_2}{v}, 0, 0 \right\}$$

$$G_0^2 = \frac{1}{\sqrt{4v^2 M_{St}^2 + g_B^2 B_S^2 (v_1^2 v_2^2 + v_S^2 v^2)}} \left\{ \frac{-g_B B_S v_1 v_2^2}{v}, \frac{-g_B B_S v_1^2 v_2}{v}, g_B B_S v v_S, 2M_{St} v \right\}. \quad (77)$$

This shows that the linear space spanned by the two Goldstones - and identified just from the V_{PQ} potential - is invariant respect to the small corrections induced by the additional non-perturbative potential given in Eq. (74).

7.3 The strength of the potential and λ_{eff}

One important comment concerns the possible size of the axion mass m_χ induced by V' at the electroweak scale. In this respect we will take into account two basic possibilities. A first possibility that we will explore is to assume that the axion mass is PQ-like, in the milli-eV region; as a second possibility we will select an axion mass around the MeV region. These choices cover a region of parameter space that has never been analyzed in these types of models, while a study of the GeV region for the axion mass has been addressed before in [43]. These choices have to be confronted with constraints coming from a) direct axion searches, b) nucleosynthesis constraints and 3) constraints on the relic densities from WMAP data.

A PQ-like axion is bound to emerge in the spectrum of the theory if the potential V' is strongly suppressed and the real mechanism of misalignment which determines its mass is the one taking place at the QCD transition. The value of λ_{eff} , under these assumptions, should be truly small and one way to achieve this would be to attribute its origin to electroweak instantons. Using the numerical relations for the electromagnetic (α) and weak couplings (α_W), $1/\alpha(M_Z) = 128$ and $\alpha_W = \alpha/\sin^2 \theta_W$ with $\sin^2 \theta_W(M_Z) = 0.23$ on the Z mass ($\alpha_W(M_Z) = 0.034$), the exponential suppression of the extra potential is controlled by $\lambda_{eff} \sim e^{-185} \equiv \lambda_{inst} = 4.5 \times 10^{-81}$. This corresponds to a mass for the axion given by $m_\chi \sim \sqrt{\lambda_{eff} v} \sim 10^{-29}$ eV. This mass would be obviously redefined at the QCD epoch.

As we have briefly mentioned in the introduction, mass values of the axion field around 10^{-33} eV (for global $U(1)$'s or of PQ type) and with a spontaneous breaking scale $f_a \sim 10^{18}$ eV have been considered as a possible origin of a cosmological constant $\Lambda^4 \sim (10^{-3} \text{eV})^4$ [11]. In such models the misalignment is purely of electroweak origin and connected to electroweak instantons. Oscillations of fields of such a mass would not take place even at the current cosmological time.

Instead, for an axion of a mass in the MeV region, the value of λ_{eff} is larger ($\sim 10^{-12}$) and will be estimated below. In this case the effect of vacuum misalignment at the QCD scale is irrelevant in determining the mass of this particle. A more massive axion, in fact, decays at a much faster rate than a very light one and the usual picture typical of a long-lived PQ-like axion, in this specific case, simply does not apply.

In order to characterize in more detail the potential in Eq. (74), we proceed with a careful analysis of the field dependence of the phase factors in the exponentials, that we expect to be written exclusively in terms of the physical fields of the CP odd sector, H_0^4 , and the axion χ ($\chi \equiv H_0^5$). In fact, this is the analogous (and a generalization) of what found in the previous section (see Eq. (67)), where the periodicity

has been shown to depend only on the axion χ . For this purpose we use the following parameterization of the fields

$$\begin{aligned} H_1^1(x) &= \frac{1}{\sqrt{2}} (\rho_1^1(x) + v_1) e^{i\Phi_1^1(x)} & H_1^2(x) &= \frac{1}{\sqrt{2}} \rho_1^2(x) e^{i\Phi_1^2(x)} \\ H_2^1(x) &= \frac{1}{\sqrt{2}} \rho_2^1(x) e^{i\Phi_2^1(x)} & H_2^2(x) &= \frac{1}{\sqrt{2}} (\rho_2^2(x) + v_2) e^{i\Phi_2^2(x)} \\ S(x) &= \frac{1}{\sqrt{2}} (\rho_S(x) + v_S) e^{i\Phi_S(x)} \end{aligned} \quad (78)$$

and select just some of the V_i in Eq. (75) in order to illustrate the general behaviour.

For instance, if we consider only the V_1 term we get the corresponding symmetric mass matrix for the total potential $V + V_1$, with V defined in Eq. (31),

$$M_{odd}^2 = -\frac{a_\lambda}{\sqrt{2}} \begin{pmatrix} \frac{v_2 v_S}{v_1} & v_S & v_2 & 0 \\ \cdot & \frac{v_1 v_S}{v_2} & v_1 & 0 \\ \cdot & \cdot & \frac{v_1 v_2}{v_S} + 8\sqrt{2} \frac{a_1}{a_\lambda} v_S^2 & -4\sqrt{2} \frac{a_1}{a_\lambda} \frac{g_B B_S v_S^3}{M_{St}} \\ \cdot & \cdot & \cdot & 2\sqrt{2} \frac{a_1}{a_\lambda} \frac{g_B^2 B_S^2 v_S^4}{M_{St}^2} \end{pmatrix} \quad (79)$$

expressed in the basis $(\Phi_1^1, \Phi_2^2, \Phi_S, \text{Im}b)$. From this matrix we get two null eigenvalues corresponding to the neutral Goldstones and two eigenvalues which correspond to the masses of the two CP-odd states H_0^4 and H_0^5 . In this specific case they take the form

$$\begin{aligned} m_{H_0^4, H_0^5}^2 &= \frac{1}{2M_{St} v_1 v_2 v_S} \left(A \pm \sqrt{A^2 - B} \right) \\ A &= 4a_1 v_1 v_2 v_S^3 (4M_{St}^2 + g_B^2 B_S^2 v_S^2) + \sqrt{2} a_\lambda M_{St}^2 (v_1^2 v_2^2 + v^2 v_S^2) \\ B &= 16\sqrt{2} a_1 a_\lambda M_{St}^2 v_1 v_2 v_S^5 (4v^2 M_{St}^2 + g_B^2 B_S^2 (v_1^2 v_2^2 + v^2 v_S^2)). \end{aligned} \quad (80)$$

In the limit of a vanishing a_1 ($\sim \lambda_{eff}$) we obtain a massless state corresponding to H_0^5 (χ) and a massive one corresponding to H_0^4 . In fact, expanding the expressions above up to first order in a_1 , which is a very small parameter due to (76), we obtain for the two eigenvalues the approximate forms

$$\begin{aligned} m_{H_0^4}^2 &\simeq \sqrt{2} a_\lambda \left(\frac{v_1 v_2}{v_S} + \frac{v_1 v_S}{v_2} + \frac{v_2 v_S}{v_1} \right) + 16a_1 \frac{v_1^2 v_2^2 v_S^2}{v^2 v_S^2 + v_1^2 v_2^2}, \\ m_{H_0^5}^2 &\simeq \frac{4a_1 v_S^4 [4v^2 M_{St}^2 + g_B^2 B_S^2 (v^2 v_S^2 + v_1^2 v_2^2)]}{M_{St}^2 (v^2 v_S^2 + v_1^2 v_2^2)}. \end{aligned} \quad (81)$$

These relations show that indeed $m_{H_0^5}$ is $O(\lambda_{eff} v)$ while $m_{H_0^4}$ is $O(v)$.

Moving to the analysis of the phase factor of the same term (V_1), the linear combination of fields that appears in the exponential factor is given by the expression

$$\bar{\theta}_1 \equiv \frac{4\Phi_S(x)}{v_S} - \frac{2g_B B_S \text{Im}b(x)}{M_{St}}. \quad (82)$$

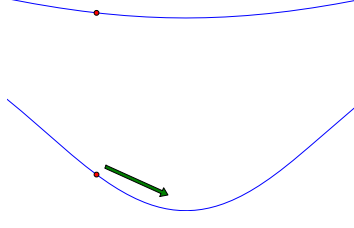


Figure 4: Illustration of the two misalignments at the electroweak (upper figure) and at the QCD phase transitions (lower figure) for a PQ-like axion (not to scale).

We rotate this linear combination on the physical basis (G_Z, G_Z, H_0^4, H_0^5) using the rotation matrix O^χ . After the rotation we can re-express the angle of misalignment as a linear combination of the physical states of the CP-odd sector in the form

$$\bar{\theta}_1 = \frac{H_0^4}{\sigma_{H_0^4}} + \frac{H_0^5}{\sigma_{H_0^5}}. \quad (83)$$

This linear combination will appear in all the operatorial terms included in V' and is a generalization of Eq. (69), with $\sigma_{H_0^4}$ and $\sigma_{H_0^5}$ defining, separately, the scales of the two angular contributions to the total phase. It is not difficult to show that the periodicity of the potential depends predominantly on H_0^4 . This can be easily seen by analyzing the size of $\sigma_{H_0^4}$ and $\sigma_{H_0^5}$. In fact, expanding to first order in a_1 we get

$$\begin{aligned} \frac{1}{\sigma_{H_0^4}} &= -\frac{4v_1v_2}{v_2 \operatorname{sgn} B_S \sqrt{v^2v_S^2 + v_1^2v_2^2}} - \frac{8\sqrt{2}v_1^2v_2^2v_S^4 [4v^2M_{St}^2 + g_B^2B_S^2(v^2v_S^2 + v_1^2v_2^2)] a_1}{a_\lambda M_{St}^2 (v^2v_S^2 + v_1^2v_2^2)^{5/2} \operatorname{sgn}(B_S)} + O(a_1^2) \\ \frac{1}{\sigma_{H_0^5}} &= -\frac{8\sqrt{2}v_1^2v_2^2v_S^4 [4v^2M_{St}^2 + g_B^2B_S^2(v^2v_S^2 + v_1^2v_2^2)] a_1}{a_\lambda M_{St}^2 (v^2v_S^2 + v_1^2v_2^2)^{5/2} \operatorname{sgn} B_S} + O(a_1^2). \end{aligned} \quad (84)$$

with a_λ being proportional to the SUSY breaking scale M_{susy} . A more careful look at the structure of these two scales shows that $\sigma_{H_0^4} \sim v_S$ ($v_S = 400$ GeV in our case) while $\sigma_{H_0^5} \sim M_{susy}/\lambda_{eff}$. Clearly, $\sigma_{H_0^5} \gg \sigma_{H_0^4}$, but the dependence of the extra potential on χ is clearly affected by the different possible sizes of λ_{eff} . For an instanton generated potential ($\lambda_{eff} \sim \lambda_{inst}$) the direction of χ is essentially flat and $\sigma_{H_0^5}$ turns out to be very large. In turn, this implies that the dependence of the potential V_1 on H_0^5 , which takes place exclusively through the exponential, is negligible, being essentially controlled by H_0^4 ($\bar{\theta}_1 \sim H_0^4/v$) with

$$V_1 \sim \lambda_{eff} v^4 \cos(\bar{\theta}_1). \quad (85)$$

We may conclude, indeed, that in this case the effect of misalignment on χ , generated at the electroweak scale, can be neglected. This feature is shown on the left panel of Fig. 5, where we plot $V'(H_0^4, \chi)$. It is immediately clear from these plots that for $\lambda_{eff} \sim \lambda_{inst}$ the only periodicity of the extra potential is in the variable H_0^4 (left panel), due to the flatness of the H_0^5 direction. For a more sizeable potential, with $\lambda_{eff} \sim 10^{-12}$, the curvature generated in χ is responsible for giving a mass to the axion in the MeV range (Fig. 5, right panel).

This result is generic for all the terms, as we are now going to show.

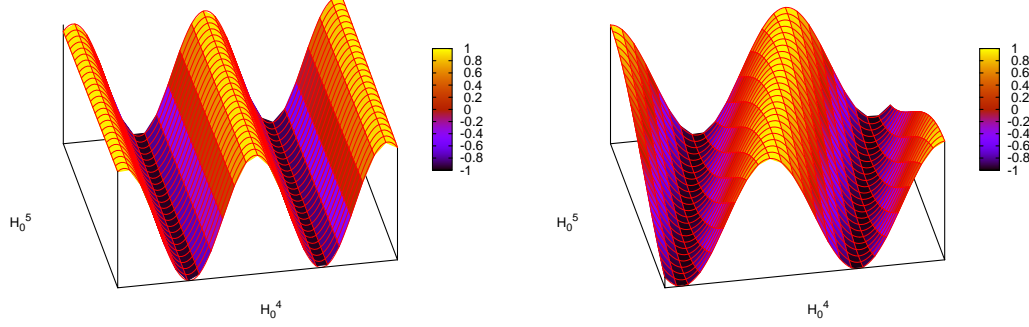


Figure 5: Shape of the extra potential V' at the electroweak scale in the CP-odd sector in the $(H_0^4, \chi \equiv H_0^5)$ plane. χ is an almost flat direction for a strength induced by the instanton vacuum at the electroweak scale (left panel) and acquires a curvature for an axion mass in the MeV region (curvature in the χ direction, right panel).

For instance, from the contribution in V_3 parametrized by a_3 ,

$$V_3 = e^{-ig_B B_S \frac{\text{Im}b}{M_{St}}} a_3 H_1^\dagger H_1 S^2 + \dots \quad (86)$$

we obtain similar expressions for the mass matrix and eigenvalues. The linear combination of fields that appears in the phase is given by

$$\bar{\theta}_3 \equiv \frac{2\Phi_S(x)}{v_S} - \frac{g_B B_S \text{Im}b(x)}{M_{St}}, \quad (87)$$

and if we rotate this linear combination we get an expression again of the form given Eq. (83), with two new scales σ' s. Expanded for small a_3 they give

$$\begin{aligned} \frac{1}{\sigma_{H_0^4}} &= -\frac{2v_1 v_2}{v_S \sqrt{v^2 v_S^2 + v_1^2 v_2^2} \text{sgn}(B_S)} - \frac{\sqrt{2} v_1^4 v_2^2 v_S^2 [4v^2 M_{St}^2 + g_B^2 B_S^2 (v^2 v_S^2 + v_1^2 v_2^2)] a_3}{a_\lambda M_{St}^2 (v^2 v_S^2 + v_1^2 v_2^2)^{5/2} \text{sgn}(B_S)} + O(a_3^2) \\ \frac{1}{\sigma_{H_0^5}} &= -\frac{\sqrt{2} v_1^4 v_2^2 v_S^2 [4v^2 M_{St}^2 + g_B^2 B_S^2 (v^2 v_S^2 + v_1^2 v_2^2)] a_3}{a_\lambda M_{St}^2 (v^2 v_S^2 + v_1^2 v_2^2)^{5/2} \text{sgn} B_S} + O(a_3^2). \end{aligned} \quad (88)$$

A closer look at this expression shows again that $\sigma_{H_0^4} \sim v_S$ and $\sigma_{H_0^5} \sim M_{susy}/\lambda_{eff}$, similarly to the previous case. We conclude that V_3 , which is proportional to a_3 , takes the same approximate form given by Eq. (85). As a final example we consider one of the contributions with the lowest mass dimension, such as

$$V_2 = e^{-ig_B 2B_S \frac{\text{Im}b}{2M_{St}}} d_1 S + \dots \quad (89)$$

with d_1 of mass dimension 3. From the operator we can extract the phase

$$\bar{\theta}_2 = \frac{g_B B_S \text{Im}b(x)}{2M_{St}} - \frac{\Phi_S(x)}{v_S} \quad (90)$$

and after the rotation we get the coefficients for the linear combination

$$\begin{aligned}\frac{1}{\sigma_{H_0^4}} &= \frac{v_1 v_2}{v_S \sqrt{v^2 v_S^2 + v_1^2 v_2^2} \operatorname{sgn} B_S} + \frac{v_1^2 v_2^2 v_S [4v^2 M_{St}^2 + g_B^2 B_S^2 (v^2 v_S^2 + v_1^2 v_2^2)] d_1}{2a_\lambda M_{St}^2 (v^2 v_S^2 + v_1^2 v_2^2)^{5/2} \operatorname{sgn} B_S} + O(d_1^2) \\ \frac{1}{\sigma_{H_0^5}} &= \frac{v_1^2 v_2^2 v_S [4v^2 M_{St}^2 + g_B^2 B_S^2 (v^2 v_S^2 + v_1^2 v_2^2)] d_1}{2a_\lambda M_{St}^2 (v^2 v_S^2 + v_1^2 v_2^2)^{5/2} \operatorname{sgn} B_S} + O(d_1^2).\end{aligned}\quad (91)$$

Also in this case the behaviour of the two normalization scales σ 's appearing in the global phase of this contribution are $\sigma_{H_0^4} \sim v_S$ while

$$\sigma_{H_0^5} \sim \frac{M_{susy}}{\lambda_{eff}} \left(\frac{M_{susy}}{v} \right)^3, \quad (92)$$

with $\sigma_{H_0^5}$ corresponding to a very large suppression scale, due to the small size of λ_{eff} . Again, as in the previous two cases, the structure of the potential is of the form given in Eq. (85).

One can draw some conclusions regarding the role played by the exponential phase and compare the supersymmetric with the non-supersymmetric case. In the non-supersymmetric case the periodicity of the potential is controlled by the weak scale (v), and is expressed directly in terms of the physical component of b (which is a real field). The size of the potential, in this case, is of order $\lambda_{eff} v^4$

$$V' \sim \lambda_{eff} v^4 \cos\left(\frac{\chi}{v}\right) \quad (93)$$

and therefore very small, while the periodicity shows that the amplitude of the axion field is $\chi \sim O(v)$. In the supersymmetric case, more generally, we obtain for a generic component V_i

$$V' \sim \lambda M_{susy}^4 \cos\left(\frac{H_0^4}{v_S} + \frac{\chi}{M_{susy}/\lambda_{eff}}\right) \quad (94)$$

from which it is clear that the curvature in the axion field is controlled by the parameter λ_{eff} . In the supersymmetric case we can think of the periodicity in Eq. (94) as essentially controlled by the massive CP-odd Higgs H_0^4 , with a period which is $O(\pi v_S)$, with superimposed a second periodicity of $O(\pi M_{susy}/\lambda_{eff})$ (with $M_{susy}/\lambda_{eff} \gg v_S$) in the perpendicular direction (χ). We conclude that the actual structure of the complete $(V + V')$ potential indeed guarantees the presence in the spectrum of a physical and light pseudoscalar field. This analysis holds, in principle, for an axion of any mass, although we do not explicitly study an axion whose mass goes beyond the MeV region. To have an axion which is long-lived, the true discriminant of our study is the axion mass, and for this reason we are going to present a study of the decay rates of this particle keeping the mass as a free parameter varying in the milli-eV - MeV interval.

8 Decay of a gauged supersymmetric axion

In this section we compute the decay rate of the axion of the supersymmetric model into two-photons, mediated both by the direct PQ interaction and by the fermion loop, which are shown in Fig. 6, keeping the axion mass as a free parameter. Denoting with $N_c(f)$ the color factor for a fermion specie, and

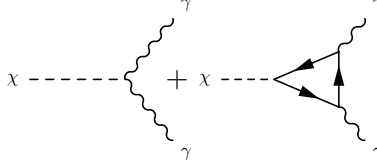


Figure 6: Contributions to the axi-Higgs decay $\chi \rightarrow \gamma\gamma$.

introducing the function $\tau_f \eta(\tau_f)$, a function of the mass of the fermions circulating in the loop with

$$\tau = 4m_f^2/m_\chi^2 \quad \eta(\tau) = \arctan^2 \frac{1}{\sqrt{-\rho_{f\chi}^2}} \quad \rho_{f\chi} = \sqrt{1 - \left(\frac{2m_f}{m_\chi}\right)^2}, \quad (95)$$

the WZ interaction in Fig. 6 is given by

$$\mathcal{M}_{WZ}^{\mu\nu}(\chi \rightarrow \gamma\gamma) = 4g_{\gamma\gamma}^\chi \varepsilon[\mu, \nu, k_1, k_2], \quad (96)$$

where $g_{\gamma\gamma}^\chi$ is the coupling, defined via the relations

$$g_{\gamma\gamma}^\chi = -\frac{g_B B_S (4c_Y g_2^2 + c_W g_Y^2)}{16g^2 M_{St}} \sqrt{\frac{v^2 v_S^2 + v_1^2 v_2^2}{4M_{St}^2 v^2 + g_B^2 B_S^2 (v^2 v_S^2 + v_1^2 v_2^2)}} \quad (97)$$

obtained from the rotation of the WZ vertices on the physical basis (we will comment in more detail on the size of this coupling in the next section). The massless contribution to the decay rate coming from the WZ counterterm $\chi F_\gamma F_\gamma$ is given by

$$\Gamma_{WZ}(\chi \rightarrow \gamma\gamma) = \frac{m_\chi^3}{4\pi} (g_{\gamma\gamma}^\chi)^2. \quad (98)$$

Combining also in this case the tree level decay with the 1-loop amplitude, we obtain for $\chi \rightarrow \gamma\gamma$ the amplitude

$$\mathcal{M}^{\mu\nu}(\chi \rightarrow \gamma\gamma) = \mathcal{M}_{WZ}^{\mu\nu} + \mathcal{M}_f^{\mu\nu}. \quad (99)$$

The second amplitude in Fig. 6 is mediated by the triangle loops and is given by the expression

$$\mathcal{M}_f^{\mu\nu}(\chi \rightarrow \gamma\gamma) = \sum_f N_c(f) iC_0(m_\chi^2, m_f) c_{\gamma\gamma}^{\chi, f} \varepsilon[\mu, \nu, k_1, k_2] \quad f = \{q_u, q_d, \nu_l, l, \chi_1^\pm, \chi_2^\pm\} \quad (100)$$

where $N_c(f)$ is the color factor for the fermions. In the domain $0 < m_\chi < 2m_f$, which is the relevant domain for our study, being the axion very light, the pseudoscalar triangle when both photons are on mass-shell is given by the expression

$$C_0(m_\chi^2, m_f) = -\frac{m_f}{\pi^2 m_\chi^2} \arctan^2 \left(\left(\frac{4m_f^2}{m_\chi^2} - 1 \right)^{-1/2} \right) = -\frac{m_f}{\pi^2 m_\chi^2} \eta(\tau) \quad (101)$$

The coefficient $c_{\gamma\gamma}^{\chi,f}$ is the factor for the vertex between the axi-Higgs and the fermion current. The expressions of these factors are

$$\begin{aligned} c^{\chi,q_u} &= -\frac{i\sqrt{2}y_u M_{St} v_1^2 v_2}{\sqrt{(v^2 v_S^2 + v_1^2 v_2^2) [4M_{St}^2 v^2 + g_B B_S (v^2 v_S^2 + v_1^2 v_2^2)]}}, \\ c^{\chi,q_d} &= -\frac{v_2 y_d}{v_1 y_u} c^{\chi,q_u}, \\ c^{\chi,l} &= \frac{y_e}{y_d} c^{\chi,q_d}. \end{aligned} \tag{102}$$

We obtain the following expression for the decay amplitude

$$\begin{aligned} \Gamma_\chi \equiv \Gamma(\chi \rightarrow \gamma\gamma) &= \frac{m_\chi^3}{32\pi} \left\{ 8(g_{\gamma\gamma}^\chi)^2 + \frac{1}{2} \left| \sum_f N_c(f) i \frac{\tau_f}{4\pi^2 m_f} \eta(\tau_f) e^2 Q_f^2 c^{\chi,f} \right|^2 \right. \\ &\quad \left. + 4g_{\gamma\gamma}^\chi \sum_f N_c(f) i \frac{\tau_f}{4\pi^2 m_f} \eta(\tau_f) e^2 Q_f^2 c^{\chi,f} \right\}, \end{aligned} \tag{103}$$

where the three terms correspond, respectively, to the point-like WZ term, to the 1-loop contribution and to their interference.

Notice that in the expression of this decay rate both the direct ($\sim (g_{\gamma\gamma}^\chi)^2$) and the interference ($\sim g_{\gamma\gamma}^\chi$) contributions are suppressed as inverse powers of the Stückelberg mass, here taken to be equal to 1 TeV. We have chosen v as the SM electroweak vev, for v_S we have chosen the value of 500 GeV. In order to have an acceptable Higgs spectrum, the Yukawa couplings have been set to give the right fermion masses of the Standard Model, while for g_B and B_S we have chosen $g_B = 0.1$ and $B_S = 4$.

We show in Figs. 7 and 8 results obtained from the numerical evaluation of the decay amplitude as a function of the mass of the axion m_χ , which clearly indicates that the decay rates are very small for a milli-eV particle, although larger than those of the PQ case [30]. We conclude that a PQ-like axion is indeed long-lived also in these models and as such could, in principle, contribute to the relic densities of dark matter. For an axion with a mass in the MeV region, instead, the particle is not stable and as such would decay rather quickly. The decay, in this case, is fast enough ($\tau \lesssim 10^{-3}$ sec) and does not interfere with the nucleosynthesis.

9 Cold dark matter by misalignment of the axion field

In the case of a long-lived axion, the generation of relic densities of axion dark matter, in this model, involves two (sequential) misalignments, generated, as we have already discussed, the first at the electroweak scale, and the second at the QCD phase transition. The presence of two misalignments at two separate scales, as discussed in [30], is typical of axions which show interactions both with the weak and with the strong sectors, due to the presence of mixed anomalies. This point has been addressed in detail within a non-supersymmetric model, but in a supersymmetric scenario the physical picture remains the same.

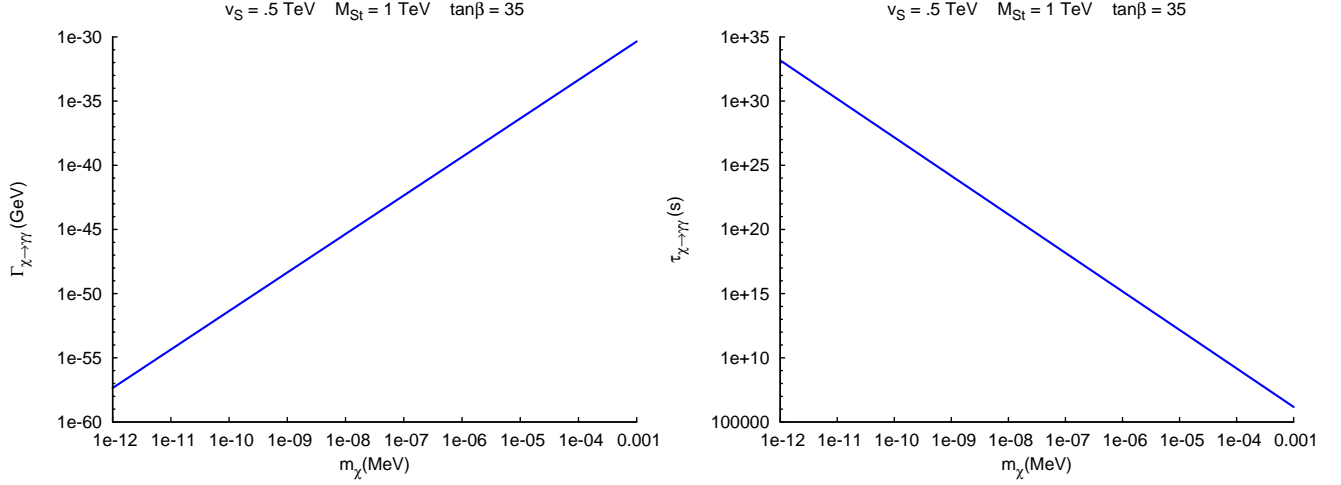


Figure 7: Decay amplitude (left panel) and mean lifetime (right panel) for $\chi \rightarrow \gamma\gamma$ as a function of the axi-Higgs mass.

In the PQ-like case, at the first misalignment, taking place at the electroweak scale, the physical axion is singled out as a component of $\text{Im } b$, with a mass which is practically zero, due to the small value of the curvature induced by the potential generated by electroweak instantons (Fig. 4, top) given in Eq. (74). In the case of a very small extra potential ($\lambda_{eff} \sim \lambda_{inst}$) it is the second misalignment to be responsible for generating an axion mass. At the second misalignment, taking place at the QCD phase transition, the mass of this pseudo Nambu-Goldstone mode is redefined from zero to a small but more significant value ($\sim 10^{-3}$ eV) induced by the QCD instantons ((Fig. 4, bottom). The final value of the mass is determined in terms of the hadronic scale Λ_{QCD} and of a second intermediate scale, M_{St}^2/v , which replaces f_a in all of the expressions usually quoted in the literature and held valid for PQ axions, as we are now going to clarify.

• MeV axion

For an MeV axion the situation is opposite, since it is the first misalignment that has to be held responsible for the generation of the axion mass. In this second case there is an overlap between the period of coherent oscillations at the QCD hadron transition and the typical lifetime at which the axion decays. This can be trivially checked by comparing the QCD time, defined as the inverse Hubble rate at the temperature of confinement ($H(T_{QCD}) \sim 10^{-11}$ eV, $T_{QCD} \sim 200$ MeV) $t_{QCD} \sim 10^{-4}$ sec with the axion lifetime in this typical mass range.

• PQ-like axion

For a PQ-like axion the effective scale (M_{St}^2/v) is the result of the product of two factors: a first factor due to the rotation matrix of the Stückelberg field $\text{Im } b$ onto χ - which is proportional to v/M - times a second factor ($1/M_{St}$) which is inherited from the original $\text{Im } b/M_{St} F\tilde{F}$ (WZ) counterterm. Specifically, starting from Eq. (73), the size of the projection of $\text{Im } b$ into χ is given by

$$\frac{1}{N_\chi} B_S g_B \sec \alpha (v^2 v_S^2 + v_1^2 v_2^2) \sim v/M_{St} \quad (104)$$

and hence a typical PQ interaction term involving the Stückelberg field b becomes

$$\frac{\text{Im } b}{M_{St}} FF' \rightarrow \frac{\chi}{M_{St}^2/v} FF'. \quad (105)$$

The physical component of b (i.e. χ), acquires an interaction to $F\tilde{F}$ which is suppressed by the scale M_{St}^2/v .

Having identified this scale, if we neglect the axion mass generated by V' (Eq. 74) at the electroweak scale, the final mass of the physical axion induced at the QCD scale is controlled by the ratio $m_\chi \sim \Lambda_{QCD}^2 v / M_{St}^2$, where the angle of misalignment is given by $\theta' = \chi v / M_{St}^2$.

Coming to the value of the abundances for a PQ-like axion - defined as the number density to entropy ratio $Y = n_\chi/s$ - these can be computed in terms of the relevant suppression scale appearing in the $\chi F\tilde{F}$ interaction. We have expanded on the structure of the computation in Appendix E. If we indicate with $\theta'(T_i)$ the angle of misalignment at the QCD hadron transition and with T_i the initial temperature at the beginning of the oscillations, the expression of the abundances takes the form

$$Y_\chi(T_i) = \left(\frac{v}{M_{St}} \right) \frac{45 M_{St}^2 (\theta'(T_i))^2}{2 \sqrt{5\pi g_{*,T}} T_i M_P}, \quad (106)$$

which depends linearly on M_{St} . As we have already mentioned, the computation of the relic densities for a non-thermal population follows rather closely the approach outlined in the non-supersymmetric case. For instance, a rather large value of M_{St} , of the order of 10^7 GeV [30], determines a sizeable contribution of the gauged axion to the relic densities of cold dark matter. These, in turn, follow rather closely the behaviour expected in the case of the PQ axion. In practice, to obtain a sizeable non-thermal populations of gauged axions, M_{St} should be such that $M_{St}^2/v \sim f_a$, with f_a the usual estimated size of the PQ axion decay constant. This allows a sizeable contribution of χ to the relic density of cold dark matter, with a partial contribution to Ω ($\Omega_\chi h^2 \sim 0.1$) in close analogy to what expected in the case of the PQ axion. These considerations, which are in close relations with what found in the non-supersymmetric construction [30], in this case will be subject to the constraints coming from the neutralino sector and its abundances, and on the acceptable values of the Stückelberg mass. These points will be analyzed in the next sections.

10 The spectrum in the neutralino sector

The neutralino sector is constructed from the eigenstates of the space spanned by the neutral fields $(-i\lambda_{W^3}, -i\lambda_Y, -i\lambda_B, \tilde{H}_1^1, \tilde{H}_2^2, \tilde{S}, -i\psi_{\mathbf{b}})$, which involve the three neutral gauginos, the two Higgsinos, the singlino (the fermion component of the singlet superfield) and the axino component of the Stückelberg supermultiplet. We denote with M_{χ_0} the corresponding mass matrix and we list its components in the appendix. The neutralino eigenstates of this mass matrix are labelled as $\tilde{\chi}_i^0$ ($i = 1, \dots, 7$) in the basis $\{-i\lambda_{W^3}, -i\lambda_Y, -i\lambda_B, \tilde{H}_1^1, \tilde{H}_2^2, \tilde{S}, -i\psi_{\mathbf{b}}\}$

$$\tilde{\chi}_i^0 = a_{i1} \lambda_{W^3} + a_{i2} \lambda_Y + a_{i3} \lambda_B + a_{i4} \tilde{H}_1^1 + a_{i5} \tilde{H}_2^2 + a_{i6} \tilde{S} + a_{i7} \psi_{\mathbf{b}}. \quad (107)$$

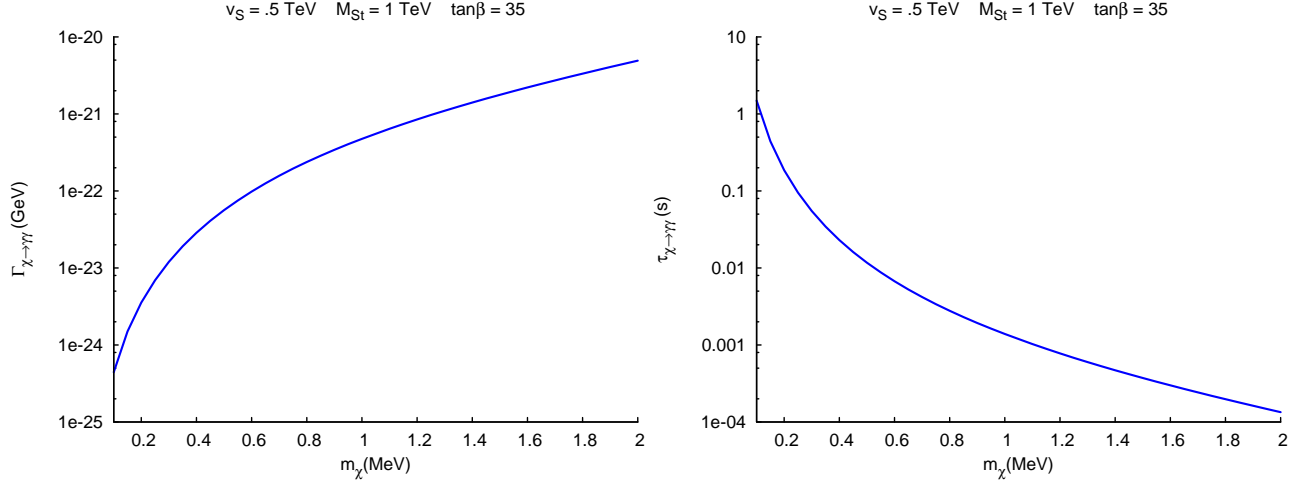


Figure 8: Decay amplitude and mean lifetime for $\chi \rightarrow \gamma\gamma$ as a function of the axi-Higgs mass for an axion whose mass in the MeV range.

We will also use the notation $c_{ij} = |a_{ij}|^2$ to denote the matrix of the components of the i -th neutralino (mass) eigenstate in the basis of the interaction eigenstates. They are ordered in mass and the lightest eigenstate corresponds to $i = 0$. We indicate with O^{χ^0} the rotation matrix that diagonalizes the neutralino mass matrix. In order to perform a numerical analysis of the model we need to fix some of the parameters, first of all requiring consistency of their choice with the masses of the Standard Model particles. For this purpose, the Higgs vev's v_1 and v_2 have been constrained in order to generate the correct mass values of the W^\pm , which depends on $v^2 = v_1^2 + v_2^2$, and of the Z gauge boson.

The ratio $\tan\beta = v_1/v_2$ has been set to 35. The Yukawa couplings have been fixed in order to give the correct masses of the SM fermions. The choice of v_S and of the parameter λ in the trilinear term $\lambda SH_1 \cdot H_2$ in the scalar potential has been made in order to obtain mass values in the Higgs sector in agreement with the limits from direct searches (with $\lambda \sim O(1)$). For this reason we have selected the values

$$\lambda = 0.3 \quad v_S = 0.4 \text{ TeV}, \quad (108)$$

and the assignment $B_{H_1} = -1, B_S = 1$ for the $U(1)_B$ charges of the Higgs and the singlet; $B_Q = 2$ for the quark doublet, and $B_L = 1$ for the lepton doublet. The supersymmetric parameters have been selected according to the relation

$$M_Y : M_W : M_G = 1 : 2 : 6, \quad (109)$$

having taken into account the unification condition for the gaugino masses. For simplicity we have set $M_{YB} \simeq M_Y$. As a further simplification, the sfermion mass parameters M_L, M_Q, m_R, m_D and m_U have been set to a unique value M_0 . We have also chosen a common value a_0 for the trilinear couplings a_e, a_d and a_u . With these choices the only free parameters left are the Stückelberg mass M_{St} , the gaugino mass

term for λ_B , denoted by M_B , and the axino mass term, M_b . Our choices are the following

$$\begin{aligned}
M_Y &= M_{YB} = 1 \text{ TeV} & M_W &= 2 \text{ TeV} & M_G &= 6 \text{ TeV} \\
M_L &= M_Q = m_R = m_D = m_U = M_0 = 0.9 \text{ TeV} \\
a_e &= a_d = a_u = a_0 = 0.8 \text{ TeV} \\
a_\lambda &= -100 \text{ GeV},
\end{aligned} \tag{110}$$

where with M_L and M_Q we have denoted the scalar mass terms for the sleptons and the squarks, assumed to be equal for all the 3 generations. We have also chosen

$$M_B = M_b = 1 \text{ TeV} \quad M_{St} = 1.4 \text{ TeV}, \tag{111}$$

with a coupling constant g_B of the anomalous $U(1)$ of 0.5. From previous investigations such values of the anomalous coupling are known to be compatible with LEP data at the Z resonance [52, 50]. In particular, the mass of the extra Z' satisfies the current constraints on the mass ($> 1 \text{ TeV}$) which make it compatible with actual searches of extra neutral currents. This parameter choice is our benchmark, which is compatible with all the SM requirements on the spectrum of the known particles. It involves SUSY breaking scales in a kinematical range which will be shortly under investigations at the LHC.

The tree-level spectrum obtained with this choice of the parameters is illustrated in Fig. 9. The plot displays the entire spectrum computed by a numerical diagonalization of all the mass matrices of the model, starting from the Higgs sector and then showing the mass spectrum of the Standard Model (SM) fermions, the W^\pm , Z and Z' gauge bosons, closing with the charginos, neutralinos, sleptons and squarks. The LSP is the lowest mass neutralino, denoted as χ_0^0 . The main features of this parameter choice correspond, on general grounds, to the selection of the TeV scale for the values of the SUSY breaking parameters, combined with a choice of the coupling of the anomalous $U(1)_B$ comparable, in size, with the $SU(2)$ coupling g_2 around the Z mass. The Stückelberg mass M_{St} is in principle free, and bound to be larger than approximately 1 TeV, since it is directly connected with the mass of the extra Z' gauge boson. We recall, as shown in Eq. (47), that $M_{Z'} \sim M_{St}$ due to the Stückelberg origin of the mass of the extra neutral gauge boson ([36] and [52]). The Z mass is also corrected, respect to the SM values, by $1/M_{St}$ contributions, which are compatible with precision data at LEP thanks to the presence of g_B as an independent parameter of the model.

Starting from the “focus point” or benchmark values fixed above, we can vary separately the three parameters M_B, M_b and M_{St} and investigate the neutralino sector in its components. The results of this numerical analysis of this spectrum are shown in the left panels of Figs. 10, 11, 12 where we vary these three parameters in the same range (0.5 TeV – 3 TeV). At the same time we show on the right panels of the same figures the i -th component c_{0i} of the lightest mass eigenvalue $\tilde{\chi}_0^0$. The mass of the lightest neutralino is always less than 100 GeV and is dominated by the singlino component, except at some special values, where the axino (ψ_b) and the bino (λ_B) components are enhanced. For instance, this is evident in Fig. 10 for $M_B \sim 2.3 \text{ TeV}$ (right panel) and in Fig. 11 for M_{St} around 0.9 TeV. More detailed 2-parameters studies of the neutralino mass as a function of two of the three scales of the model are shown in 3 panels presented in Fig. 13, where we vary, respectively, the pairs (M_B, M_b) , (M_{St}, M_B) and (M_{St}, M_b) . The

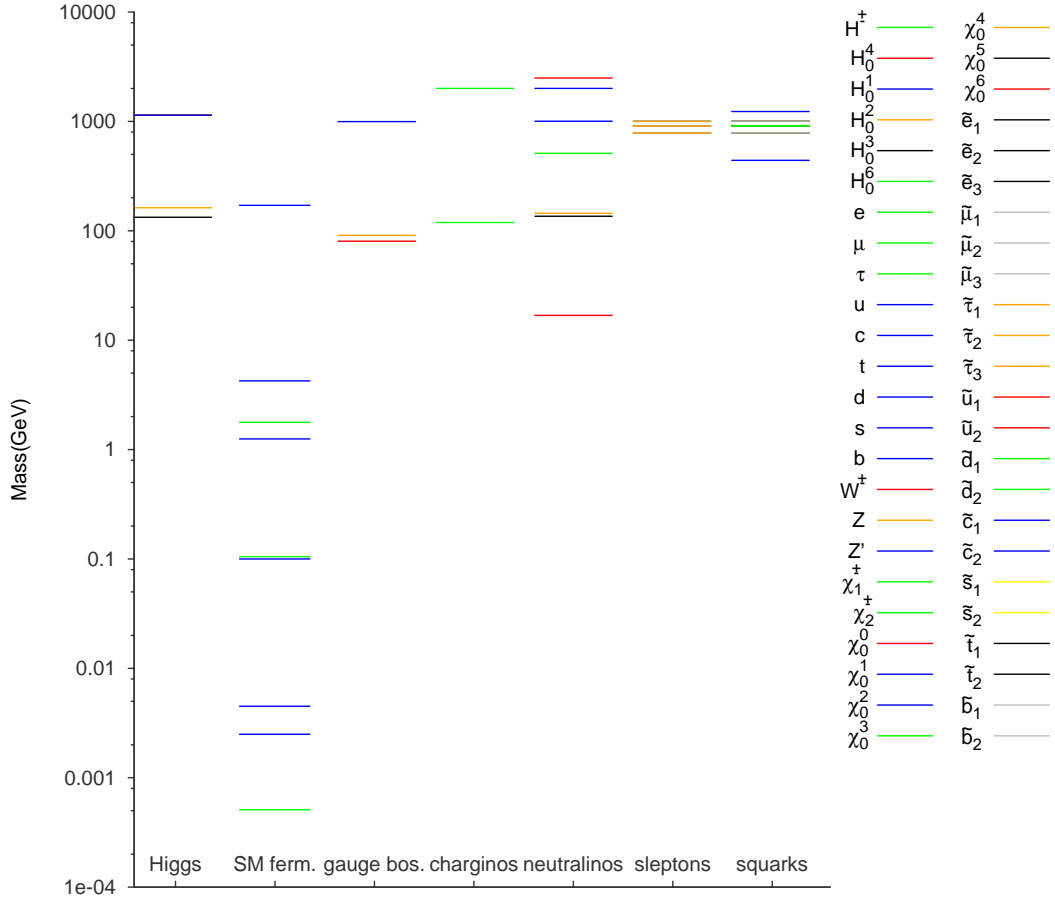


Figure 9: Mass spectrum of all the particles of the model obtained with the parameter values illustrated in Sec. 10

study shows clearly that the neutralino mass remains in an acceptable range, below the 100 GeV upper limit. This scenario, characterized by a low energy breaking of supersymmetry, contains features which are standard in most of the literature on supersymmetric models and is not much affected by variations on the specific values of the SUSY breaking parameters, as far as we select a breaking scale in the TeV region. We mention this point in order to be clear about the absolute generality of the benchmark values that we have chosen.

We will proceed with this choice of parameters to a complete simulation of the neutralino relic densities, trying to compare the values of such densities with the WMAP data [34].

11 Neutralino relic densities and cosmological bounds

As it is well known, the evaluation of the relic densities requires the calculation of a great number of thermally averaged cross sections, given the number of particles which are present. Before coming to the discussion of the results of this very involved analysis, which is summarized just in some simple plots of the relic densities of the lightest neutralino - as a function both of M_{St} and of the SUSY breaking scales M_b and M_B , - we present a general description of the structure of the interactions in the model. We also list the 2-to-2 processes that have been considered in the coupled Boltzmann equations.

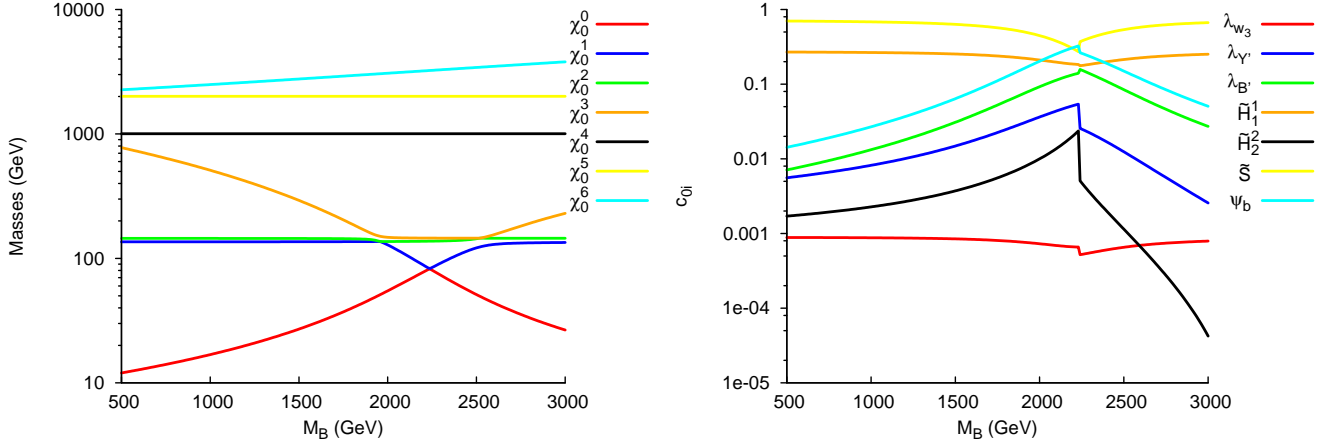


Figure 10: Neutralino masses (left panel) and components of the lightest neutralino (right panel) as functions of M_B . The neutralino is denoted as χ_0^0 and corresponds to the continuous red line. The dominant singlino component \tilde{S} (~ 1) is the continuous yellow line.

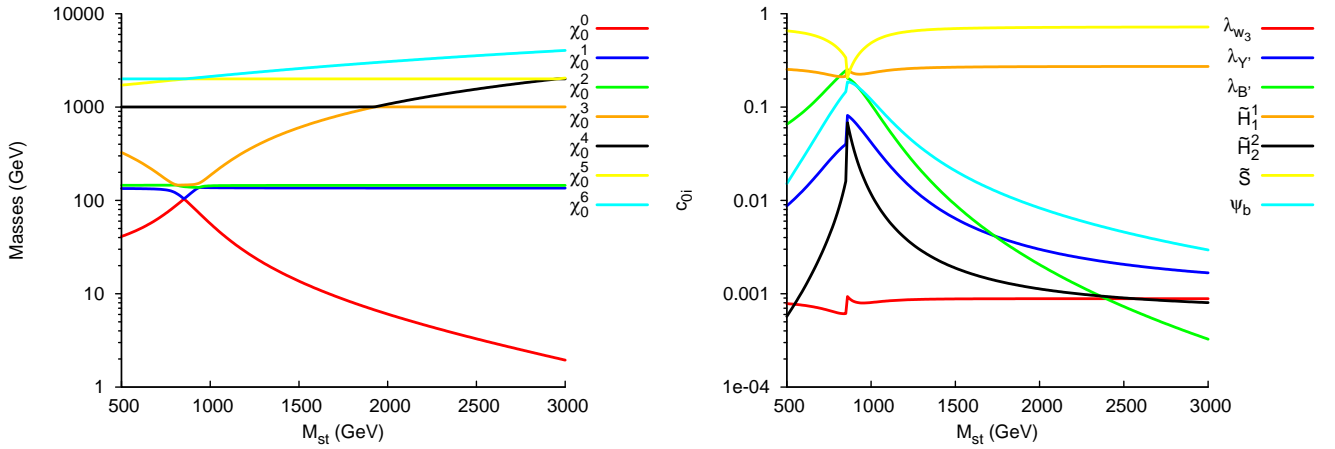


Figure 11: Masses of the neutralinos (left panel) and components of the LSP (right panel) as functions of M_{st}

We start from the action involving the physical axion (H_0^5) and its interactions with the various sectors. These involve, typically, interactions with the Higgs sector via bilinear vertices (proportional to $R^{H_0^5 HH}$), and trilinear ones (proportional to $R^{H_0^5 HHH}$) in H , with H denoting generically CP-even and CP-odd Higgs eigenstates. Other interactions in the same component of the Lagrangian involve axion-neutralino terms ($R^{H_0^5 \chi_i^0 \chi_j^0}$) plus axion-charginos ($R^{H_0^5 \chi_i^\pm \chi_j^\mp}$). Other terms are those involving interactions of the axion with the sleptons ($R^{H_0^5 \tilde{l}_i^\dagger \tilde{l}_j}$) and the squarks ($R^{H_0^5 \tilde{q}_i^\dagger \tilde{q}_j}$); vertices involving gauge bosons (for instance $R^{H_0^5 A \chi_i^\pm \chi_j^\mp}$, with a photon A and two charginos) and quartic contributions with 2, 3 and 4 axion lines.

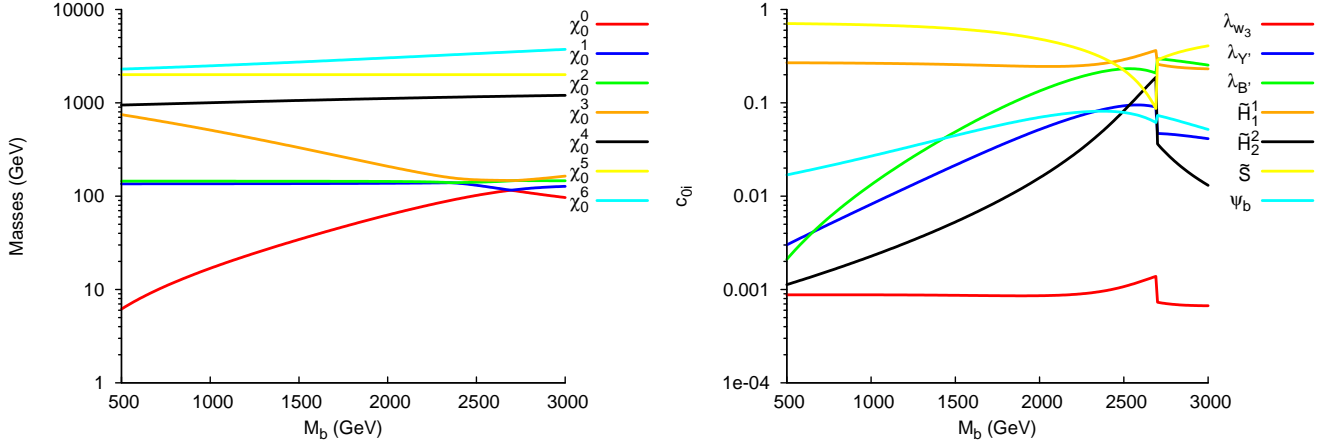


Figure 12: masses of the neutralinos (left panel) and components of the LSP (right panel) as functions of M_b

The Lagrangian describing all the tree-level interactions involving the axion is

$$\begin{aligned}
\mathcal{L}_{H_0^5-int} = & R^{H_0^5 H_0^4 H_0^i} H_0^5 H_0^4 H_0^i + R^{H_0^5 {}^2 H_0^i} (H_0^5)^2 H_0^i + R^{H_0^5 H_0^4 H_0^i H_0^j} H_0^5 H_0^4 H_0^i H_0^j + R^{H_0^5 {}^2 H_0^i H_0^j} (H_0^5)^2 H_0^i H_0^j + \\
& R^{H_0^5 H_0^4 {}^3 H_0^i} H_0^5 H_0^4 {}^3 H_0^i + R^{H_0^5 {}^2 H_0^4 {}^2} (H_0^5)^2 (H_0^4)^2 + R^{H_0^5 {}^3 H_0^4} (H_0^5)^3 H_0^4 + R^{H_0^5 {}^4} (H_0^5)^4 + \\
& R^{H_0^5 \chi_i^0 \chi_j^0} H_0^5 \chi_i^0 \chi_j^0 + R^{H_0^5 \chi_i^\pm \chi_j^\mp} H_0^5 \chi_i^\pm \chi_j^\mp + R^{H_0^5 \tilde{l}_i \tilde{l}_j} H_0^5 \tilde{l}_i^\dagger \tilde{l}_j + R^{H_0^5 \tilde{q}_i \tilde{q}_j} H_0^5 \tilde{q}_i^\dagger \tilde{q}_j + \\
& R^{H_0^5 A \chi_i^\pm \chi_j^\mp} H_0^5 A^\mu \bar{\chi}_i^\pm \gamma_\mu \chi_j^\mp + R^{H_0^5 Z \chi_i^\pm \chi_j^\mp} H_0^5 Z^\mu \bar{\chi}_i^\pm \gamma_\mu \chi_j^\mp + R^{H_0^5 Z' \chi_i^\pm \chi_j^\mp} H_0^5 Z'^\mu \bar{\chi}_i^\pm \gamma_\mu \chi_j^\mp + \\
& R^{H_0^5 W^\mp \chi_i^\pm \chi_j^0} H_0^5 W_\mu^\mp \bar{\chi}_j^0 \gamma^\mu \chi_i^\pm + R^{\chi_i^0 \chi_j^\pm H^\mp} H_0^5 \chi_i^0 \chi_j^\pm H^\mp + R^{\chi_i^0 \chi_j^0 H^4} \chi_i^0 \chi_j^0 H_0^5 H_0^4. \quad (112)
\end{aligned}$$

The explicit expressions of these vertices have been listed in Appendix D. Other interactions appearing in the interaction Lagrangian involve derivative couplings with the gauge bosons and the Higgses and they are given by

$$\begin{aligned}
\mathcal{L}_{H_0^5-int} = & R^{H_0^5 H^\pm W^\mp} H_0^5 W_\mu^\mp \partial^\mu H^\pm + R^{H_0^5 H_0^i A} H_0^5 A_\mu \partial^\mu H_0^i + R^{H_0^5 H_0^i Z} H_0^5 Z_\mu \partial^\mu H_0^i + \\
& R^{H_0^5 H_0^i Z'} H_0^5 Z'_\mu \partial^\mu H_0^i. \quad (113)
\end{aligned}$$

Similar interactions are also typical for H_0^4 , the CP-odd Higgs. Some of the vertices are illustrated in Fig. 14.

Besides the interaction with the axi-Higgs, we have the following vertices involving neutralinos

$$\begin{aligned}
\mathcal{L}_{\chi_0-int} = & R^{\chi_i^0 \chi_j^0 Z} Z^\mu \bar{\chi}_i^0 \gamma_\mu \chi_j^0 + R^{\chi_i^0 \chi_j^0 Z'} Z'^\mu \bar{\chi}_i^0 \gamma_\mu \chi_j^0 + R^{\chi_i^0 \chi_j^\pm W^\mp} W_\mu^\mp \bar{\chi}_i^0 \gamma_\mu \chi_j^\pm + R^{\chi_i^0 \chi_j^\pm H^\mp} H^\mp \bar{\chi}_i^0 \gamma_\mu \chi_j^\pm + \\
& R^{\chi_i^0 \chi_j^0 H_0^k} H_0^k \bar{\chi}_j^0 \gamma_\mu \chi_i^0 + R^{\chi_i^0 f \tilde{f}} \chi_i^0 f \tilde{f}_{1,2} + R^{\chi_i^0 \chi_j^\pm \tilde{q}^\dagger \tilde{q}} \chi_i^0 \chi_j^\pm \tilde{q}_k^\dagger \tilde{q}_l + R^{\chi_i^0 \chi_j^\pm \tilde{f}^\dagger \tilde{f}} \chi_i^0 \chi_j^\pm \tilde{f}_k^\dagger \tilde{f}_l + \\
& R^{\chi_i^0 \chi_j^\pm H^\mp H_0^k} \chi_i^0 \chi_j^\pm H^\mp H_0^k + R^{\chi_i^0 \chi_j^0 H_0^k H_0^l} \chi_i^0 \chi_j^0 H_0^k H_0^l + R^{\chi_i^0 \chi_j^0 H^\pm H^\mp} \chi_i^0 \chi_j^0 H^\pm H^\mp. \quad (114)
\end{aligned}$$

Some of these vertices are illustrated in Fig. 15.

These vertices, identified in configuration space, are converted into a form which can be input into LanHEP using our translator, which allows to automatize the procedure. LanHEP generates the files containing the informations on the spectrum and the interactions of the model. These files can then be fed into micrOMEGAs which computes the scattering cross section needed for the relic density calculation. The

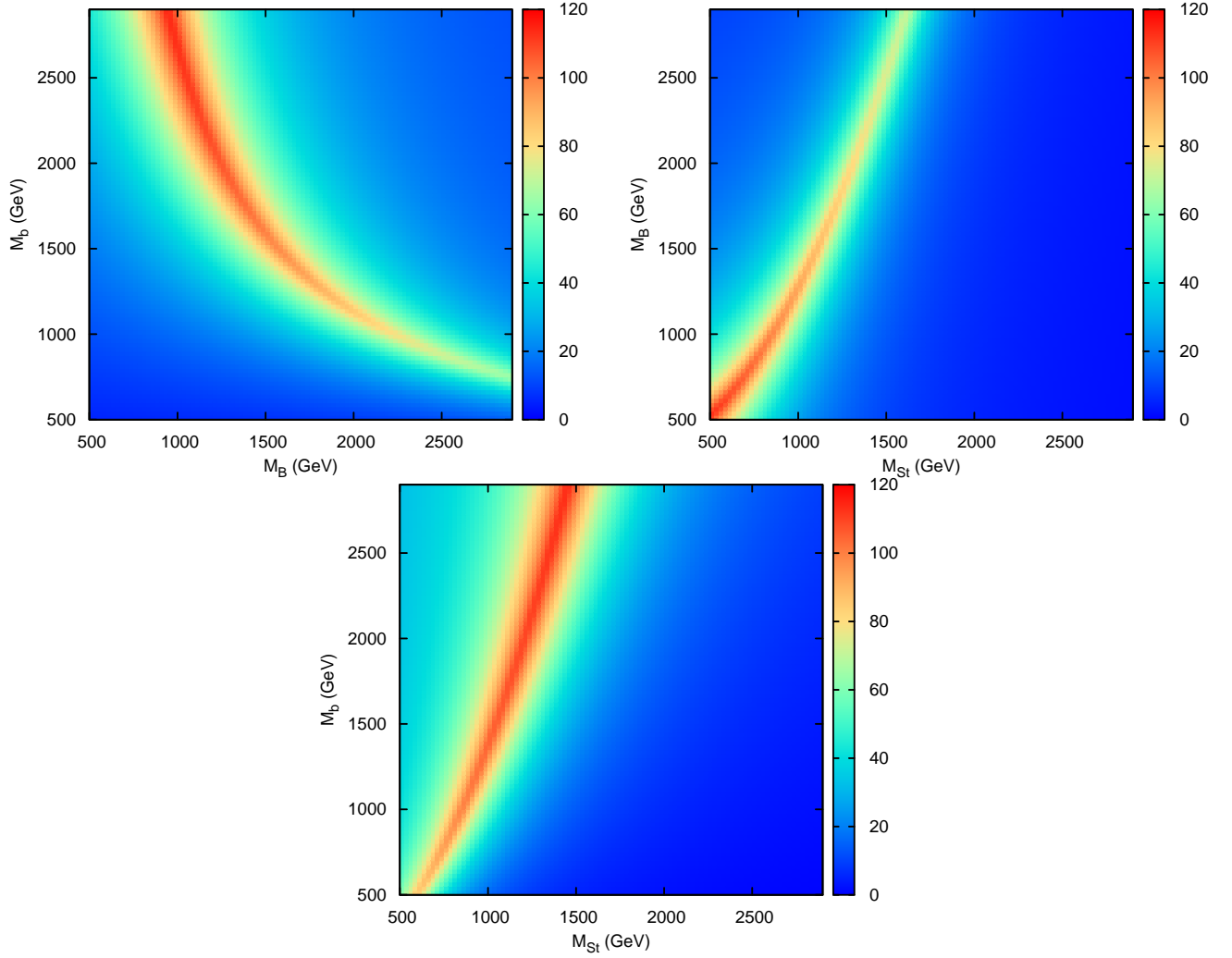


Figure 13: Mass of the LSP as a function of the combinations of the three pairs of two parameters, with the third fixed at the benchmark value.

program relies on CalcHEP for the actual computation of the 2-to-2 scatterings, according to the specified model files.

In Tab. 3 we show all the tree level annihilation processes in the different kinematical channels involving two neutralinos. These are the relevant processes for the computation of the relic densities. We show in Tab. 3 a list of the most relevant 2-to-2 processes which are generated in the s , t and u channels having neutralinos in the initial state (in), while the possible final states are shown on the right-hand side of the same table (out). The cross sections associated to these processes are then averaged with a Boltzmann distribution and inserted into the corresponding Boltzmann equations by micrOMEGAs, which allows us to obtain predictions for the relic densities of the LSP according to various scenarios.

The result of our simulation study are all contained in Fig. 16 where we plot the relic densities of the neutralino as functions of the SUSY breaking scales M_b and M_B and of the Stückelberg mass M_{St} . We show in green the regions characterized by large contributions coming from the co-annihilations of neutralinos. It appears evident, from a cursory glance at these plots, that the choice of 1.8-3 TeV for

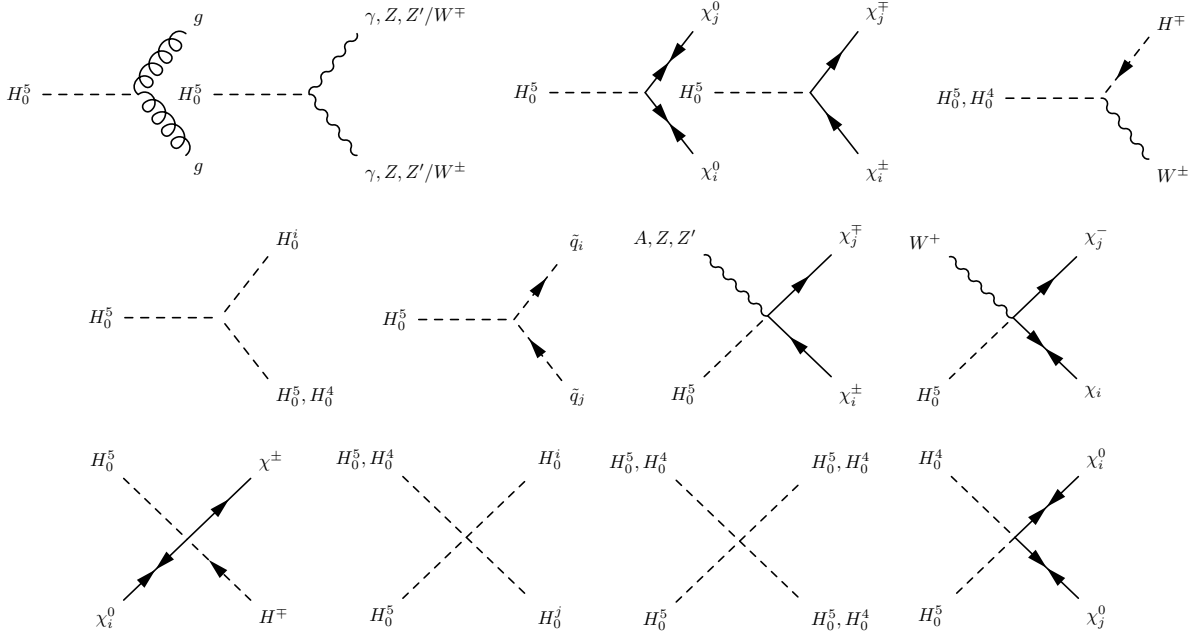


Figure 14: Axi-Higgs (H_0^5) interactions. The double arrows denote Majorana particles (neutralinos).

the allowed region of the SUSY breaking parameters appears consistent with the experimental bounds coming from WMAP on Ωh^2 . These bounds provide a robust estimate for the allowed contributions to the cosmological relic densities of our universe coming from dark matter, with $\Omega h^2 \sim 0.1$. The WMAP constraints at 2σ level are shown as horizontal tick lines in the plots of Fig. 16.

It is then clear, from this numerical analysis, that we can match this constraint, within a low energy scenario for supersymmetry breaking, only if the Stückelberg mass stays below the 1.5 TeV region. The bound appears to be rather robust and independent of the charge assignment chosen for the model. The constraints derived on the value of the Stückelberg mass indicate that in a rather standard scenario with low energy SUSY breaking it is not possible to increase arbitrarily this parameter without violating the WMAP bounds on dark matter. This constraint originates from the structure of the Stückelberg multiplet which induces a large matrix element in the neutralino mass matrix due to the mixing between the gaugino λ_B and the axino ψ_b which is proportional to M_{St} . As M_{St} grows, the neutralino becomes lighter and the contribution from the co-annihilation region tends to vanish. This is rather evident from Fig. 16, where the suppression of the relic densities generated by the co-annihilation is no longer efficient as M_{St} grows too large or too small compared to the SUSY breaking scale, which defines the size of the other parameters in the neutralino mass matrix.

12 Summary: windows on the axion mass

At this point, before coming to our conclusions, we can try to gather all the information that we have obtained so far in the previous sections, summarizing the basic properties of axions in these types of models.

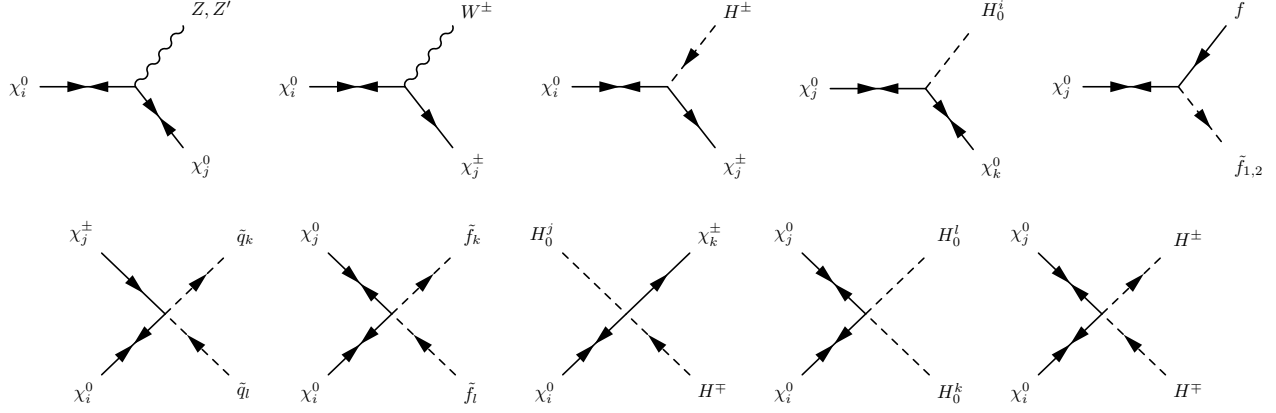


Figure 15: Neutralino interactions

in	s-channel	out
$\chi_i^0 \chi_j^0$	Z, Z'	$H^\pm H^\mp, H_0^k H_0^4, H_0^k H_0^5, Z/Z' H_0^k, \bar{f}f, \tilde{f}^\dagger \tilde{f}$
	H_0^k	$H^\pm H^\mp, H_0^l H_0^m, H_0^4 H_0^4, H_0^4 H_0^5, H_0^5 H_0^5, Z/Z' H_0^4/H_0^5, W^\pm H^\mp, Z/Z' Z/Z', W^\pm W^\mp, \bar{f}f, \tilde{f}^\dagger \tilde{f}$
	H_0^4, H_0^5	$H_0^k H_0^4, H_0^k H_0^5, Z/Z' H_0^k, W^\pm H^\mp, \bar{f}f, \tilde{f}^\dagger \tilde{f}$
in	t/u-channel	out
$\chi_i^0 \chi_j^0$	χ_k^0	$H_0^l H_0^m, H_0^l H_0^4/H_0^5, H_0^4/H_0^5 H_0^4/H_0^5, Z/Z' H_0^l/H_0^4/H_0^5, Z/Z' Z/Z'$
	χ_k^\pm	$W^\pm/H^\pm W^\mp/H^\mp$
	\tilde{f}	$\bar{f}f$

Table 3: Tree level neutralino annihilation processes in the 3 kinematic channels

• The milli-eV (PQ-like) axion

One possibility that we have explored in this work is that V' , the extra potential which is periodic in the axion field, may be generated around TeV scale or at the electroweak phase transition. The actual strength of the potential, remains, in our construction, undetermined and the physical features of the axion (primarily its mass), depend upon this parameter. We have tried to describe the various possibilities, in this respect, and the essential features for each choice for the value of the mass. In particular, if the extra potential is generated by non-perturbative effects at the electroweak phase transition, then the mass of the axion is tiny, and the true mechanism of misalignment which determines its mass takes place at a second stage, at the QCD phase transition. In this case the physical axion of the model would be no much different from an ordinary PQ axion and would be rather long-lived. At the same time, its abundances are fixed by the possible value of the scale M_{St}^2/v , which should be rather large ($\sim 10^{10} - 10^{12}$ GeV), of the same order of f_a in typical of axion models, to be a significant component of cold dark matter.

We have seen, however, that a complete simulation of the model (using current WMAP data) bounds the Stückelberg mass M_{St} to be around the TeV scale, indicating that the contribution to dark matter

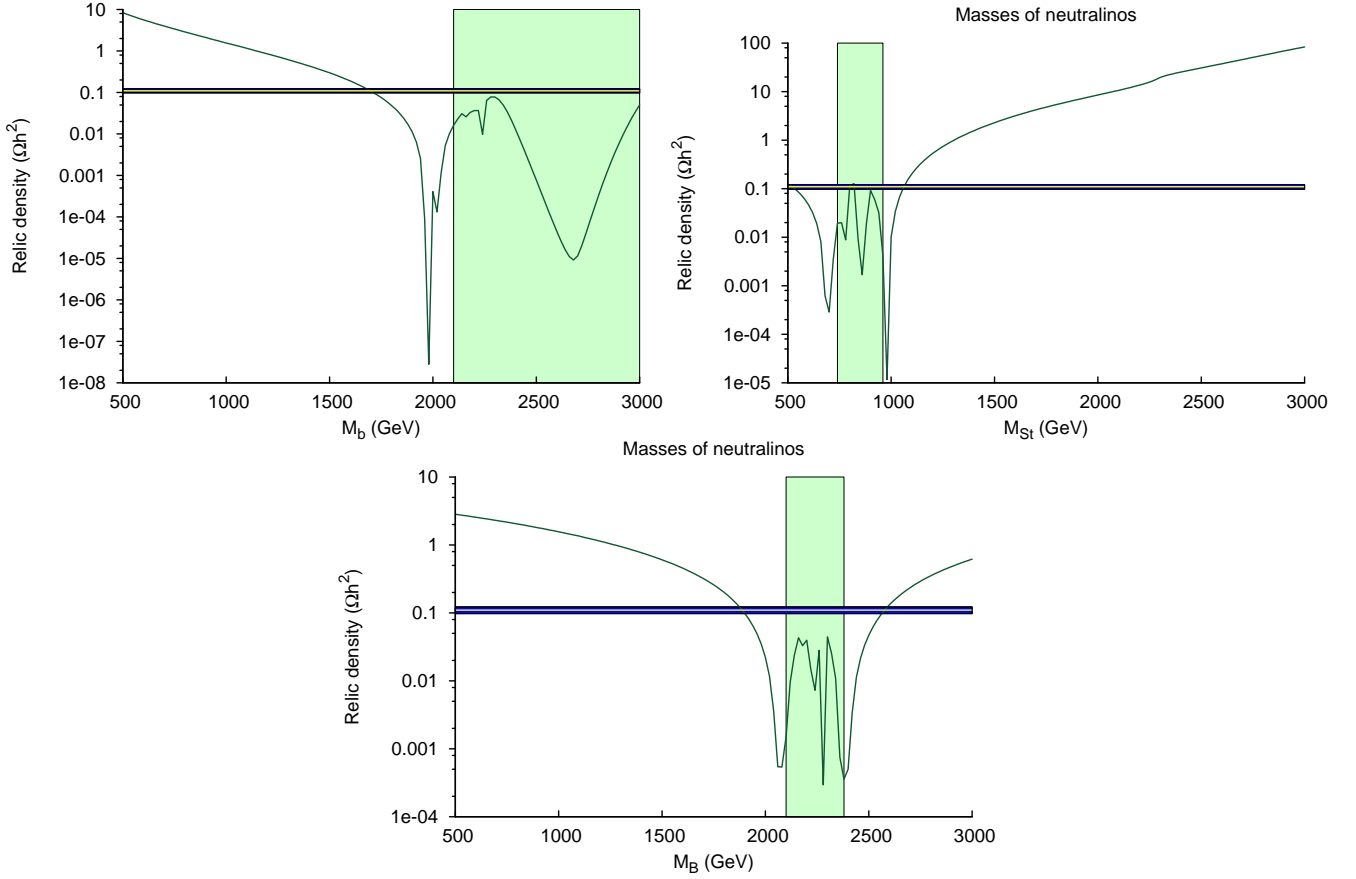


Figure 16: Relic density of the lightest neutralino as a function of M_{St} ; the horizontal line represents the physical dark matter density value extracted from WMAP data with its 2σ error bar

from misalignment of the axion field, in this case, should be small.

A second important constraint on this particle, in this mass range, comes from direct axion searches, which also requires the interaction of the axions with the gauge fields (in particular the photon) to be suppressed by a large f_a . For this reason, the strong upper bound on M_{St} emerging from our direct simulations, indicates that an axion of this mass, in fact, could be excluded by typical searches with detectors of Sikivie type. The reason is rather obvious, since axions in the milli-eV mass range could be copiously produced at the center of the sun and probably should have been seen by now in ground based detectors (helioscopes), such as CAST [53]. We recall that one of the goals of searches with helioscopes is to set a lower bound on the suppression scale f_a of the axion-photon vertex, which is currently experimentally constrained, as we have already mentioned, to be rather large.

However, given the new types of interactions of the axion present in this model respect to those of the standard PQ axion, which modify its interaction with a medium, this experimental exclusion limits on this mass window may not apply after all. In this respect, while the cosmological relic densities of this particle are small, they could be produced at current colliders and contribute to standard missing energy processes.

- **The meV axion**

A second possibility that we have investigated is that the extra potential appearing in the CP-odd sector is unrelated to instanton corrections in the electroweak vacuum. In this case the mass of the axion remains a free parameter. The range that we have explored in this second case involves an axion mass in the MeV region, discussing the several constraints that emerge from the model. In this case the axion is, in general, not long-lived and as such is not a component of dark matter. On the other hand, the constraints from CAST can be avoided, since the particle would not be produced at the center of the sun, being its mass above the keV range. Obviously, in this case other constraints emerge from nucleosynthesis requirements, since a particle in this mass range has to decay fast enough in order not to generate a late entropy release at nucleosynthesis time. We have seen that an axion in the MeV range is consistent with these two requirements. An axion of this type could be searched for at colliders, and in this respect the analysis of its possible detection at the LHC would follow quite closely the patterns described by two of us in [43]. As in this previous (non-supersymmetric) study, where the axion is Higgs-like (of a mass in the GeV region) typical channels where to look for this particle would be a) the associated production of an axion and a direct photon; b) the multi-axion production channel, and c) the associated production of one axion and other Higgses of the CP-even sector. The modifications, compared to that previous study, would now involve 1) the lower value of the mass of the axion (MeV rather than GeV); 2) the presence of extra supersymmetric interactions and, finally, 3) the bound on M_{St} which appears only in the supersymmetric case, being related to the neutralino sector.

13 Conclusions

The investigation of the phenomenological role played by models containing anomalous gauge interactions from abelian extensions of the Standard Model, we believe that will receive further attention in the future. These studies can be motivated within several scenarios, including string and supergravity theories, in which gauged axionic symmetries are introduced for anomaly cancellation. In turn, these modified mechanism of cancellation of the anomalies, which involve an anomalous fermion spectrum and an axion, are essentially connected with the UV completion of these field theories, which in a string framework are realized by the Green-Schwarz mechanism.

Our description, in a non-gravitational and, henceforth, rather simplified context, is supposed to capture some of the main features of these more general constructions. For this purpose, we have used the approach of the 1-loop (gauge invariant) effective action, constructed around a flat spacetime, but with the inclusion of supersymmetry.

The model that we have investigated (the USSM-A) summarizes the most salient physical features of these types of constructions, where a Stückelberg supermultiplet is associated to an anomalous abelian structure in order to restore the gauge invariance of the anomalous effective action. The Stückelberg supermultiplet is accompanied, for this reason, by supersymmetric Wess-Zumino interactions which induce local operators both of the form $\text{Re } b F F'$ and $\text{Im } b F \tilde{F}$, suppressed by the Stückelberg mass. Stückelberg mass terms for the anomalous gauge boson and for the saxion, and the mechanism of Higgs-axion mixing of the axion with the scalar CP-odd sector, remain the most salient features of this extension. It departs considerably from the USSM, and opens new scenarios for dark matter studies.

In this work we have tried to characterize in detail some among the main phenomenological implications of these models, which are particularly interesting for cosmology. The physical axion of this construction, or gauged axion, emerges as a component of the Stückelberg field $\text{Im } b$. We have pointed out that the mechanism of sequential misalignment, formerly discussed in the non-supersymmetric case [30], finds a natural application also in the presence of supersymmetry, with minor modifications.

One relevant feature of these models, already notice in [30], is that their axions do not contribute to the isocurvature perturbations of the early universe, being gauge degrees of freedom at the scale of inflation.

We have followed a specific pattern in order to come out with specific results in these types of models, using for this purpose a particular superpotential (the NMSSM superpotential with one extra singlet superfield), whose essential features, however, may well be generic.

Building on previous results in the MLSOM, here we have tried to generalize our reasonings in regard to the role of axions and neutralinos, which are present in the theory, by computing their cosmological relic densities.

We have presented an accurate study of such densities, showing that the Stückelberg mass, which coincides with the tree-level mass of the anomalous gauge boson, can't be larger than 1.5 TeV. Only in this case the WMAP constraints [34] on the contribution to Ω coming from dark matter can be satisfied. Thus, in these models, the Stückelberg scale is essentially constrained by cosmological considerations to lay around the supersymmetry breaking scale, here chosen around 1 TeV, and possibly not far from it.

Combined with the information coming from exclusion limits on extra neutral gauge bosons, which are around 0.9 TeV [35], the kinematical window for confirming scenarios of this type at the LHC could be experimentally close. Notice that such a value of the Stückelberg mass is a lower bound on the possible mass of the extra Z prime in this model, since the total mass of the new gauge boson would acquire an additional contribution coming from the standard Higgs mechanism.

We find this features rather interesting, for being essentially unique among models containing extra neutral currents and, furthermore, for being, unexpectedly, of cosmological origin.

Finally, we have seen that with a Stückelberg mass in the TeV range the non-thermal population of axions does not contribute significantly to the dark matter densities if these axions are PQ-like. These types of constraints, obviously, are typical of supersymmetric constructions and are avoided in a non-supersymmetric context. In this second case, as discussed in [30], a Stückelberg scale around 10^7 GeV is sufficient to revert this trend.

We have also pointed out that gauged axions in this mass range (milli-eV) are probably difficult to reconcile with current bounds from direct searches, while the case for detecting MeV or heavier axions, in these types of models, remains a wide open possibility. In this second case, cascade decays of these light particles and their associated production with photons should be seen as their possible event signatures at the LHC.

Acknowledgements

We thank Nikos Irges, George Lazarides and Antonio Racioppi for discussions. This work is supported in part by the European Union through the Marie Curie Research and Training Network UniverseNet (MRTN-CT-2006-035863).

A Appendix. D terms and kinetic mixing

After the rotation we have the following equations of motion for the abelian D-fields

$$\begin{aligned}
D_{Y'} = & g_Y \left(\frac{1}{2} H_1^\dagger H_1 - \frac{1}{2} H_2^\dagger H_2 + \frac{1}{2} \tilde{L}^\dagger \tilde{L} - \tilde{R}^\dagger \tilde{R} - \frac{1}{6} \tilde{Q}^\dagger \tilde{Q} + \frac{2}{3} \tilde{U}_R^\dagger \tilde{U}_R - \frac{1}{3} \tilde{D}_R^\dagger \tilde{D}_R \right) + \\
& \frac{c_Y}{M_{St}} \left(\frac{1}{\sqrt{2}} \tan \alpha (\lambda_{B'} \psi_{\mathbf{b}} + \bar{\lambda}_{B'} \bar{\psi}_{\mathbf{b}}) - \frac{1}{\sqrt{2}} (\lambda_{Y'} \psi_{\mathbf{b}} + \bar{\lambda}_{Y'} \bar{\psi}_{\mathbf{b}}) \right) - \\
& \frac{1}{\sqrt{2}} \frac{c_{YB}}{M_{St}} \sec \alpha (\lambda_{B'} \psi_{\mathbf{b}} + \bar{\lambda}_{B'} \bar{\psi}_{\mathbf{b}}) - 4 \frac{c_{YB}}{M_{St}} D_{B'} \text{Re} b \sec \alpha - \xi_Y; \\
D_{B'} \sec \alpha = & -g_Y \tan \alpha \left(\frac{1}{2} H_1^\dagger H_1 - \frac{1}{2} H_2^\dagger H_2 + \frac{1}{2} \tilde{L}^\dagger \tilde{L} - \tilde{R}^\dagger \tilde{R} - \frac{1}{6} \tilde{Q}^\dagger \tilde{Q} + \frac{2}{3} \tilde{U}_R^\dagger \tilde{U}_R - \frac{1}{3} \tilde{D}_R^\dagger \tilde{D}_R \right) + \\
& -\frac{1}{2} g_B \sec \alpha \left(B_{H_1} H_1^\dagger H_1 + B_{H_2} H_2^\dagger H_2 + B_S S^\dagger S + B_L \tilde{L}^\dagger \tilde{L} - B_R \tilde{R}^\dagger \tilde{R} + B_Q \tilde{Q}^\dagger \tilde{Q} - \right. \\
& \left. B_{U_R} \tilde{U}_R^\dagger \tilde{U}_R - B_{D_R} \tilde{D}_R^\dagger \tilde{D}_R \right) + \frac{1}{\sqrt{2}} \frac{c_Y}{M_{St}} \tan \alpha \left[\lambda_{Y'} \psi_{\mathbf{b}} + \bar{\lambda}_{Y'} \bar{\psi}_{\mathbf{b}} - \tan \alpha (\lambda_{B'} \psi_{\mathbf{b}} + \bar{\lambda}_{B'} \bar{\psi}_{\mathbf{b}}) \right] + \\
& \frac{c_{YB}}{M_{St}} \sec \alpha \left[\sqrt{2} \tan \alpha (\lambda_{B'} \psi_{\mathbf{b}} + \bar{\lambda}_{B'} \bar{\psi}_{\mathbf{b}}) - \frac{1}{\sqrt{2}} (\lambda_{Y'} \psi_{\mathbf{b}} + \bar{\lambda}_{Y'} \bar{\psi}_{\mathbf{b}}) \right] - \frac{1}{\sqrt{2}} \frac{c_B}{M_{St}} \sec^2 \alpha (\lambda_{B'} \psi_{\mathbf{b}} + \bar{\lambda}_{B'} \bar{\psi}_{\mathbf{b}}) \\
& - M_{St} \text{Re} b \sec \alpha - 4 \frac{c_{YB}}{M_{St}} D_{Y'} \text{Re} b \sec \alpha + 8 \frac{c_{YB}}{M_{St}} D_{B'} \text{Re} b \sec \alpha \tan \alpha + \tan \alpha \xi_Y - \sec \alpha \xi_B. \quad (115)
\end{aligned}$$

B Appendix. Scalar CP even sector

In the basis $(\text{Re} H_1^1, \text{Re} H_2^2, \text{Re} S, \text{Re} b)$ we have the following mass matrix

$$\begin{aligned}
M_{even \ 11}^2 = & \frac{1}{2} v_1^2 (g^2 + g_B^2 B_{H_1}^2) - a_\lambda \frac{v_2 v_S}{v_1}, \\
M_{even \ 12}^2 = & \frac{1}{2} [v_1 v_2 (g_B^2 B_{H_1} B_{H_2} - g^2 + 4\lambda^2) + 2a_\lambda v_S], \\
M_{even \ 13}^2 = & v_1 v_S \left(\frac{1}{2} g_B^2 B_{H_1} B_S + 2\lambda^2 \right) + a_\lambda v_2, \\
M_{even \ 14}^2 = & \frac{g_B v_1}{\sqrt{2}} \left[M_{St} B_{H_1} - 2 \frac{c_{YB}}{M_{St}} g_Y (2B_{H_1} v_1^2 - B_{H_1} v_2^2 + B_{H_2} v_2^2 + B_S v_S^2) \right], \\
M_{even \ 22}^2 = & \frac{1}{2} v_2^2 (g^2 + g_B^2 B_{H_1}^2) - a_\lambda \frac{v_1 v_S}{v_2}, \\
M_{even \ 23}^2 = & v_2 v_S \left(\frac{1}{2} g_B^2 B_{H_2} B_S + 2\lambda^2 \right) + a_\lambda v_1, \\
M_{even \ 24}^2 = & \frac{1}{\sqrt{2}} g_B v_2 \left[M_{St} B_{H_2} + 2 \frac{c_{YB}}{M_{St}} g_Y (B_{H_1} v_1^2 - B_{H_2} v_1^2 + 2B_{H_2} v_2^2 + B_S v_S^2) \right], \\
M_{even \ 33}^2 = & \frac{1}{2} g_B^2 B_S^2 v_S^2 - a_\lambda \frac{v_1 v_2}{v_S}, \\
M_{even \ 34}^2 = & \frac{1}{2} g_B B_S v_S \left[M_{St} - \frac{c_{YB}}{M_{St}} g_Y (v_1^2 - v_2^2) \right], \\
M_{even \ 44}^2 = & 4 \frac{c_{YB}^2}{M_{St}^2} \left[g_Y^2 (v_1^2 - v_2^2)^2 + g_B^2 (B_{H_1} v_1^2 + B_{H_2} v_2^2 + B_S v_S^2)^2 \right] - 4g_Y c_{YB} (v_1^2 - v_2^2) + M_{St}^2. \quad (116)
\end{aligned}$$

This matrix has been obtained setting the kinetic mixing α and the Fayet-Iliopoulos parameter ξ_Y and ξ_B to zero. The diagonalization of this matrix is performed numerically and with our parameter choice we get a state that has a dominant saxion component and a mass of the order of the Stückelberg scale. The rotation matrix is implicitly defined as

$$\begin{pmatrix} H_0^1 \\ H_0^2 \\ H_0^3 \\ H_0^b \end{pmatrix} = O^{ev} \begin{pmatrix} \text{Re}H_1^1 \\ \text{Re}H_2^2 \\ \text{Re}S \\ \text{Re}b \end{pmatrix}. \quad (117)$$

We have defined as H_0^b the CP-even physical state which, given the parameter values (see Sec. 10), consists essentially of the saxion field $\text{Re}b$.

C Appendix. Mass matrices and kinetic mixing

In the sections that follow we show the structure of the mass matrices in the presence of the kinetic mixing between the two abelian gauge factors.

C.1 Mass matrices of the neutral gauge boson

After electroweak symmetry breaking, the mass matrix of the neutral sector in the basis $(V_\mu^3, A_\mu^{Y'}, B'_\mu)$ is given by

$$\begin{aligned} M_{gauge\ 11}^2 &= -\frac{1}{4}g_2^2 v^2 & M_{gauge\ 12}^2 &= \frac{1}{4}g_2 g_Y v^2 & M_{gauge\ 13}^2 &= -\frac{1}{4}g_2 \sec \alpha [x_B + g_Y v^2 \sin \alpha] \\ M_{gauge\ 22}^2 &= -\frac{1}{4}g_Y^2 v^2 & M_{gauge\ 23}^2 &= \frac{1}{4}g_Y \sec \alpha [x_B + g_Y v^2 \sin \alpha] \\ M_{gauge\ 33}^2 &= \frac{1}{4}(-4M_{st}^2 - N_{BB} \sec^2 \alpha - g_Y^2 v^2 \tan^2 \alpha - 2x_B g_Y \sec \alpha \tan \alpha). \end{aligned} \quad (118)$$

The eigenvalues are given by Eq. (45).

C.2 Sfermion sectors

In the expressions that follow we understand the generation and family indices for squarks and sleptons. The sfermion sectors are affected by the presence of the mixing and FI. Looking at the **slepton sector**,

in the basis $(\tilde{L}^2, \tilde{R}^\dagger)$ we have the following mass matrix

$$\begin{aligned}
M_{\tilde{l}11}^2 &= \frac{1}{16} \sec^2 \alpha \left\{ 8m_l^2 + (-g_2^2 + 2g_Y^2 + 2g_B^2 B_{H_1} B_L) v_1^2 + (g_2^2 - 2g_Y^2 + 2g_B^2 B_{H_2} B_L) v_2^2 + 2g_B^2 B_L B_S v_S^2 + \right. \\
&\quad \left. 4v_1^2 y_e^2 + 8g_B B_L \xi_B - 8g_Y \xi_Y + [(v_2^2 - v_1^2) g_2^2 + 8m_l^2 + 4v_1^2 y_e^2] \cos 2\alpha + \right. \\
&\quad \left. 2 \sin \alpha [4g_Y \xi_B + g_B g_Y (B_{H_1} v_1^2 + B_L v_1^2 + B_{H_2} v_2^2 - B_L v_2^2 + B_S v_S^2) - 4B_L g_B \xi_Y] \right\}, \\
M_{\tilde{l}12}^2 &= \frac{1}{2} \left(\sqrt{2} a_e v_1 - \lambda v_2 v_S y_e \right), \\
M_{\tilde{l}22}^2 &= \frac{1}{8} \sec^2 \alpha \left\{ 4m_R^2 + (2y_e^2 - 2g_Y^2 - g_B^2 B_{H_1} B_R) v_1^2 + (2g_Y^2 - g_B^2 B_{H_2} B_R) v_2^2 - g_B^2 B_R B_S v_S^2 - \right. \\
&\quad \left. 4g_B B_R \xi_B + 8g_Y \xi_Y + 2 \cos 2\alpha (2m_R^2 + v_1^2 y_e^2) - [8g_Y \xi_B + g_B g_Y \sin \alpha (2B_{H_1} v_1^2 + B_R v_1^2 + \right. \\
&\quad \left. 2B_{H_2} v_2^2 - B_R v_2^2 + 2B_S v_S^2) - 4g_B B_R \xi_Y] \right\}. \tag{119}
\end{aligned}$$

This matrix can be easily diagonalized with a rotation matrix parametrized by a single angle given by

$$\tan 2\theta_{\tilde{l}} = \frac{2M_{\tilde{l}12}^2}{M_{\tilde{l}22}^2 - M_{\tilde{l}11}^2}; \tag{120}$$

the rotation matrix is defined as follows

$$\begin{pmatrix} \tilde{l}_1 \\ \tilde{l}_2 \end{pmatrix} = O^{\tilde{l}} \begin{pmatrix} \tilde{L}^2 \\ \tilde{R}^\dagger \end{pmatrix} \quad O^{\tilde{l}} = \begin{pmatrix} \sin \theta_{\tilde{l}} & \cos \theta_{\tilde{l}} \\ \cos \theta_{\tilde{l}} & -\sin \theta_{\tilde{l}} \end{pmatrix}. \tag{121}$$

The mass parameter for the third slepton state can be obtained directly from the Lagrangian. We obtain

$$\begin{aligned}
M_{\tilde{l}3}^2 &= \frac{1}{16} \sec^2 \alpha \left\{ 8m_l^2 + (-g_2^2 + 2g_Y^2 + 2g_B^2 B_{H_1} B_L) v_1^2 + (g_2^2 - 2g_Y^2 + 2g_B^2 B_{H_2} B_L) v_2^2 + 2g_B^2 B_L B_S v_S^2 + \right. \\
&\quad \left. 4v_1^2 y_e^2 + 8g_B B_L \xi_B - 8g_Y \xi_Y + [(v_2^2 - v_1^2) g_2^2 + 8m_l^2 + 4v_1^2 y_e^2] \cos 2\alpha + \right. \\
&\quad \left. 2 \sin \alpha [4g_Y \xi_B + g_B g_Y (B_{H_1} v_1^2 + B_L v_1^2 + B_{H_2} v_2^2 - B_L v_2^2 + B_S v_S^2) - 4B_L g_B \xi_Y] \right\}. \tag{122}
\end{aligned}$$

We recall that the family index is understood.

Now we will consider the **squark sector**. In the basis $(\tilde{Q}_2, \tilde{D}_R^\dagger)$ we obtain the mass matrix

$$\begin{aligned}
M_{\tilde{d}11}^2 &= \frac{1}{48} \sec^2 \alpha \left\{ 24m_Q^2 + (-3g_2^2 - 2g_Y^2 + 6g_B^2 B_{H_1} B_Q) v_1^2 + (3g_2^2 + 2g_Y^2 + 6g_B^2 B_{H_2} B_Q) v_2^2 + \right. \\
&\quad \left. 6g_B^2 B_Q B_S v_S^2 + 12v_1^2 y_d^2 + 24g_B B_Q \xi_B + 8g_Y \xi_Y + 3[(v_2^2 - v_1^2) g_2^2 + 8m_Q^2 + 4v_1^2 y_d^2] \cos 2\alpha - \right. \\
&\quad \left. 2 \sin \alpha [4g_Y \xi_B + g_B g_Y (B_{H_1} v_1^2 - 3B_Q v_1^2 + B_{H_2} v_2^2 + 3B_Q v_2^2 + B_S v_S^2) + 12g_B B_Q \xi_Y] \right\}, \\
M_{\tilde{d}12}^2 &= \frac{1}{2} \left(\sqrt{2} a_d v_1 - \lambda v_2 v_S y_d \right), \\
M_{\tilde{d}22}^2 &= \frac{1}{24} \sec^2 \alpha \left\{ 12m_{D_R}^2 - (2g_Y^2 + 3g_B^2 B_{D_R} B_{H_1}) v_1^2 + (2g_Y^2 v_2^2 - 3g_B^2 B_{D_R} B_{H_2}) v_2^2 - 3g_B^2 B_{D_R} B_S v_S^2 + \right. \\
&\quad \left. 6v_1^2 y_d^2 - 12g_B B_{D_R} \xi_B + 8g_Y \xi_Y + 6(2m_{D_R}^2 + v_1^2 y_d^2) \cos 2\alpha - [8g_Y \xi_B + \right. \\
&\quad \left. g_B g_Y (3B_{D_R} v_1^2 + 2B_{H_1} v_1^2 - 3B_{D_R} v_2^2 + 2B_{H_2} v_2^2 + 2B_S v_S^2) - 12g_B B_{D_R} \xi_Y] \sin \alpha \right\}. \tag{123}
\end{aligned}$$

The other two squark states can be extracted from the mass matrix in the basis $(\tilde{Q}_1, \tilde{U}_R^\dagger)$

$$\begin{aligned}
M_{\tilde{u}}^2{}_{11} &= \frac{1}{48} \sec^2 \alpha \left\{ 24m_Q^2 + (3g_2^2 - 2g_Y^2 + 6g_B^2 B_{H_1} B_Q) v_1^2 + (-3g_2^2 + 2g_Y^2 + 6g_B^2 B_{H_2} B_Q) v_2^2 + \right. \\
&\quad \left. 6g_B^2 B_Q B_S v_S^2 + 12v_2^2 y_u^2 + 24g_B B_Q \xi_B + 8g_Y \xi_Y + 3[(v_1^2 - v_2^2) g_2^2 + 8m_Q^2 + 4v_2^2 y_u^2] \cos 2\alpha - \right. \\
&\quad \left. 2 \sin \alpha [4g_Y \xi_B + g_B g_Y (B_{H_1} v_1^2 - 3B_Q v_1^2 + B_{H_2} v_2^2 + 3B_Q v_2^2 + B_S v_S^2) + 12g_B B_Q \xi_Y] \right\}, \\
M_{\tilde{u}}^2{}_{12} &= \frac{1}{2} \left(\lambda v_1 v_S y_u - \sqrt{2} a_u v_2 \right), \\
M_{\tilde{u}}^2{}_{22} &= \frac{1}{24} \sec^2 \alpha \left\{ 12m_{U_R}^2 + (4g_Y^2 - 3g_B^2 B_{H_1} B_{U_R}) v_1^2 - (4g_Y^2 + 3g_B^2 B_{H_2} B_{U_R}) v_2^2 - 3g_B^2 B_S B_{U_R} v_S^2 + \right. \\
&\quad \left. 6v_2^2 y_u^2 - 12g_B B_{U_R} \xi_B - 16g_Y \xi_Y + 6(2m_{U_R}^2 + v_2^2 y_u^2) \cos 2\alpha + [16g_Y \xi_B + g_B g_Y (4B_{H_1} v_1^2 - \right. \\
&\quad \left. 3B_{U_R} v_1^2 + 4B_{H_2} v_2^2 + 3B_{U_R} v_2^2 + 4B_S v_S^2) + 12g_B B_{U_R} \xi_Y] \sin \alpha \right\}. \tag{124}
\end{aligned}$$

The diagonalization of these matrices is analogous to that of the sleptons mass matrix; the angles that define the rotation on the physical basis can be easily defined following Eq. (120).

C.3 Neutralino sector and kinetic mixing

Now we turn to the neutralino sector; the mass matrix in the basis $(\lambda_{w_3}, \lambda_Y, \lambda_B, -i\tilde{H}_1^1, -i\tilde{H}_2^2, -i\tilde{S}, \psi_{\mathbf{b}})$ takes the form

$$M_{\chi^0} = \begin{pmatrix} M_{\chi^0}^{11} & 0 & 0 & M_{\chi^0}^{14} & M_{\chi^0}^{15} & 0 & M_{\chi^0}^{17} \\ \cdot & M_{\chi^0}^{22} & M_{\chi^0}^{23} & M_{\chi^0}^{24} & M_{\chi^0}^{25} & 0 & M_{\chi^0}^{27} \\ \cdot & \cdot & M_{\chi^0}^{33} & M_{\chi^0}^{34} & M_{\chi^0}^{35} & M_{\chi^0}^{36} & M_{\chi^0}^{37} \\ \cdot & \cdot & \cdot & 0 & M_{\chi^0}^{45} & M_{\chi^0}^{46} & 0 \\ \cdot & \cdot & \cdot & \cdot & 0 & M_{\chi^0}^{56} & 0 \\ \cdot & \cdot & \cdot & \cdot & \cdot & 0 & 0 \\ \cdot & \cdot & \cdot & \cdot & \cdot & \cdot & M_{\chi^0}^{77} \end{pmatrix} \tag{125}$$

with

$$\begin{aligned}
M_{\chi^0}^{11} &= \frac{M_w}{2} & M_{\chi^0}^{14} &= -\frac{g_2 v_1}{4} & M_{\chi^0}^{15} &= \frac{g_2 v_2}{4} & M_{\chi^0}^{17} &= -\frac{b_W g_2 (v_2^2 - v_1^2)}{64\sqrt{2}} \\
M_{\chi^0}^{22} &= \frac{M_Y}{2} & M_{\chi^0}^{23} &= \frac{1}{4} M_{YB} \sec \alpha & M_{\chi^0}^{24} &= \frac{g_Y v_1}{4} & M_{\chi^0}^{25} &= -\frac{g_Y v_2}{4} \\
M_{\chi^0}^{27} &= -\frac{1}{8\sqrt{2}} \sec^2 \alpha \left\{ -\frac{c_{YB}}{M_{St}} (g_B B_{H_1} v_1^2 + g_B B_{H_2} v_2^2 + g_B B_S v_S^2 + 4\xi_B) + \frac{c_Y}{M_{St}} [(v_1^2 - v_2^2) g_Y - 4\xi_Y] + \right. \\
&\quad \left. \sin \alpha \left\{ \frac{c_Y}{M_{St}} (g_B B_{H_1} v_1^2 + g_B B_{H_2} v_2^2 + g_B B_S v_S^2 + 4\xi_B) + \frac{c_{YB}}{M_{St}} [(v_2^2 - v_1^2) g_Y + 4\xi_Y] \right\} \right\} \\
M_{\chi^0}^{33} &= \frac{1}{2} (M_B - M_{YB} \sec \alpha \tan \alpha) & M_{\chi^0}^{34} &= -\frac{1}{4} v_1 \sec \alpha (g_B B_{H_1} + g_Y \sin \alpha) \\
M_{\chi^0}^{35} &= -\frac{1}{4} v_2 \sec \alpha (g_B B_{H_2} - g_Y \sin \alpha) \\
M_{\chi^0}^{36} &= -\frac{1}{4} g_B B_S v_S \sec \alpha
\end{aligned}$$

$$\begin{aligned}
M_{\chi^0}^{37} = & \frac{1}{16\sqrt{2}} \sec^3 \alpha \{ (-3 \frac{c_{YB}}{M_{St}} g_Y + 2 \frac{c_B}{M_{St}} g_B B_{H_1} + \frac{c_Y}{M_{St}} g_B B_{H_1}) v_1^2 + (3 \frac{c_{YB}}{M_{St}} g_Y + 2 \frac{c_B}{M_{St}} g_B B_{H_2} + \frac{c_Y}{M_{St}} g_B B_{H_2}) v_2^2 + \\
& (2 \frac{c_B}{M_{St}} g_B B_S + \frac{c_Y}{M_{St}} g_B B_S) v_S^2 + 4 M_{st} + 8 \frac{c_B}{M_{St}} \xi_B + 4 \frac{c_Y}{M_{st}} \xi_B + 12 \frac{c_{YB}}{M_{St}} \xi_Y + \\
& \cos 2\alpha \{ 4 M_{st} - \frac{c_Y}{M_{St}} (g_B B_{H_1} v_1^2 + g_B B_{H_2} v_2^2 + g_B B_S v_S^2 + 4 \xi_B) + \frac{c_{YB}}{M_{St}} [(v_1^2 - v_2^2) g_Y - 4 \xi_Y] \} + \\
& 2 \sin \alpha \{ -2 \frac{c_{YB}}{M_{St}} (g_B B_{H_1} v_1^2 + g_B B_{H_2} v_2^2 + g_B B_S v_S^2 + 4 \xi_B) + (\frac{c_Y}{M_{St}} + \frac{c_B}{M_{St}}) [(v_1^2 - v_2^2) g_Y - 4 \xi_Y] \} \} \\
M_{\chi^0}^{45} = & -\frac{\lambda v_S}{2\sqrt{2}} \quad M_{\chi^0}^{46} = -\frac{\lambda v_2}{2\sqrt{2}} \quad M_{\chi^0}^{56} = -\frac{\lambda v_1}{2\sqrt{2}} \quad M_{\chi^0}^{77} = \frac{M_b}{2}
\end{aligned} \tag{126}$$

The rotation matrix for this sector is implicitly defined as O^{χ^0} and

$$\begin{pmatrix} \lambda_{w_3} \\ \lambda_Y \\ \lambda_B \\ -i\tilde{H}_1^1 \\ -i\tilde{H}_2^2 \\ -i\tilde{S} \\ \psi_{\mathbf{b}} \end{pmatrix} = O^{\chi^0} \begin{pmatrix} \chi_0^0 \\ \chi_1^0 \\ \chi_2^0 \\ \chi_3^0 \\ \chi_4^0 \\ \chi_5^0 \\ \chi_6^0 \end{pmatrix}. \tag{127}$$

The numerical study of this matrix can be found in Sec. 10.

C.4 Chargino sector

We recall here the structure of the chargino sector and the diagonalization procedure. We define

$$\lambda_{w^+} = \frac{1}{\sqrt{2}}(\lambda_{w_1} - i\lambda_{w_2}) \quad \lambda_{w^-} = \frac{1}{\sqrt{2}}(\lambda_{w_1} + i\lambda_{w_2}) \tag{128}$$

and in the basis $(\lambda_{w^+}, \tilde{H}_2^1, \lambda_{w^-}, \tilde{H}_1^2)$ we obtain the mass matrix

$$M_{\tilde{\chi}^\pm}^2 = \begin{pmatrix} 0 & 0 & M_W & g_2 v_1 \\ 0 & 0 & g_2 v_2 & \lambda v_S \\ M_W & g_2 v_2 & 0 & 0 \\ g_2 v_1 & \lambda v_S & 0 & 0 \end{pmatrix}; \tag{129}$$

from the diagonalization we get the squared eigenvalues

$$m_{\tilde{\chi}_{1,2}^\pm} = \frac{1}{2} \left[M_W^2 + \lambda^2 v_S^2 + g_2^2 v^2 \mp \sqrt{(M_W^2 + \lambda^2 v_S^2 + g_2^2 v^2)^2 - 4(\lambda v_S M_W - g_2^2 v_1 v_2)^2} \right] \tag{130}$$

If we define

$$\psi^+ = \begin{pmatrix} \lambda_{w^+} \\ \tilde{H}_2^1 \end{pmatrix} \quad \psi^- = \begin{pmatrix} \lambda_{w^-} \\ \tilde{H}_1^2 \end{pmatrix} \tag{131}$$

and define the mass eigenstates as

$$\chi^+ = V \psi^+ \quad \chi^- = U \psi^- \tag{132}$$

where U and V are two unitary matrices that perform the diagonalization of this sector. If we define

$$X = \begin{pmatrix} M_W & g_2 v_2 \\ g_2 v_1 & \lambda v_S \end{pmatrix} \quad (133)$$

then these unitary matrices are defined in such a way that

$$V X^\dagger X V^{-1} = U^* X X^\dagger U^T = M_{\chi^\pm, diag}; \quad (134)$$

where $M_{\chi^\pm, diag}$ is given by

$$M_{\chi^\pm, diag} = \begin{pmatrix} m_{\tilde{\chi}_1^\pm} & 0 \\ 0 & m_{\tilde{\chi}_2^\pm} \end{pmatrix}. \quad (135)$$

D Appendix. Axi-Higgs interactions

In this section we report the expressions of the vertices involving the axi-Higgs. We have trilinear and quadrilinear vertices involving the other neutral Higgs states, leptons, quarks, neutralinos, sleptons, squarks and charginos. For simplicity's sake, in these expressions we denote implicitly some of the matrices that define the rotation on the physical basis. We use O^{ev} for the 4×4 rotation matrix of the CP-even Higgs sector, defined in Sec. B, O^{χ^0} for the 7×7 rotation matrix of the neutralino sector, defined in Sec. C.3, $O^{\tilde{l}}$, $O^{\tilde{u}}$ and $O^{\tilde{d}}$ for the 2×2 matrices of the slepton and squark sectors, defined in Sec. C.2. We denote with H_0^i ($i = 1, 2, 3$) the CP-even Higgs states; we leave aside the couplings with H_0^b since we assume that it is completely decoupled at the electroweak scale (see Sec. 8).

$$\begin{aligned} N &= \frac{v_1^2 v_2^2 + v^2 v_S^2}{M_{st}} \sqrt{4v^2 M_{st}^2 + g_B^2 B_S^2 (v_1^2 v_2^2 + v^2 v_S^2)} \\ R^{H_0^5 H_0^i H_0^4} &= \frac{1}{2N} \left\{ 2\sqrt{2} a_\lambda v_1^2 v_2^2 (O_{i1}^{ev} v_1 + O_{i2}^{ev} v_2) + v_1 v_2 v_S \left[O_{i1}^{ev} (B_{H_1} (B_S - B_{H_2}) g_B^2 + g_2^2 + g_Y^2) v_1^3 - \right. \right. \\ &\quad O_{i1}^{ev} (B_{H_1} (B_{H_1} - B_S) g_B^2 + g_2^2 + g_Y^2 - 4\lambda^2) v_2^2 v_1 + 4\sqrt{2} a_\lambda O_{i3}^{ev} v_2 v_1 \\ &\quad \left. - O_{i2}^{ev} v_2 v_1^2 (B_{H_2} (B_{H_2} - B_S) g_B^2 + g_2^2 + g_Y^2 - 4\lambda^2) + O_{i2}^{ev} (B_{H_2} (B_S - B_{H_1}) g_B^2 + g_2^2 + g_Y^2) v_2^3 \right] + \\ &\quad v_S^2 \left[O_{i3}^{ev} v_1 v_2 (g_B^2 B_S ((B_S - B_{H_2}) v_1^2 + (B_S - B_{H_1}) v_2^2) - 4\lambda^2 v^2) - \right. \\ &\quad \left. \left. 2\sqrt{2} a_\lambda (O_{i1}^{ev} v_1 + O_{i2}^{ev} v_2) v^2 \right] \right\} \quad (136) \end{aligned}$$

$$\begin{aligned} R^{H_0^5 H_0^5 H_0^i} &= \frac{(v_1^2 v_2^2 + v^2 v_S^2)}{2N^2} \left\{ -g_B^2 O_{i3}^{ev} B_S^2 v^4 v_S^3 - v^4 v_S^2 [B_S (O_{i1}^{ev} B_{H_1} v_1 + O_{i2}^{ev} B_{H_2} v_2) g_B^2 + 4\lambda^2 (O_{i1}^{ev} v_1 + O_{i2}^{ev} v_2)] - \right. \\ &\quad v_1 v_2 \left[4\sqrt{2} a_\lambda (O_{i1}^{ev} v_1 + O_{i2}^{ev} v_2) v^2 + O_{i3}^{ev} v_1 v_2 (B_S (B_{H_2} v_1^2 + B_{H_1} v_2^2) g_B^2 + 4\lambda^2 v^2) \right] v_S + \\ &\quad g_2^2 v_1^2 v_2^2 (v_1^2 - v_2^2) (O_{i1}^{ev} v_1 - O_{i2}^{ev} v_2) + v_1^2 v_2^2 \left[O_{i1}^{ev} (-B_{H_1} B_{H_2} g_B^2 + g_Y^2 - 4\lambda^2) v_1^3 - \right. \\ &\quad O_{i1}^{ev} (g_Y^2 + g_B^2 B_{H_1}^2) v_2^2 v_1 - O_{i2}^{ev} (g_Y^2 + g_B^2 B_{H_2}^2) v_1^2 v_2 + 4\sqrt{2} a_\lambda O_{i3}^{ev} v_2 v_1 + \\ &\quad \left. \left. O_{i2}^{ev} (-B_{H_1} B_{H_2} g_B^2 + g_Y^2 - 4\lambda^2) v_2^3 \right] \right\} \quad (137) \end{aligned}$$

$$\begin{aligned} R^{H_0^5 H_0^4 H_0^i H_0^j} &= \frac{v_1 v_2 v_S}{(1 + \delta^{ij}) 2N} \left\{ (O_{i1}^{ev} O_{j1}^{ev} - O_{i2}^{ev} O_{j2}^{ev}) (v_1^2 - v_2^2) g_2^2 + \left[4\lambda^2 (O_{i2}^{ev} O_{j2}^{ev} - O_{i3}^{ev} O_{j3}^{ev}) - \right. \right. \\ &\quad \left. \left. g_B^2 (B_{H_2} - B_S) (O_{i1}^{ev} O_{j1}^{ev} B_{H_1} + O_{i2}^{ev} O_{j2}^{ev} B_{H_2} + O_{i3}^{ev} O_{j3}^{ev} B_S) \right] v_1^2 + \left[4\lambda^2 (O_{i1}^{ev} O_{j1}^{ev} - O_{i3}^{ev} O_{j3}^{ev}) - \right. \right. \end{aligned}$$

$$g_B^2(B_{H_1} - B_S)(O_{i1}^{ev}O_{j1}^{ev}B_{H_1} + O_{i2}^{ev}O_{j2}^{ev}B_{H_2} + O_{i3}^{ev}O_{j3}^{ev}B_S)\Big]v_2^2 + g_Y^2(O_{i1}^{ev}O_{j1}^{ev} - O_{i2}^{ev}O_{j2}^{ev})(v_1^2 - v_2^2)\Big\} \quad (138)$$

$$R^{H_0^5 H_0^i H_0^j} = -\frac{(v_2^2 v_S^2 + v_1^2 v_2^2)}{(1 + \delta^{ij})2N^2} \left\{ v_2^2 v_1^4 \left[B_{H_2}(O_{i1}^{ev}O_{j1}^{ev}B_{H_1} + O_{i2}^{ev}O_{j2}^{ev}B_{H_2} + O_{i3}^{ev}O_{j3}^{ev}B_S)g_B^2 + 4\lambda^2(O_{i1}^{ev}O_{j1}^{ev} + O_{i3}^{ev}O_{j3}^{ev}) \right] + v_2^4 v_1^2 \left[B_{H_1}(O_{i1}^{ev}O_{j1}^{ev}B_{H_1} + O_{i2}^{ev}O_{j2}^{ev}B_{H_2} + O_{i3}^{ev}O_{j3}^{ev}B_S)g_B^2 + 4\lambda^2(O_{i2}^{ev}O_{j2}^{ev} + O_{i3}^{ev}O_{j3}^{ev}) \right] + v^4 v_S^2 \left[B_S(O_{i1}^{ev}O_{j1}^{ev}B_{H_1} + O_{i2}^{ev}O_{j2}^{ev}B_{H_2} + O_{i3}^{ev}O_{j3}^{ev}B_S)g_B^2 + 4\lambda^2(O_{i1}^{ev}O_{j1}^{ev} + O_{i2}^{ev}O_{j2}^{ev}) \right] - g^2(O_{i1}^{ev}O_{j1}^{ev} - O_{i2}^{ev}O_{j2}^{ev})(v_1^2 - v_2^2)v_2^2 v_1^2 \right\} \quad (139)$$

$$R^{H_0^5 H_0^4 3} = \frac{v_1 v_2 v_S}{4N(v_2^2 v_S^2 + v_1^2 v_2^2)} \left\{ -g^2(v_1^2 - v_2^2)^2 v_S^2 - g_B^2 \left[(B_{H_2} - B_S)v_1^2 + (B_{H_1} - B_S)v_2^2 \right] \left[B_S v_1^2 v_2^2 + (B_{H_2} v_1^2 + B_{H_1} v_2^2) v_S^2 \right] + 4\lambda^2 \left[(v_1^4 + v_2^4) v_S^2 - v_1^2 v_2^2 v^2 \right] \right\} \quad (140)$$

$$R^{H_0^5 H_0^4 2} = \frac{1}{4N^2} \left\{ g_B^2 \left[-B_S v_1^4 v_2^4 (B_{H_2} v_1^2 + B_{H_1} v_2^2) - v_1^2 v_2^2 v_S^2 \left((3B_{H_2}^2 - 4B_S B_{H_2} + 3B_S^2) v_1^4 + (10B_S^2 + 6B_{H_1} B_{H_2}) v_2^2 v_1^2 + (3B_{H_1}^2 - 4B_S B_{H_1} + 3B_S^2) v_2^4 \right) - B_S v^4 (B_{H_2} v_1^2 + B_{H_1} v_2^2) v_S^4 \right] - 3g^2 v_2^2 v_1^2 (v_1^2 - v_2^2)^2 v_S^2 + 4\lambda^2 \left[-v_1^4 v^2 v_2^4 + 2v_1^2 v_2^2 v_S^2 (2v_1^4 + v_2^2 v_1^2 + 2v_2^4) - v^6 v_S^4 \right] \right\} \quad (141)$$

$$R^{H_0^5 H_0^4} = \frac{v_1 v_2 v_S (v_1^2 v_2^2 + v^2 v_S^2)}{N^3} \left\{ - (B_{H_2}(B_{H_2} - B_S)g_B^2 + g_2^2 + g_Y^2 - 4\lambda^2) v_2^2 v_1^6 + \left[(B_{H_1} + B_{H_2})B_S - 2B_{H_1} B_{H_2} \right] g_B^2 + 2g_2^2 + 2g_Y^2 \right] v_2^4 v_1^4 - (B_{H_1}(B_{H_1} - B_S)g_B^2 + g_2^2 + g_Y^2 - 4\lambda^2) v_2^6 v_1^2 - v^4 \left[B_S \left((B_{H_2} - B_S)v_1^2 + (B_{H_1} - B_S)v_2^2 \right) g_B^2 + 4\lambda^2 v^2 \right] v_S^2 \right\} \quad (142)$$

$$R^{H_0^5 4} = \frac{(v_1^2 v_2^2 + v^2 v_S^2)^2}{4N^4} \left\{ - (g_2^2 + g_Y^2 + g_B^2 B_{H_2}^2) v_2^4 v_1^8 + 2(-B_{H_1} B_{H_2} g_B^2 + g_2^2 + g_Y^2 - 4\lambda^2) v_2^6 v_1^6 - (g_2^2 + g_Y^2 + g_B^2 B_{H_1}^2) v_2^8 v_1^4 - 2v_2^2 v^4 \left[B_S (B_{H_2} v_1^2 + B_{H_1} v_2^2) g_B^2 + 4\lambda^2 v^2 \right] v_S^2 v_1^2 - g_B^2 B_S^2 v^8 v_S^4 \right\} \quad (143)$$

$$R^{H_0^5 i \bar{i}} = \frac{i\sqrt{2}M_{st}v_1 v_2^2 y_i}{\sqrt{(v_1^2 v_2^2 + v_S^2 v^2)(4v^2 M_{st}^2 + g_B^2 B_S^2 (v_1^2 v_2^2 + v_S^2 v^2))}} \quad i = e, \mu, \tau, d, c, b \quad (144)$$

$$R^{H_0^5 j \bar{j}} = -\frac{i\sqrt{2}M_{st}v_2 v_1^2 y_j}{\sqrt{(v_1^2 v_2^2 + v_S^2 v^2)(4v^2 M_{st}^2 + g_B^2 B_S^2 (v_1^2 v_2^2 + v_S^2 v^2))}} \quad j = u, s, t \quad (145)$$

$$R^{H_0^5 \chi_i^0 \chi_j^0} = i \frac{\sqrt{v_1^2 v_2^2 + v_S^2 v^2}}{(1 + \delta^{ij})N} \left\{ g_2 v_1 v_2 \left[(O_{i5}^{\chi^0} O_{j1}^{\chi^0} + O_{i1}^{\chi^0} O_{j5}^{\chi^0}) v_1 - (O_{i4}^{\chi^0} O_{j1}^{\chi^0} + O_{i1}^{\chi^0} O_{j4}^{\chi^0}) v_2 \right] + \sqrt{2}\lambda \left[v_1^2 v_2 (O_{i6}^{\chi^0} O_{j4}^{\chi^0} + O_{i4}^{\chi^0} O_{j6}^{\chi^0}) + v_1 v_2^2 (O_{i6}^{\chi^0} O_{j5}^{\chi^0} + O_{i5}^{\chi^0} O_{j6}^{\chi^0}) - v^2 v_S (O_{i5}^{\chi^0} O_{j4}^{\chi^0} + O_{i4}^{\chi^0} O_{j5}^{\chi^0}) \right] \right\} \quad (146)$$

$$R^{H_0^5 \tilde{e}_i \tilde{e}_j} = -\frac{i\sqrt{v_1^2 v_2^2 + v_S^2 v^2}}{(1 + \delta^{ij})N} \left(O_{i2}^{\tilde{e}_1} O_{j1}^{\tilde{e}_1} - O_{i1}^{\tilde{e}_1} O_{j2}^{\tilde{e}_1} \right) \left(\lambda v_2 v_S y_{e_1} - \sqrt{2} a_{e_1} v_1 \right) v_2^2 \quad (147)$$

$$R^{H_0^5 \tilde{q}_d i \tilde{q}_d j} = - \frac{i \sqrt{v_1^2 v_2^2 + v_S^2 v^2}}{(1 + \delta^{ij})N} \left(O_{i2}^{\tilde{d}_1} O_{j1}^{\tilde{d}_1} - O_{i1}^{\tilde{d}_1} O_{j2}^{\tilde{d}_1} \right) \left(\lambda v_2 v_S y_{d_1} - \sqrt{2} a_{d_1} v_1 \right) v_2^2 \quad (148)$$

$$R^{H_0^5 \tilde{q}_u i \tilde{q}_u j} = \frac{i \sqrt{v_1^2 v_2^2 + v_S^2 v^2}}{(1 + \delta^{ij})N} \left(O_{i2}^{\tilde{u}_1} O_{j1}^{\tilde{u}_1} - O_{i1}^{\tilde{u}_1} O_{j2}^{\tilde{u}_1} \right) \left(\lambda v_1 v_S y_{u_1} - \sqrt{2} a_{u_1} v_2 \right) v_1^2 \quad (149)$$

$$R^{H_0^5 \chi_i^+ \chi_j^-} = \frac{i \sqrt{2(v_1^2 v_2^2 + v_S^2 v^2)}}{N} [\lambda v_S v^2 V^{j2} U^{i2} + g_2 v_1 v_2 (v_2 V^{j2} U^{i1} + v_1 V^{j1} U^{i2})] \quad (150)$$

The matrices V and U appearing in the coupling of the axi-higgs with the charginos are the standard matrices that realize the diagonalization of the chargino mass matrix in the MSSM, since this matrix is not modified in our model. They are defined in Appendix C.4.

E Appendix. Relic densities at the second misalignment

In this appendix we fill in the gaps in the derivation of the expression of the abundances generated by the mechanism of vacuum misalignment. We start from the Lagrangian

$$\mathcal{S} = \int d^4x \sqrt{g} \left(\frac{1}{2} \dot{\chi}^2 - \frac{1}{2} m_\chi^2 \Gamma_\chi \dot{\chi} \right), \quad (151)$$

where Γ_χ is the decay rate of the axion and we have expanded the potential around its minimum up to quadratic terms. The same action is derived from the quadratic approximation to the general expression

$$\mathcal{S} = \int d^4x R^3(t) \left(\frac{1}{2} \sigma_\chi^2 (\partial_\alpha \theta)^2 - \mu^4 (1 - \cos \theta) - V_0 \right) \quad (152)$$

which, in our case, is constructed from the expression of V' given in Eq. (67), with $\mu \sim v$, the electroweak scale. We also set other contributions to the vacuum potential to vanish ($V_0 = 0$). In a Friedmann-Robertson-Walker spacetime metric with a scaling factor $R(t)$, this action gives the equation of motion

$$\frac{d}{dt} \left[(R^3(t) (\dot{\chi} + \Gamma_\chi)) \right] + R^3 m_\chi^2(T) \chi = 0. \quad (153)$$

We will neglect the decay rate of the axion in this case and set $\Gamma_\chi \approx 0$. At this point, since the potential V' is of non-perturbative origin, we can assume that it vanishes far above the electroweak scale (or temperature T_{ew}). For this reason $m_\chi = m_b = 0$ for $T \gg T_{ew}$, which is essentially equivalent to assume that the Stückelberg axion is not subject to any mixing far above the weak scale. The general equation of motion derived from Eq. (153), introducing a temperature dependent mass, can be written as

$$\ddot{\chi} + 3H\dot{\chi} + m_\chi^2(T)\chi = 0, \quad (154)$$

which clearly allows as a solution a constant value of the misalignment angle $\theta = \theta_i$. The T-dependence of the mass term should be generated, for consistency, from a generalization to finite temperature of V' . In practice this is not necessary in our case, being the role of the first misalignment negligible in determining the final mass of the axion.

The axion energy density is given by

$$\rho = \frac{1}{2}\dot{\chi}^2 + \frac{1}{2}m_\chi^2\chi^2, \quad (155)$$

which after a harmonic averaging gives

$$\langle \rho \rangle = m_\chi^2 \langle \chi^2 \rangle. \quad (156)$$

Notice that after differentiating Eq. (155) and using the equation of motion in (154), followed by the averaging Eq. (156) one obtains the relation

$$\langle \dot{\rho} \rangle = \langle \rho \rangle \left(-3H + \frac{\dot{m}}{m} \right), \quad (157)$$

where the time dependence of the mass is through its temperature $T(t)$, while $H(t) = \dot{R}(t)/R(t)$ is the Hubble parameter. By inspection one easily finds that the solution of this equation is of the form

$$\langle \rho \rangle = \frac{m_\chi(T)}{R^3(t)} \quad (158)$$

showing a dilution of the energy density with an increasing space volume, valid even for a T -dependent mass. At this point, the universe must be (at least) as old as the required period of oscillation in order for the axion field to start oscillating and to appear as dark matter, otherwise θ is misaligned but frozen; this is the content of the condition

$$m_\chi(T_i) = 3H(T_i), \quad (159)$$

which allows to identify the initial temperature of the coherent oscillation of the axion field χ , T_i , by equating $m_\chi(T)$ to the Hubble rate, taken as a function of temperature.

To quantify the relic densities at the current temperature T_0 ($T_0 \equiv T(t_0)$, at current time t_0) we define preliminarily the two standard effective couplings

$$\begin{aligned} g_{*,S,T} &= \sum_B g_i \left(\frac{T_i}{T} \right)^3 + \frac{7}{8} \sum_F g_i \left(\frac{T_i}{T} \right)^3 \\ g_{*,T} &= \sum_B g_i \left(\frac{T_i}{T} \right)^4 + \frac{7}{8} \sum_F g_i \left(\frac{T_i}{T} \right)^4, \end{aligned} \quad (160)$$

functions of the massless relativistic degrees of freedom of the primordial state, with $T \gg T_{ew}$. The counting of the degrees of freedom is: 2 for a Majorana fermion and for a massless gauge boson, 3 for a massive gauge boson and 1 for a real scalar. In the radiation era, the thermodynamics of all the components of the primordial state is entirely determined by the temperature T , being the system at equilibrium. We exclude for simplicity all sorts of possible source of entropy due to any inhomogeneity (see, for instance, [54]). Pressure and entropy are then just given as a function of the temperature

$$\begin{aligned} \rho &= 3p = \frac{\pi^2}{30} g_{*,T} T^4 \\ s &= \frac{2\pi^2}{45} g_{*,S,T} T^3, \end{aligned} \quad (161)$$

while the Friedmann equation allows to relate the Hubble parameter and the energy density

$$H = \sqrt{\frac{8}{3}\pi G_N \rho}, \quad (162)$$

with $G_N = 1/M_P^2$ being the Newton constant and M_P the Planck mass. The number density of axions n_χ decreases as $1/R^3$ with the expansion, as does the entropy density $s \equiv S/R^3$, where S indicates the comoving entropy density - which remains constant in time ($\dot{S} = 0$) - leaving the ratio $Y_a \equiv n_\chi/s$ conserved. We define, as usual, the abundance variable of χ

$$Y_\chi(T_i) = \frac{n_\chi}{s} \Big|_{T_i} \quad (163)$$

at the temperature of oscillation T_i , and observe that at the beginning of the oscillations the total energy density is just the potential one

$$\rho_\chi = n_\chi(T_i)m_\chi(T_i) = 1/2 m_\chi^2(T_i)\chi_i^2. \quad (164)$$

We then obtain for the initial abundance at $T = T_i$

$$Y_\chi(T_i) = \frac{1}{2} \frac{m_\chi(T_i)\chi_i^2}{s} = \frac{45m_\chi(T_i)\chi_i^2}{4\pi^2 g_{*,S,T} T_i^3} \quad (165)$$

where we have inserted at the last stage the expression of the entropy of the system at the temperature T_i given by Eq. (161). At this point, plugging the expression of ρ given in Eq. (161) into the expression of the Hubble rate as a function of density given in Eq. (162), the condition for oscillation Eq. (159) allows to express the axion mass at $T = T_i$ in terms of the effective massless degrees of freedom evaluated at the same temperature, that is

$$m_\chi(T_i) = \sqrt{\frac{4}{5}\pi^3 g_{*,T_i}} \frac{T_i^2}{M_P}. \quad (166)$$

This gives for Eq. (165) the expression

$$Y_\chi(T_i) = \frac{45\sigma_\chi^2 \theta_i^2}{2\sqrt{5\pi g_{*,T_i}} T_i M_P}, \quad (167)$$

where we have expressed χ in terms of the angle of misalignment θ_i at the temperature when oscillations start. We assume that $\theta_i = \langle \theta \rangle$ is the zero mode of the initial misalignment angle after an averaging. As we have already mentioned, T_i should be determined consistently by Eq. (159). However, the presence of two significant and unknown variables in the expression of m_χ , which are the coupling of the anomalous $U(1)$, g_B , and the Stückelberg mass M , forces us to consider the analysis of the T-dependence of χ phenomenologically less relevant. It is more so if the Stückelberg mass is somehow close to the TeV region, in which case the zero temperature axion mass m_χ acquires corrections proportional to the bare coupling ($m_\chi \sim \lambda v(1 + O(g_B))$).

For this reason, assuming that the oscillation temperature T_i is close to the electroweak temperature T_{ew} , Eq. (166) provides an upper bound for the mass of the axion at which the oscillations occur, assuming that they start around the electroweak phase transition. Stated differently, mass values of χ such that

$m(T_i) \ll 3H(T_i)$ correspond to frozen degrees of freedom of the axion at the electroweak scale. This is clearly an approximation, but it allows to define the oscillation mass in terms of the Hubble parameter for each given temperature.

We recall that the relic density due to misalignment can be extracted from the relations

$$\Omega_\chi^{mis} \equiv \frac{\rho_{\chi 0}^{mis}}{\rho_c} = \frac{(n_{\chi 0} m_\chi)}{\rho_c} = \left(\frac{n_{\chi 0}}{s_0} \right) \frac{m_\chi s_0}{\rho_c} \quad (168)$$

where we have denoted with $n_{\chi 0}$ the current number density of axions and with $\rho_{\chi 0}^{mis}$ their current energy density due to vacuum misalignment. This expression can be rewritten as

$$\Omega_\chi^{mis} = \frac{n_\chi}{s} \bigg|_{T_i} m_\chi \frac{s_0}{\rho_c} \quad (169)$$

using the conservation of the abundance $Y_{a0} = Y_a(T_i)$. Notice that in Eq. (169) we have neglected a possible dilution factor $\gamma = s_{osc}/s_0$ which may be present due to entropy release. We have introduced the variable

$$\rho_c = \frac{3H_0^2}{8\pi G_N} \quad (170)$$

which is the critical density and

$$s_0 = \frac{2\pi^2}{45} g_{*,T_0} T_0^3 \quad (171)$$

which is the current entropy density. To fix g_{*,T_0} we just recall that at the current temperature T_0 the relativistic species contributing to the entropy density s_0 are the photons and three families of neutrinos with

$$g_{*,T_0} = 2 + \frac{7}{8} \times 3 \times 2 \left(\frac{T_\nu}{T_0} \right)^3 \quad (172)$$

where, from entropy considerations, $T_\nu/T_0 = (4/11)^{1/3}$.

To proceed with the computation of the massless degrees of freedom above the electroweak phase transition we just recall the structure of the model. We have 13 gauge bosons corresponding to the gauge group $SU(3) \times SU(2) \times U_Y(1) \times U_B(1)$, 2 Higgs doublets, 3 generations of leptons and 3 families of quarks. Above the energy of the electroweak transition we have only massless fields with the exception of the $U_B(1)$ gauge boson, since this symmetry takes the Stückelberg form above the electroweak scale, giving $g_{*,T} = 110.75$. Below the same scale this number is similarly computed with $g_{*,T} = 91.25$. Other useful parameters are the critical density and the current entropy

$$\rho_c = 5.2 \cdot 10^{-6} \text{GeV/cm}^3 \quad s_0 = 2970 \text{ cm}^{-3}, \quad (173)$$

with $\theta_i \simeq 1$. It is clear, by inserting these numbers into Eq. (168) that Ω_χ^{mis}

$$\frac{45\sigma_\chi^2 \theta_i^2}{2\sqrt{5\pi g_{*,T_i}} T_i M_P} \frac{m_\chi s_0}{\rho_c} \quad (174)$$

is negligible unless $\sigma_\chi \sim M_{St}^2/v$ is of the same order of $f_a \sim 10^{12}$ GeV, the standard PQ constant. This choice would correspond to $\Omega_\chi \sim 0.1$, but the value of M_{St} should be of $O(10^7)$ GeV, which is clearly excluded in our case, being in conflict with the WMAP data.

References

- [1] R. D. Peccei and H. R. Quinn, Phys. Rev. **D16**, 1791 (1977).
- [2] R. D. Peccei, Lect. Notes Phys. **741**, 3 (2008), arXiv:hep-ph/0607268.
- [3] S. Weinberg, Phys. Rev. Lett. **40**, 223 (1978).
- [4] F. Wilczek, Phys. Rev. Lett. **40**, 279 (1978).
- [5] M. Dine, W. Fischler, and M. Srednicki, Phys. Lett. **B104**, 199 (1981).
- [6] A. R. Zhitnitsky, Sov. J. Nucl. Phys. **31**, 260 (1980).
- [7] J. E. Kim, Phys. Rev. Lett. **43**, 103 (1979).
- [8] M. A. Shifman, A. I. Vainshtein, and V. I. Zakharov, Nucl. Phys. **B166**, 493 (1980).
- [9] Supernova Search Team, A. G. Riess *et al.*, Astron. J. **116**, 1009 (1998), arXiv:astro-ph/9805201.
- [10] Supernova Cosmology Project, S. Perlmutter *et al.*, Astrophys. J. **517**, 565 (1999), arXiv:astro-ph/9812133.
- [11] Y. Nomura, T. Watari, and T. Yanagida, Phys. Lett. **B484**, 103 (2000), arXiv:hep-ph/0004182.
- [12] P. Sikivie, Lect. Notes Phys. **741**, 19 (2008), arXiv:astro-ph/0610440.
- [13] S. Chang, C. Hagmann, and P. Sikivie, (1998), arXiv:hep-ph/9812327.
- [14] CAST, E. Arik *et al.*, JCAP **0902**, 008 (2009), arXiv:0810.4482.
- [15] The ADMX, S. J. Asztalos *et al.*, Phys. Rev. Lett. **104**, 041301 (2010), arXiv:0910.5914.
- [16] L. D. Duffy and K. van Bibber, New J. Phys. **11**, 105008 (2009), arXiv:0904.3346.
- [17] G. G. Raffelt, Lect. Notes Phys. **741**, 51 (2008), arXiv:hep-ph/0611350.
- [18] L. Visinelli and P. Gondolo, Phys. Rev. **D80**, 035024 (2009), arXiv:0903.4377.
- [19] M. Ahlers, H. Gies, J. Jaeckel, J. Redondo, and A. Ringwald, Phys. Rev. **D77**, 095001 (2008), arXiv:0711.4991.
- [20] M. Ahlers, H. Gies, J. Jaeckel, J. Redondo, and A. Ringwald, Phys. Rev. **D76**, 115005 (2007), arXiv:0706.2836.
- [21] A. De Angelis, O. Mansutti, and M. Roncadelli, Phys. Lett. **B659**, 847 (2008), arXiv:0707.2695.
- [22] A. De Angelis, O. Mansutti, and M. Roncadelli, Phys. Rev. **D76**, 121301 (2007), arXiv:0707.4312.
- [23] A. Mirizzi and D. Montanino, JCAP **0912**, 004 (2009), arXiv:0911.0015.

- [24] Z. G. Berezhiani, A. S. Sakharov, and M. Y. Khlopov, *Sov. J. Nucl. Phys.* **55**, 1063 (1992).
- [25] Z. G. Berezhiani, M. Y. Khlopov, and A. S. Sakharov, DFTUZ-91-29.
- [26] C. Corianò, N. Irges, and S. Morelli, *JHEP* **07**, 008 (2007), arXiv:hep-ph/0701010.
- [27] C. Corianò, N. Irges, and S. Morelli, *Nucl. Phys.* **B789**, 133 (2008), arXiv:hep-ph/0703127.
- [28] J. De Rydt, J. Rosseel, T. T. Schmidt, A. Van Proeyen, and M. Zagermann, *Class. Quant. Grav.* **24**, 5201 (2007), arXiv:0705.4216.
- [29] J.-P. Derendinger, P. M. Petropoulos, and N. Prezas, *Nucl. Phys.* **B785**, 115 (2007), arXiv:0705.0008.
- [30] C. Corianò, M. Guzzi, G. Lazarides, and A. Mariano, (2010), arXiv:1005.5441.
- [31] B. de Carlos, J. A. Casas, F. Quevedo, and E. Roulet, *Phys. Lett.* **B318**, 447 (1993), arXiv:hep-ph/9308325.
- [32] T. Banks, M. Dine, and M. Graesser, *Phys. Rev.* **D68**, 075011 (2003), arXiv:hep-ph/0210256.
- [33] C. Corianò, M. Guzzi, A. Mariano, and S. Morelli, *Phys. Rev.* **D80**, 035006 (2009), arXiv:0811.3675.
- [34] WMAP, G. Hinshaw *et al.*, *Astrophys. J. Suppl.* **180**, 225 (2009), arXiv:0803.0732.
- [35] CDF, T. Aaltonen *et al.*, *Phys. Rev.* **D77**, 051102 (2008), arXiv:0710.5335.
- [36] C. Corianò, N. Irges, and E. Kiritsis, *Nucl. Phys.* **B746**, 77 (2006), arXiv:hep-ph/0510332.
- [37] C. Corianò, M. Guzzi, N. Irges, and A. Mariano, *Phys. Lett.* **B671**, 87 (2009), arXiv:0811.0117.
- [38] M. Cvetič, D. A. Demir, J. R. Espinosa, L. L. Everett, and P. Langacker, *Phys. Rev.* **D56**, 2861 (1997), arXiv:hep-ph/9703317.
- [39] P. Anastasopoulos *et al.*, *Phys. Rev.* **D78**, 085014 (2008), arXiv:0804.1156.
- [40] F. Fucito, A. Lionetto, A. Mammarella, and A. Racioppi, (2008), arXiv:0811.1953.
- [41] A. Lionetto and A. Racioppi, *Nucl. Phys.* **B831**, 329 (2010), arXiv:0905.4607.
- [42] C. Corianò, M. Guzzi, and S. Morelli, *Eur. Phys. J.* **C55**, 629 (2008), arXiv:0801.2949.
- [43] C. Corianò and M. Guzzi, *Nucl. Phys.* **B826**, 87 (2010), arXiv:0905.4462.
- [44] K. Dimopoulos, G. Lazarides, D. Lyth, and R. Ruiz de Austri, *JHEP* **05**, 057 (2003), arXiv:hep-ph/0303154.
- [45] G. Belanger, F. Boudjema, A. Pukhov, and A. Semenov, *Comput. Phys. Commun.* **177**, 894 (2007).
- [46] A. Pukhov, (2004), arXiv:hep-ph/0412191.
- [47] A. Semenov, *Comput. Phys. Commun.* **180**, 431 (2009), arXiv:0805.0555.

- [48] D. Feldman, Z. Liu, P. Nath, and G. Peim, Phys. Rev. **D81**, 095017 (2010), arXiv:1004.0649.
- [49] B. Kors and P. Nath, JHEP **12**, 005 (2004), arXiv:hep-ph/0406167.
- [50] C. Corianò, A. E. Faraggi, and M. Guzzi, Phys. Rev. **D78**, 015012 (2008), arXiv:0802.1792.
- [51] D. Feldman, Z. Liu, and P. Nath, Phys. Rev. **D75**, 115001 (2007), arXiv:hep-ph/0702123.
- [52] R. Armillis, C. Corianò, M. Guzzi, and S. Morelli, Nucl. Phys. **B814**, 15679 (2009), arXiv:0809.3772.
- [53] CAST, E. F. Ribas, (2009), arXiv:0912.4222.
- [54] G. Lazarides, R. K. Schaefer, D. Seckel, and Q. Shafi, Nucl. Phys. **B346**, 193 (1990).